Theses and Dissertations   Graduate School

2020

TRANSCRIPTOMIC PROFILING OF POSTMORTEM PREFRONTAL CORTEX AND NUCLEUS ACCUMBENS FROM CHRONIC ALCOHOL ABUSERS.

Eric S. Vornholt

TRANSCRIPTOMIC PROFILING OF POSTMORTEM PREFRONTAL CORTEX AND NUCLEUS ACCUMBENS FROM CHRONIC ALCOHOL ABUSERS.

A Dissertation submitted in partial fulfillment of the requirements for the degree of Doctor of Philosophy at Virginia Commonwealth University.

By
Eric Vornholt

August 2016 to December 2020

Advisor: Vladimir Vladimirov, MD, PhD

Virginia Commonwealth University
Richmond, Virginia
December 2020

ACKNOWLEDGEMENTS

I cannot fully express my gratitude and appreciation to my mentor and PhD advisor, Dr. Vladimir Vladimirov. The leadership, time, patience, and flexibility Dr. Vladimirov has given me while I navigated the complex world of molecular research and academia has been influential in both my professional development and personal life. Few people have had the ability to keep me focused while also giving me the trust and freedom to push myself forward, and for that I am forever grateful.

I especially want to thank my colleagues in the Vladimirov Lab. Omari McMichael, John Drake, and Nathan Taylor, thank you for helping me hone my bench techniques and work through statistical and theoretical study design. I am so proud of the work we have accomplished together.

To the faculty at VIPBG and VCU School of Medicine who have provided support as members of my advisory committee, thank you. Drs. Brien Riley, Alexis Edwards, Joseph McClay, and Nathan Gillespie have each provided unique perspectives and influences on my work that I will carry with me as a future mentor and researcher. Each of you has contributed to the scientist I am now and will grow to become. Additionally, I am grateful to Drs. Kenneth Kendler, Silviu-Alin Bacanu, and Michael Miles who have served as collaborators for my F31, my first major professional achievement that has instilled the confidence that moves me today.

I am so incredibly grateful to the graduate students and postdoctoral fellows at both VIPBG and as part of the ILS program who have provided emotional support and comradery as we have all grown as scientists. Thank you for the lunches at City Dogs and unofficial happy hours. I want to also thank all of my friends in Richmond for accepting me unconditionally and making these years some of the best in my life.

I am overwhelmingly appreciative to my family. Their unwavering love has provided me with the motivation, confidence and energy that has allowed me to succeed as a student and as a person. To my sister, Sarah, who has provided emotional support during the hardest times when I have needed them the most. I am so proud of you and the strength you bring to all of us, and I am a better friend, son, and husband because of you. To my parents, John and Nancy, who from the beginning have believed in me. Because of you, I have always known what true happiness and love feels like. The foundation you have built for me and our family is the springboard that has propelled me forward, knowing nothing could stop me from achieving my dreams. Thank you.

Lastly, I want to thank the love of my life, Allie, who has given up so much so that I could pursue my dreams of becoming a scientist seeking to understand one of the last final frontiers, the human brain. I will never be able to express enough gratitude to her, as she has challenged me to reach a potential I never thought possible. I would not be the person I am today without her. And most notably, I want to thank the unconditional and unapologetic love from my two cats, Brian and Eloise, who sat up with me at all hours of the night providing both comfort and an appropriate amount of skepticism. Thank you everyone.

TABLE OF CONTENTS

LIST OF FIGURES AND TABLES

FIGURES

TABLES

ABBREVIATIONS & ACRONYMS

AD = alcohol dependence

ADH = alcohol dehydrogenase

AIC = Akaike information criteria

AUD = alcohol use disorder

CC = Cauchy Combination

cDNA = complementary DNA

circRNA = circular RNA

COGA = Collaborative Study on the Genetics of Alcoholism

DEG = differentially expressed gene

DSM-IV/V = Diagnostic and Statistical Manual of Mental Disorder

eQTL = expression quantitative trait loci

FDR = false discovery rate

GO = gene ontology

GS = gene significance

GSCAN = GWAS & Sequencing Consortium of Alcohol and Nicotine Use

GWAS = genome-wide association studies

LD = linkage disequilibrium

MCL = mesocorticolimbic system

ME = module eigengene

miRNA = microRNA

MM = module membership

mRNA = messenger RNA

MTs = metallothioneins

NAc = nucleus accumbens

ncRNA = non-coding RNA

NSW TRC = New South Wales Tissue Resource Centre

PFC = prefrontal cortex

PGC = Psychiatric Genetics Consortium

PMI = postmortem interval

RIN = RNA integrity number

RT-qPCR = reverse-transcriptase quantitative polymerase chain reaction

SNP = single nucleotide polymorphism

SUD = substance use disorder

VTA = ventral tegmental area

WGCNA = weighted gene co-expressed network analysis

ABSTRACT

Alcohol use disorder (AUD) is a debilitating psychiatric illness that develops from a combination of genetic and environmental factors. While it is well documented that AUD is heritable, the shift from recreational alcohol use to abuse/dependence is poorly understood. In this dissertation, using postmortem brain tissue from individuals with alcohol dependence (AD), we profiled the genome-wide expression of circular RNA (circRNA), microRNA (miRNA), and messenger RNA (mRNA) to better understand the impact of gene expression on the development of AUD. To achieve this, we performed two independent studies that explore transcriptome differences between AD cases and controls. The first of which examines differentially expressed gene (DEG) networks associated with AD that show either high or low levels of network preservation between two key areas of the mesocorticolimbic system (MCL), the prefrontal cortex (PFC) and nucleus accumbens (NAc). The second is a pilot study that interrogates the function of circRNA as miRNA sponges to impact the expression of mRNA. Overall, our findings corroborate results from recent studies while also providing novel evidence for biological processes that are differentially expressed between the PFC and NAc. Additionally, the second study is the first to explore circRNA:miRNA:mRNA interactions in the brains of chronic alcohol abusers and the role of circRNA as potential regulators of known AUD risk genes. Finally, we integrate genetic information in the form of eQTL analyses to determine the clinical relevance of these findings within the context of recent GWAS of AUD and other addiction phenotypes.

CHAPTER 1

INTRODUCTION

Alcohol has played a pivotal role in the evolution of human civilization and is among the most commonly used recreational drugs throughout the world [1]. As much as alcohol continues to be a hallmark of modern society, there is no denying that chronic alcohol consumption leads to negative health outcomes [2]. Some researchers focus on understanding health complications associated with excessive alcohol consumption in peripheral organs (i.e. liver failure and heart disease) [3, 4], whereas others seek to understand the neurobiological underpinnings of addictive behaviors that lead to the development of alcohol use disorder (AUD) [5]. This research focuses on the intersection of these two approaches by investigating transcriptomic changes that occur in etiologically relevant brain tissue after years of chronic alcohol abuse. Through identifying differentially expressed transcripts associated with alcohol dependence (AD), we hope to elucidate biomarkers that can help implicate potential therapeutic targets, either as implicit AUD risk genes or proteins/pathways sensitive to ethanol activity. While we are not the first to attempt this, this dissertation expands upon previous postmortem brain research by comparing expression changes between cortical and subcortical areas of the mesocorticolimbic system (MCL) from the brains of chronic alcohol abusers. Additionally, we explore circular RNA (circRNA) and microRNA (miRNA) as potential regulators of differential gene expression within the context of AUD.

Here, a brief outline of the study design is provided, followed by an overview of concepts and background information that offers justification for the presented research. Next, the two independent studies that address our overarching research aims to explore the biological processes dysregulated within the MCL of chronic alcohol abusers via comparative transcriptomics are

detailed. Finally, is an overview of the results from both studies and a discussion of potential limitations while looking forward to future research possibilities.

1.1) STUDY DESIGN

Through this dissertation, we investigate transcriptomic changes associated with AUD at various levels (circRNA, miRNA and mRNA) within the postmortem prefrontal cortex (PFC) and nucleus accumbens (NAc) from chronic alcohol abusers. To achieve this, we performed two independent studies with mutually exclusive hypotheses on 35 matched AD cases and controls (***Table 1***). It is important to note that AD and AUD are used interchangeably throughout this dissertation, given samples were obtained from individuals diagnosed with AD prior to the merging of AD and alcohol abuse into the DSM-V's AUD diagnosis [6].

Samples (n=35)	18 Cases; 17 Controls
Age	56 ± 9.6
Sex	100% Male
Brain pH	6.59 ± 0.22
Brain Weight (g)	1413.6 ± 121.25
PMI	29.8 ± 12.47
RIN	PFC = 4.51±2.04; NAc = 6.85±0.84
Hemisphere	0 = left; 1 = right
Neuropathology	0 = normal, 1 = abnormal
Hepatology	0 = normal; 1 = abnormal; 9 = N/A
Toxicology	0 = normal; 1 = alcohol; 2 = other drugs; 9 = N/A
Smoking Status	0 = never; 1 = smoker; 2 = ex-smoker; 9 = N/A

Table 1: Sample demographics and covariate dummy coding.

1.1.1) Study 1: Network preservation reveals shared and unique biological processes associated with chronic alcohol abuse in NAc and PFC.

The aim of this study to is to explore differentially expressed gene (DEG) networks associated with AD and their respective regulatory mechanisms (miRNA interactions or genetic variation) within two separate regions of the MCL, the PFC and NAc. More importantly, we sought to identify biological processes enriched within these gene networks that are shared or unique between the PFC and NAc. DEGs associated with AD were clustered into co-expressed gene networks via weighted gene co-expressed network analysis (WGCNA). We then performed a network preservation analysis to determine which of these gene networks show strong or weak levels of conservation between brain regions. Using the same analytical approach, we identified differentially expressed miRNA networks and interrogated their role in regulating AD significant mRNA networks at both the network and individual transcript level. Next, the potential impact of genetic variation on hub gene and miRNA expression was explored via expression quantitative trait loci (eQTL) analysis. Significant findings were interpreted within the current understanding that functional specialization differences between evolutionarily newer PFC and older, more conserved NAc contribute to different aspects of the proposed cycle of addiction [7]. Based on previous research, we hypothesized that we would see shared expression changes among immune response mechanisms between brain regions [8] and that neurosignalling pathways will show more region-specific changes based on known differences of cell composition between the cortical and subcortical brain regions [9].

1.1.2) Study 2: Identifying a novel biological mechanism for alcohol addiction associated with circRNA networks acting as potential miRNA sponges in the nucleus accumbens of chronic alcohol users.

This pilot study provides the first look into circRNA expression in the human brain and its potential role in regulating DEGs associated with AD. While circRNA can impact the expression of genes through various mechanisms, we focus on their role as miRNA sponges. For this analysis, we follow an analytical pipeline similar to the previous study. Differentially expressed circRNA associated with AD are partitioned into co-expressed networks via WGCNA and significant hubs are extracted for downstream analyses to identify meaningful circRNA:miRNA:mRNA interactions. Significant circRNA:miRNA:mRNA interactions within the framework of the miRNA sponge hypothesis were explored via a series of statistical and bioinformatic tests including correlation, non-coding RNA (ncRNA) target prediction, and moderation regression. Additionally, we determined whether genetic factors have a significant impact on the expression of circRNA hubs via (eQTL) analysis. Finally, we interrogated the clinical relevance of significant eQTLs by assessing their overlap with recent GWAS of smoking and AUD. As mentioned previously, this study is the first to identify significant circRNA networks associated with AD and outlines their roles as miRNA sponges that can potentially regulate the expression of DEGs in a disease-specific manner. We hypothesized that these results would show significant miRNA sponge interactions enriched for neurobiological processes based on the understanding that circRNA are abundantly and dynamically expressed in the brain [10].

1.2) CONSIDERATIONS

We acknowledge that the postmortem brain samples used for this research are representative of a unique and very specific demographic of alcohol users: individuals diagnosed with severe AD after years of chronic alcohol abuse. That being said, we must be careful in interpreting the causal nature of the reported results. It is difficult to know if expression changes are predictive of AUD or in response to chronic alcohol consumption over years. To combat this, we integrate genotypic information via eQTL analysis to isolate potential genetic risk factors for AUD that might help us make inferences about causality. Even though these results primarily represent biological shifts in the brain that occur in response to ethanol activity, the scientific and clinical value of this dissertation is not diminished because differentially expressed mRNA, miRNA, and circRNA can still serve as potential biomarkers for AUD by revealing dysregulated biological processes underlying alcohol-facilitated synaptic plasticity and conditioning that further reinforce alcohol abuse and relapse.

CHAPTER 2

BACKGROUND

2.1) Alcohol Use Disorder (AUD)

AUD is a debilitating psychiatric illness with negative health, economic and social consequences affecting nearly 15.1 million adults worldwide [11, 12]. AUD specifically is diagnosed in individuals who meet two or more of the DSM-V criteria over the course of one year, with severity (mild, moderate, and severe) determined based on the number of criteria endorsed [13]. As mentioned previously, the DSM-IV defined diagnoses of AD and alcohol abuse were combined in the DSM-V to form a single AUD diagnosis based on the belief that alcohol dependence and abuse are not mutually exclusive; often times dependence cannot exist without abuse and vice versa [6]. Depending on specific individual differences, the dangers of chronic alcohol use are enhanced by ethanol's qualities as a highly addictive substance [14]. The framework for understanding how recreational alcohol use transitions to AUD follows various models of addiction [7]. Specifically, it is believed AUD development follows three distinct stages of addiction, each with their own hypothesized neurobiological mechanisms: binge/intoxication; withdrawal/negative affect; and preoccupation/anticipation (i.e. craving) [15]. Within this cyclical model of addiction, two brain regions, the PFC and NAc, are believed to play different roles in the development of AUD as part of the larger MCL [16, 17]. Specifically, the PFC is important for executive functioning and has been linked to the preoccupation/anticipation stage, whereas NAc based allostatic conditioning of reward response is associated to both binge/intoxication and withdrawal/negative affect [7]. While the current model of alcohol addiction is useful for

understanding neuroanatomical correlates of the broader behavioral adaptations associated with AUD, most of the molecular underpinnings for these functional processes remain unknown.
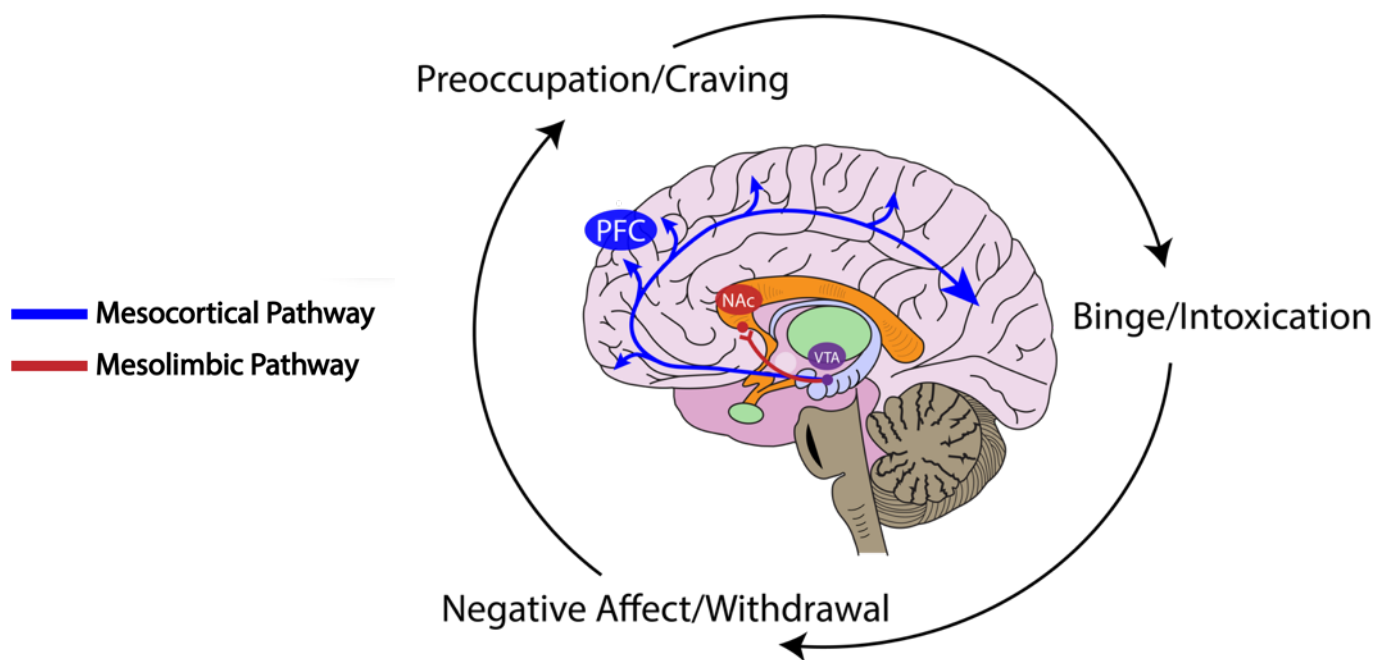
Figure 1: The mesocorticolimbic system and cycle of addiction. Visual representation of the dopaminergic mesocortical and mesolimbic pathways connecting the VTA to the PFC and NAc as well as an outline of the three stages of addiction as proposed by Koob and Volkow [18].

2.2) Mesocorticolimbic System and AUD

Chronic alcohol use, and more specifically AUD, leads to widespread damage to vital organs as the body constantly metabolizes ethanol, effectively increasing the risk of liver disease and cardiomyopathy [19]. In addition to affecting digestive and cardiovascular systems, ethanol and its metabolites have a substantial impact on brain chemistry and associated neurobiology. The MCL, connecting the ventral tegmental area (VTA) to the PFC and NAc (*Figure 1*), has proven especially susceptible to alcohol associated neuroadaptations [20, 21]. The functional specialization of the MCL in conjunction with postmortem brain research can link alcohol sensitive neurobiological mechanisms to AUD specific behaviors. For example, alcohol facilitated

disruption of the PFC can result in an impaired response inhibition, a hallmark of addictive behaviors [22]. In contrast, positive reinforcement mechanisms of reward seeking is regulated by the mesolimbic pathway via increased firing rates of dopaminergic neurons within the VTA and NAc [23]. Over time, alcohol induced mesolimbic conditioning and dysfunction can lead to increased incentive salient (wanting) behaviors and the development of AUD [15]. Alcohol associated dysfunction of the MCL creates the complex behavioral network that reinforces alcohol cravings based on emotional memory processing, reward conditioning, and a lack of impulse inhibition regardless of negative health or social consequences [24]. Little is known about the molecular mechanisms underlying these functional processes or if these mechanisms are conserved between cortical and subcortical MCL structures. Thus, the goal of ***Study 1*** is to elucidate the predicted biological function associated with DEG networks shared or unique to the PFC and NAc.

2.3) **Molecular Targets of Alcohol**

Ethanol, the main alcohol present in wine, spirits and beer, is a relatively simple two-carbon molecule (C_2H_5OH) which primarily interacts with other biomolecules via weak hydrophobic interactions and hydrogen bonding [25]. Unlike other drugs of abuse, alcohol lacks specificity in its neuronal binding profile and is easily able to traverse cell membranes, interacting directly or indirectly to both intercellular and intracellular molecular targets [26]. The most commonly understood direct molecular targets for ethanol is alcohol dehydrogenase (ADH) and aldehyde dehydrogenase (ALDH) which are responsible for the primary and secondary oxidization of alcohol into its respective aldehydes and ketones [27]. While ADH facilitated alcohol metabolism predominantly occurs in the liver, alcohol in the brain is converted into acetate by the catalase and cytochrome P450 2E1 (CYP2E1) enzymes [28]. Among the proteins responsible for ethanol

metabolism, genes within the ADH cluster along with ALDH2 have been robustly associated with AUD in multiple genome-wide association studies (GWAS) [29–31]. These single nucleotide polymorphisms (SNPs) have been shown to lead to deficits in alcohol metabolism, effectively serving as a protective factor for AUD by increasing the negative side effects of alcohol consumption [32].

Direct and indirect ethanol targets in the brain are much more ambiguous and centered around proteins primarily associated with synaptic transmission and plasticity. More specifically, two types of signaling pathways have been shown to be important for regulating addictive behaviors through either reinforcing excessive drinking, craving and relapse ("go" pathways) or protecting against excessive activation of the go-pathway ("stop" pathways") [33]. The "go pathway" in the brain is primarily mediated by the activity PKA (protein kinase A), FYN (tyrosine kinase fyn), and HRAS. Alcohol leads to activation of PKA through interacting with adenylyl cyclase (AC) which in turn leads to the increased activation of adenosine and dopamine G_sa-coupled protein receptors ($A_{23}R$ and DR1 respectively) [34]. FYN is activated through the phosphorylation and subsequent inactivation of STEP by PKA, resulting in enhanced NMDAR and CaMKII mediated AMPAR activity [35–37]. Alcohol also indirectly impacts HRAS via interactions with PKA and RAS-specific guanine nucleotide-releasing factor 1/2 (RAS-GRF1/2) [38, 39]. HRAS activation begins a downstream signaling cascade to various proteins (ERK1/2, mTORC1, and AKT) that support the transcription/translation of genes associated with microtubule assembly and postsynaptic density organization [34]. In summary, alcohol associated activation of the "go" signaling pathway results in altered synaptic plasticity resulting from the conditioning of reward response and emotional memory processing as individuals experience positive affect while drinking followed by negative affect during withdrawal. This cycle, thus, reinforces continued/excessive alcohol consumption and relapse. The "stop" pathway is important

for regulating the over-activation of the go pathway mainly through the activity of BDNF/GDNF during periods of moderate, but not excessive alcohol consumption [33]. While the exact mechanism by which this pathway regulates excessive alcohol consumption is relatively unknown, evidence from animal models show that moderate drinking leads to increased BDNF expression [40, 41], with other experimental studies indicating that either the overexpression or knockout of BDNF can lead to decreased or increased alcohol consumption respectively [42, 43]. Overall, it is believed that individual differences in respect to the activity/expression of these neurotropic factors is important for determining why some people who drink to excess develop AUD, when others do not [44]. Within the context of this research, we are interested in exploring if the dysregulation of these neuronal mechanisms/pathways primarily studied in animal models are translatable to the postmortem brain transcriptome of chronic alcohol abusers.

2.4) Utility of Human Postmortem Brains

It is important to study the molecular consequences of chronic alcohol abuse in etiologically relevant brain tissue so we can better understand the complex biological underpinnings of AUD. While proxy tissues such as model organisms, blood, or cell cultures have been used to understand the molecular underpinnings of substance use disorders, they provide little explanation for the complex behavioral adaptations we often associate with addiction in humans. Within the context of AUD, none of these models recapitulate the complexity of neurophysiological changes that occur after chronic alcohol use or how the complex interaction of genetic and environmental factors can help predict neurobiological outcomes. The human brain is characterized by relatively high levels of expression when compared to other non-neuronal tissues [45, 46] and/or the brains of mammalian model organisms [47–50]. Additionally, the observed transcriptome complexity is

greater within the human brain, which is reflected by higher levels of alternative isoforms and an increased magnitude of alternative splice events when compared to other tissue types [51–53].

The complex nature of assessing specific psychological symptoms associated with AUD is not easily translatable to model organisms. For instance, animal studies rely on loose behavioral models to simulate desired phenotypes [54] which does little to recapitulate the internalizing and externalizing symptoms that promote relapse during periods of withdrawal [55]. While some models have been validated though extensive research, e.g. stress-based tests for modeling anxiety like behaviors [56–58], there are limited paradigms for modeling impulsivity and other personality based risk factors for AUD and other SUDs [59]. Additionally, the lack of meaningful model systems for replicating the complex behaviors associated with AUD is exacerbated by an often co-morbid psychiatric diagnosis among chronic alcohol abusers [60]. With that being said, our current understanding of the molecular underpinnings of addiction and AUD are derived primarily from model organisms. This is due to the increased experimental control within model systems [61] and the overall limited availability of postmortem brain tissue from AUD cases [62]. Here, the transcriptome is profiled at multiple levels (circRNA, miRNA, and mRNA) within etiologically relevant postmortem brain tissue to yield novel findings about the molecular underpinnings of AUD previously unexplored in proxy tissues.

2.5)   Utility of Gene Expression Studies

Among the cascade of biological changes important for disease development, gene expression serves as an important biological intermediate between genetic predisposition and protein function. Most modern approaches for assessing gene expression are adapted from methodology used for identifying sequence variation within a targeted loci [63]. For decades, the

"gold" standard approach for targeted gene expression analysis and experimental validation of microarray and RNA-seq has been reverse-transcriptase quantitative PCR (RT-qPCR) [64]. RT-qPCR works by converting RNA to complementary DNA (cDNA) through the use of a reverse transcriptase which can be quantified via PCR by comparing the exponential growth of amplification against a stable "housekeeping" gene [65]. With advancements in genome-wide sequencing technologies, methods for quantifying gene expression have evolved in parallel. Among the most predominantly used methods of assessing genome-wide expression levels (microarray and RNA-seq) here, microarray is used to assess transcript abundance at three different levels (circRNA, miRNA, and mRNA). Gene expression microarrays are based on the principles of cDNA synthesis and nucleic acid hybridization to assess the expression of thousands of transcripts in parallel [66]. Once gene expression has been quantified, researchers employ a variety of network based approaches to meaningfully interpret differential expression [67]. WGCNA is one of the most commonly used network based methods in which large sets of DEG are partitioned into modules containing transcripts with correlated expression [68]. From these co-expressed modules, researchers are able to identify gene networks enriched for biological processes relevant to the phenotype of interest [69], as well as isolate highly intramodular connected hub genes, which serve as predicted drivers of expression for entire modules [70]. Finally, gene expression has the additional benefit of providing potential functional explanations for diseases associated genetic variants identified in GWAS via eQTL mapping [71]. In eQTL studies, gene expression levels treated as quantitative traits are mapped to genetic variants either within 500kb of the transcription start site (cis-eQTL) or across the entire genome (trans-eQTL) [72]. While the utility of gene expression goes beyond what is presented here, this dissertation utilizes microarray, WGCNA, and cis-eQTL analyses to gain insight into the molecular underpinnings of AUD within the postmortem brains of chronic alcohol abusers.

2.6) Gene Expression and AUD

Transcriptomic profiling of postmortem brains can provide valuable insight into the biological consequences of chronic alcohol abuse while also providing functional explanations for genetic variants associated with AUD. While most studies observe relatively small fold changes when comparing expression differences between AUD cases and controls, about 20-50% of the transcriptome is differentially expressed [73]. Because of small effect sizes, gene expression studies have limited power to interpret the importance of individual genes in respect to AUD etiology. Network based approaches such as WGCNA, however, aggregate related genes into co-expressed networks to allow for the identification of specific biological processes that are dysregulated in the postmortem brains of chronic alcohol abusers [68, 74–76]. Studies show the most notable DEG networks associated with AUD are linked to immune/stress response, synaptic plasticity, and neurotransmission. More specifically, studies from our lab and others have shown that immune/inflammatory genes are upregulated throughout the brain of chronic alcoholics, which is believed to be a product of the cellular response to ethanol's neurotoxic properties [74, 77]. While our understanding of how immune/stress response reinforces addictive behaviors is limited, it is suggested that stress-induced signaling is important for the negative affect states often associated with withdrawal, thus leading to conditioning that promotes relapse [8].

Aside from immune response mechanisms, we see the dysregulation of genes important for synaptic transmission and neuroplasticity. Multiple studies have shown decreased expression of $GABA_A$ and $GABA_B$ subunits within the hippocampus and PFC of alcoholics [78, 79]. GABAergic receptors play an important role at each step in the previously mentioned cycle of addiction by regulating reward response in the NAc and hippocampus [80]. Ionotropic and metabotropic glutamate receptors, as previously mentioned, are important for the development of AUD through

modulating the release of dopamine during periods of intoxication, leading to the formation of alcohol dependent synaptic connections [81]. Postmortem brain studies have shown the significant upregulation of NMDAR and AMPR subunits in the PFC of individuals diagnosed with AD [78, 82]. The same study [82] also identified increased expression of genes (*GIPC1* and *MIB2)* involved in the trafficking and ubiquitination of NMDAR subunit 2B [83, 84]. Ethanol's ability to promote glutamate activity in the brain at NMDAR and AMPR is important for neurogenesis that promotes relapse and continued alcohol abuse despite negative consequences [85]. This dissertation builds upon these recent findings by determining transcriptome changes associated with AUD that are either conserved or unique to the PFC and NAc.

2.7) MiRNA Biogenesis and Function

Another class of molecules that have been extensively studied using postmortem brain tissue from cases with various neuropsychiatric and substance use disorders (SUDs) are miRNA. These are small non-coding RNA (≈22 base pair), the biogenesis of which is a three-step process starting in the cell nucleus and ending with the generation of the mature miRNA in the cytoplasm [86]. The primary miRNA transcript measuring over 1kb in length is cleaved in the nucleus to form an intermediate molecule called precursor miRNA (pre-miRNA). The pre-miRNA is exported to the cytoplasm, where it is further cleaved and loaded onto the RNA-Induced Silencing Complex (RISC) to generate the mature miRNA sequence [87]. Most miRNA regulate gene function negatively through imperfect binding with the 3' untranslated region (3'UTR) of mRNA [88, 89]. Animal miRNAs pair with 3'UTR of their target genes though the "seed" region (consisting of nucleotides 2-7) at the 5' end of the mature strand. Depending on homology, miRNA can impact an mRNA target either through degradation or translational inhibition [90]. It has been estimated

that miRNAs may influence as much as 30% of the human transcriptome [91]. MiRNA further contribute to the transcriptome complexity of the brain. Aside from being highly enriched in the brain [92, 93], miRNAs have been shown to be potential biomarkers for psychiatric disorders and more specifically AUD [94, 95]. Our lab and others have made strides in profiling miRNA expression and identifying co-expressed miRNA-mRNA networks within the postmortem brains of chronic alcohol users [74, 96]. These studies combined with studies from animal models have revealed alcohol associated dysregulation of miRNAs with mRNA targets important for immune response and synaptic function [97, 98]. Here we attempt to expand upon this previous research by comparing AD significant mRNA:miRNA interaction networks between brain regions (NAc vs. PFC) to better understand how miRNA regulate addiction related biological processes. Additionally, we explore miRNA within the framework of circRNA:miRNA:mRNA interactions to provide a regulatory mechanism for genes associated with AUD.

2.8) Circular RNA

With the recent technological advancements in the study of transcriptomics circRNA have emerged as important ncRNA with implications for gene regulation and disease. CircRNA are unique from miRNA and most other ncRNA in that they form circular secondary structures, resulting in increased stability [99]. The biogenesis of circRNA consists of spliceosome-mediated canonical splicing followed by backsplicing of pre-mRNA in which the 5' and 3' ends of spliced exons/introns are covalently bonded to form a closed end loop structure [100]. CircRNA have been reported to alter the expression of their host mRNA as well as the expression of distal genes through various mechanisms [10]. **Study 2** focuses solely on the mechanism by which circRNAs act as miRNA sponges in order to alter the expression of target genes in a disease dependent

manner. As mentioned previously, miRNA can lead to the translational repression and/or degradation of target mRNAs by interacting with the 3'UTR [101]. CircRNA act as a competitive endogenous RNA (ceRNA) by sequestering homologous miRNAs that would otherwise interact with their target mRNA, effectively increasing the expression of the target gene [102]. Within the context of AUD and other neuropsychiatric disorders, circRNA is of particular interest for researchers based on their dynamic and abundant expression within the mammalian brain [103]. Additionally, the transcriptional landscape of circRNA in the brain is more diverse relative to other tissues, with one study identifying 141 of the 339 profiled circRNA were unique to the cerebral cortex [104]. Among these circRNA, several are derived from host genes important for neuronal function that have been significantly associated with alcohol use in previous studies (*HOMER1*, and *NTRK2*) [105, 106]. Given the study of circRNA is still in its infancy, researchers do not fully understand how circRNA interact with neurobiological systems to contribute to the etiology of AUD and other psychiatric disorders. While differentially expressed circRNA have been associated with both alcoholic liver disease and cardiomyopathy in animal models [107−109], to the best of our knowledge, ***Study 2*** provides the first profiling of circRNA expression in the postmortem brains of chronic alcohol abusers. More specifically, this dissertation provides the framework for investigating circRNA networks associated with chronic alcohol abuse and their predicted function in regulating AUD risk genes via miRNA sponge interactions.

CHAPTER 3

STUDY 1: *Network preservation reveals shared and unique biological processes associated with chronic alcohol abuse in NAc and PFC.*

3.1) INTRODUCTION

AUD is a debilitating psychiatric illness with negative health, economic, and social consequences for nearly 15.1 million affected adults worldwide [12]. AUD risk is dependent upon both genetic and environmental factors, with a heritability of 0.49 [110]. The neurobiological framework for understanding how benign, recreational alcohol use leads to AUD follows various hypotheses [34, 111, 112], with the most commonly accepted being the cyclical model of addiction [18]. This hypothesis provides valuable insight into the functional specialization of different brain regions that underlie behavioral maladaptations associated with AUD [15]. However, the genetic architecture and molecular mechanisms contributing to alcohol-facilitated neuroadaptations remain widely unknown.

Postmortem brain studies provide the unique opportunity to interrogate neurobiological changes associated with addiction across brain regions and neural pathways [113, 114]. Among these, the MCL, which connects the VTA to the PFC, and NAc, has proven especially sensitive to alcohol-associated neuroadaptations [16, 17, 115]. Recent postmortem brain studies of AUD have focused on examining gene and miRNA expression as the biological intermediate between genetic variation and molecular function [74–76, 116–119]. Studying mRNA and miRNA interactions may also reveal functional relationships that mediate the differential expression of risk AUD genes based on the role miRNAs play in the destabilization and degradation of their target genes [101].

While single gene expression differences are continuously explored, network approaches, such as WGCNA, allows genes with correlated expression, and therefore likely related functions, to cluster into modules that then can be analyzed to identify dysregulated biological processes and molecular pathways associated with AUD [120]. Others and we have successfully implemented this method to identify gene networks associated with AUD within the MCL and other brain regions [74, 75]. While postmortem brain expression differences alone are insufficient to infer a causal relationship between AUD and neurobiological function, the integration of genetic information via eQTL analysis can help elucidate the regulatory mechanisms by which genetic variants associated with AUD impact gene expression [121].

Thus, in this study, we seek to expand upon previous research by jointly analyzing two key MCL areas, the NAc and PFC, to identify unique and shared neurobiological processes associated with AD. To achieve this, we utilize a case/control study design to identify genes and co-expressed gene networks associated with AD. We then performed a network preservation analysis to determine how well significant modules and their respective biological processes are conserved between the PFC and NAc of chronic alcohol abusers. Within the significant modules, we identified the most connected genes (termed hubs), which were then integrated with miRNA expression data analyzed using the same methodological framework. Finally, we assessed the genetic factors that might impact the functions of risk AD genes via eQTL. The miRNA and eQTL analyses were performed in order to identify the regulatory mechanisms by which gene networks identified in PFC and NAc contribute to alcohol addiction.

3.2) MATERIALS AND METHODS

3.2.1) Tissue Processing and RNA Extraction

Postmortem brain tissue from 41 AD cases and 41 controls was provided by the Australian Brain Donor Programs of New South Wales Tissue Resource Centre (NSW TRC) under the support of The University of Sydney, National Health and Medical Research Council of Australia, Schizophrenia Research Institute, National Institute of Alcohol Abuse and Alcoholism, and the New South Wales Department of Health [113]. Samples were excluded based on: (1) history of infectious disease, (2) circumstances surrounding death, (3) substantial brain damage, and (4) post-mortem interval > 48 hours. Total RNA was isolated from PFC (the superior frontal gyrus) and NAc tissue using the mirVANA-PARIS kit (Life Technologies, Carlsbad, CA) following the manufacturer's suggested protocol. RNA concentrations and integrity (RIN) were assessed via Quant-iT Broad Range RNA Assay kit (Life Technologies) and Agilent 2100 Bioanalyzer (Agilent Technologies, Inc., Santa Clara, CA) respectively. Samples were matched for RIN, age, sex (all male), ethnicity, brain pH, and post mortem interval (PMI) as part of a previous study [74] yielding a total of 18 case-control matched pairs (n=36). Due to our matching, the RINs in PFC were slightly lower (mean=4.5, ±2.04) compared to NAc (mean=6.9, ±0.84). Previous reports, however, have demonstrated that in post-mortem brain studies reliable results are readily obtained even with RINs ≤4 [122]. For demographic information see **_Appendix I_**.

3.2.2) Gene Expression Microarray and Data Normalization

Gene expression was assayed using Affymetrix GeneChip Human Genome U133A 2.0 (HG-U133A 2.0) on 22,214 probe sets spanning ~ 18,400 mRNA transcripts, and the Affymetrix GeneChip miRNA 3.0 microarray interrogating the expression of 1733 mature miRNAs as previously described [123]. None of the mRNA or miRNA probes were excluded based on quality control criteria outlined in previous studies [74]. Raw probe data were GCRMA background

corrected, log$_2$ transformed, and quantile normalized using Partek Genomics Suite v6.23 (PGS; Partek Inc., St. Louis, MO) to obtain relative gene expression values. A principal component analysis was used to identify potential outlier samples. Only one case sample was removed from the analyses, leaving 18 controls and 17 cases (n= 35) for both brain regions. It has become widely accepted to verify a subset of microarray-generated gene expression changes via an independent platform such as qPCR. Considering limited tissue availability and our extensive use of the Affymetrix platform in the past, we did not include microarray validation in this study which is similar to what other groups have done in the past [124]. We have previously 'validated' the same array and platform in independent qPCR experiments with a concordance between microarray and qPCR platforms exceeding 80% in the past [74].

3.2.3) Analysis of Differential Gene Expression

The relationship between AD case status and gene expression in PFC and NAc was analyzed via bidirectional stepwise regression for each gene. This approach is better suited to adjust for the confounding effect of covariates within each transcript's regression model than the robust linear regression approach employed previously in the analyses of NAc [74]. The gene expression analysis between our AD cases and matched controls was performed in RStudio (ver. 1.1.463) with the Stats package (ver. 3.5.1) using a bi-directional stepwise regression model for both mRNA and miRNA normalized expression data generated from NAc and PFC. The bidirectional stepwise regression analysis cycles through all available covariates (i.e. age, RIN, pH, PMI, brain weight, hemisphere, toxicology, hepatology, neuropathology, and smoking) to identify the best-fitting model with the lowest Akaike information criteria (AIC) for each transcript (Mean AIC: NAc= -129.10, PFC= -71.07). We further observed that brain pH, RIN, and neuropathology were the

most influential covariates in the analyses of NAc expression data, while RIN and smoking history were the two most important covariates in the PFC expression analysis. Finally, we assessed proportion of variance explained by each covariate via the variancePartition package (ver. 1.20) [125].

3.2.4) Network Analyses

WGCNA was performed using the WGCNA package in RStudio (ver. 1.66). All nominally significant genes (p≤0.05) were used to generate a signed similarity matrix via pair-wise Pearson correlations. The nominal significance was chosen to (1) include genes with smaller effect sizes, albeit true positive signals, (2) exclude genes with low disease variance, i.e., likely not associated with AD and (3) to provide a sufficient number of genes for the network analysis. In the WGCNA, our similarity matrix was raised to a power (mRNA β = 14; miRNA β = 6) to approximate the scale-free topography of the adjacency matrix, in which stronger correlations are emphasized over weaker ones. Transcript interconnectedness was determined from the calculated topological overlay measure (TOM). The default, unsupervised hierarchical clustering method was used to partition modules at specified dendrogram branch cut sites using the Dynamic Tree Cut method. Highly correlated modules were then merged based on minimum merge height of r^2 = .8 and minimum module size of 35. Conventional colors were used to categorically label co-expressed networks and the sum of relative expression within each module is represented as a single value (module eigengene (ME)) for downstream phenotypic analysis.

MEs were correlated to AD case-status and available demographic/biological covariates. To validate WGCNA module clustering, we performed a bootstrap based resampling of 100 iterations with replacement. Next, using WGCNA with the clusterRepro (ver. 0.9) package in

RStudio, we identified the level of module preservation between the PFC and NAc by comparing adjacency matrices and calculating the composite preservation statistic ($Z_{summary}$). A $Z_{summary}$ >10 indicates strong evidence for network preservation, $Z_{summary}$ <10 >2 indicates weak evidence of network preservation and $Z_{summary}$ <2 indicates no module preservation, as outlined previously [126].

3.2.5) Gene Set Enrichment Analysis

Gene set enrichment was performed using ShinyGo (ver. 0.61) gene annotation database [127]. Gene lists from the significant AD modules from NAc and PFC were enriched using GO biological processes consisting of 15,796 gene sets from the Ensembl BioMart release 96; all p-values for significantly enriched gene sets are false discovery rate (FDR) adjusted (FDR of 5%). We further performed cell type enrichment using the "*userListEnrichment*" option within the WGCNA package in R (ver. 1.66) as previously described [74]. Statistical significance of brain-list enrichment was determined via a hypergeometric test; all p-values were adjusted at FDR of 5%.

3.2.6) Hub Gene Prioritization

Hub genes were defined based on the strength of intramodular connectedness, (also referred as module membership (MM)) calculated from the absolute value of the Pearson's correlation coefficient between ME and expression values. Hub genes were prioritized for downstream analysis based on MM of r≥0.80 and a significant gene correlation with AD (at p ≤0.05).

3.2.7) eQTL Analysis and GWAS/GTEx Enrichment

DNA from the postmortem brain sample was processed and genotyped as part of a larger GWAS study [74]. Genotypes with excessive missingness (greater than 20%) and monomorphic for homozygous major and minor alleles were removed. We then selected only, local, cis-eQTLs, defined as SNPs 500kb from the start/stop positions for each hub gene. Such selected SNPs were pruned with Plink v1.9 to exclude variants in linkage disequilibrium (LD) ($R^2 \geq 0.7$). For eQTL detection, SNP effect on hub gene expression was analyzed via MatrixEQTL package (ver. 2.2) in R using a linear regression model adjusting for covariates. To identify potential disease risk eQTLs, we further tested for an interaction (SNP x AD) term between genotype and AD status using the "*modelLINEAR_CROSS*" argument. A significant genotype/disease interaction for a SNP/gene pair would indicate that the effect of genotype on expression is significantly different in AD cases versus controls. To determine the overlap between the eQTLs in our sample (at $p \leq 0.002$) and significant GWAS hits (at $p \leq 1E-4$) from previously reported alcohol and smoking GWAS [128, 129], we employed the Simes enrichment test [130]. We further tested the overlap between eQTLs obtained from our analyses against eQTLs obtained from GTEx consortium [131]. The significance of this overlap was assessed via a Fisher's exact test at $p \leq 0.05$ threshold. See ***Appendix II*** for a detailed description of GWAS and GTEx enrichment.

3.2.8) mRNA/miRNA Target Prediction

The relationship between significant miRNA and mRNA modules from each brain region was examined by performing a Pearson's correlation on the miRNA and mRNA module MEs using the Stats package (ver. 3.5.1) in RStudio. Significant miRNA/mRNA ME correlations (at FDR of 5%) were followed up with a more detailed series of analyses, in which individual mRNA

hub and miRNA expression was correlated via Pearson's correlations using the miRLAB package in R (ver. 1.14.3).

3.3) RESULTS

3.3.1) AD Case/Control Differentially Expressed Genes (DEG)

A bidirectional stepwise regression revealed 3,536 and 6,401 DEGs in PFC and NAc, respectively, at the nominal p ≤0.05, of which 1,279 DEG were shared between the two regions (*Figure 2A/B*). Among these, 603 and 494 genes were downregulated and upregulated, respectively, and 182 genes were expressed in opposite directions between the two regions. Within the DEGs in NAc, nine genes (*ADH1B, ADH1C, H2AFZ, EIF4E, FTO, DRD2, SLC39A8*, and *VRK2*) were implicated in the largest and most recent AD GWAS [31]. At FDR of 5%, we identified 1,841 DEG from the NAc and 70 from the PFC. The miRNA regression analysis identified 430 and 170 nominally significant miRNAs in the NAc and PFC, respectively, with 168 miRNAs differentially expressed in NAc at FDR of 5% with no miRNA reaching FDR significance in PFC. To maintain an identical analytical pipeline for both brain regions and optimize the selection for the most influential confounding factors, we co-jointly analyzed the PFC expression data generated in this study with our previously published NAc expression data [74]. We observed a highly significant overlap between the DEGs identified in NAc from both studies (Fisher's exact test, $p=1E-10$). When we assess each covariate's contribution to the overall gene expression variance, we see that the impact of any given covariate is highly variable depending on the gene (*Figure 2C/D*). This helps validate our approach for utilizing a different set of covariates for each gene's regression model in order to control for confounds that contribute to the highest proportion of the variance.
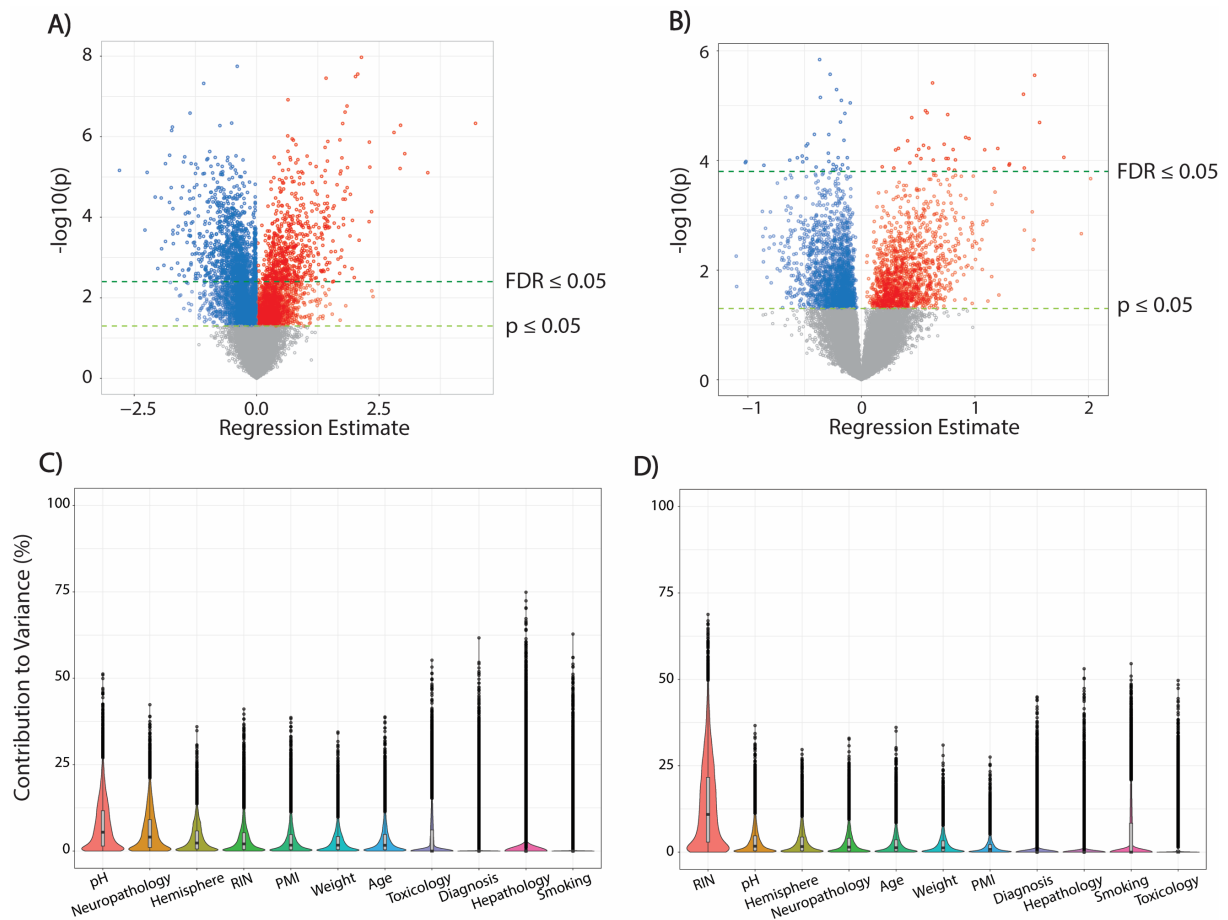
Figure 2: Volcano plots and variance partitioning of differentially expressed mRNA from NAc and PFC. *A*) NAc regression analysis reveals 6,401 DEG at the nominal p≤0.05 and 1,841 after FDR 5% correction. *B)* PFC regression shows 3,536 DEG at p≤0.05 and 70 after FDR 5% correction. Violin plot of each covariate's percent contribution to the variance for NAc (*C*) and PFC (*D*) gene expression.

3.3.2) mRNA Gene Network Module Clustering

In NAc, at a Bonferroni adjusted p≤0.05, we identified 6 modules significantly correlated with AD case status (**Figure 3A**). Among these, NAc$_{darkgreen}$ was the only negatively correlated module, whereas NAc$_{darkorange}$, NAc$_{purple}$, NAc$_{magenta}$, NAc$_{skyblue}$, and NAc$_{greenyellow}$ were all positively correlated with AD cases relative to controls (**Figure 3B**). In PFC, we identified 3 modules significantly correlated to AD at Bonferroni adjusted p≤0.05 (**Figure 3C**). Of these, the PFC$_{pink}$ module was negatively correlated, while PFC$_{darkred}$ and PFC$_{lightgreen}$ were positively correlated with AD cases (**Figure 3D**). To assess the validity of these network modules, we performed a bootstrap resampling that showed consistent module clustering when compared to the original gene networks (**Figure 4**).
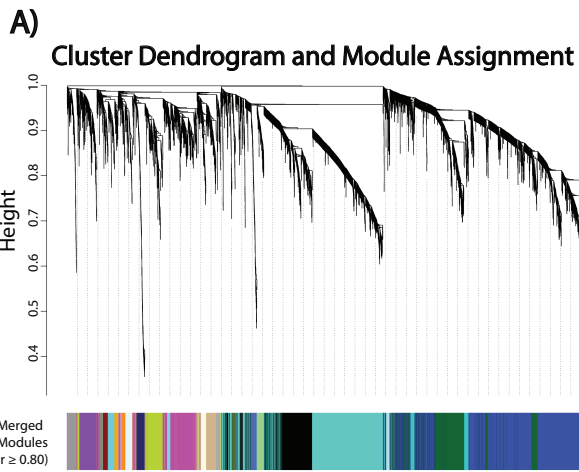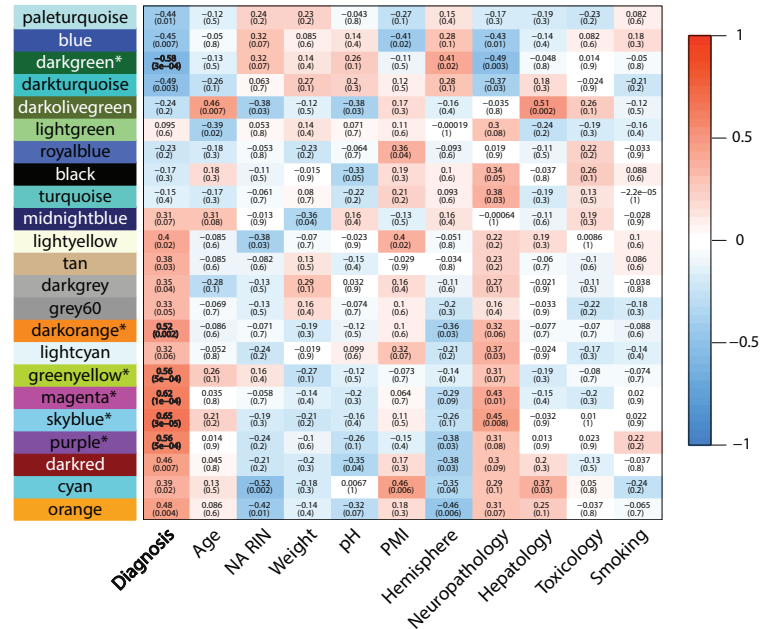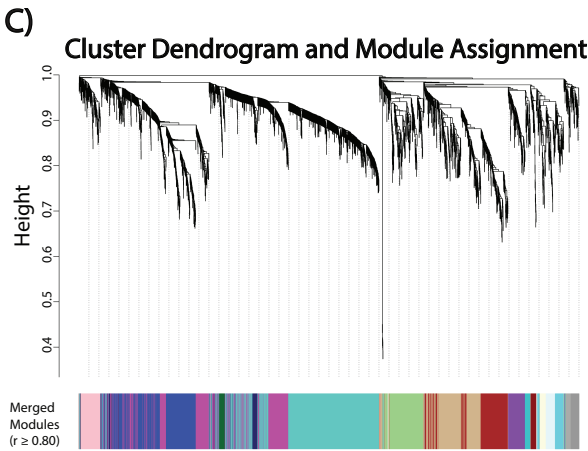
Figure 3: WGCNA clustering and module-trait relationships. A) NAc cluster dendrogram and module assignment with dissimilarity based on topological overlap. The 6,401 selected transcripts were clustered into 23 distinct modules. **B)** NAc module-trait relationship heatmap correlating (Pearson's) module MEs with AD diagnosis and covariates. Uncorrected p-values are given in parenthesis below each correlation coefficient. 6 AD associated significant modules (NAc$_{darkgreen}$, NAc$_{darkorange}$, NAc$_{greenyellow,}$ NAc$_{magenta}$, NAc$_{skyblue}$, and NAc$_{purple,}$) were identified after Bonferroni correcting p-values (*=p≤0.05). **C)** PFC cluster dendrogram and module assignment. The 3,536 selected transcripts were clustered into 17 different co-expressed modules. **D)** PFC module-trait relationship heatplot created as previously described. We identified 3 AD associated modules (PFC$_{pink}$, PFC$_{darkred}$, and PFC$_{lightgreen}$) after Bonferroni correcting p-values (*= p≤0.05).
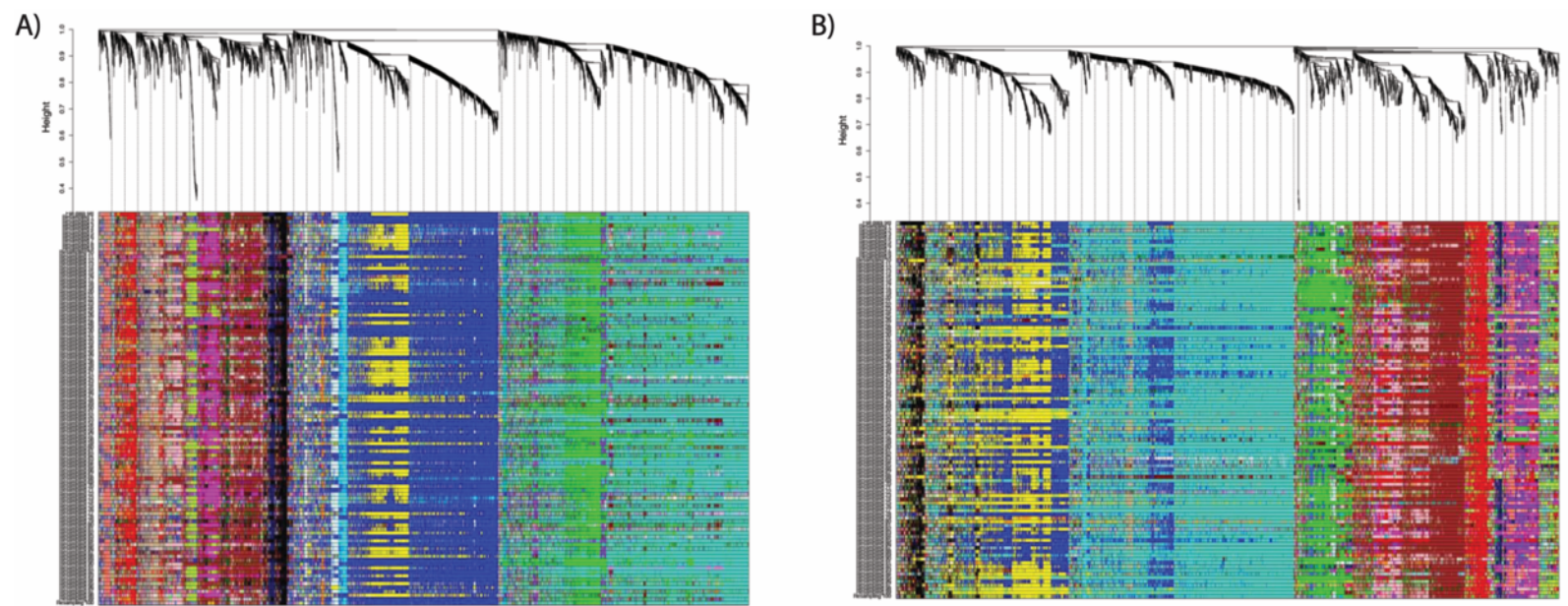
Figure 4 : Robust mRNA module clustering dendrogram. To ensure network robustness and minimize the potential effect of outlier samples on network structure, we used the robust 'bootstrapped' version of WGCNA (rWGNCA). We performed 100 iterations in which networks were created after randomly subsetting 2/3 of the total sample. The resulting 100 networks were merged into one large, final consensus network with the individual sub-networks showing reasonably high consistency with the final networks. *A)* NAc. *B)* PFC.

3.3.3) NAc and PFC Network Preservation

We performed a network preservation analysis to determine how well co-expressed networks from the PFC are conserved in NAc and vice versa. We focused primarily on the $Z_{summary}$ and *Median Rank* network preservation statistics because $Z_{summary}$ estimates network overlap by also taking into consideration network connectivity. *Median Rank* being invariant to module size, provides a more accurate estimate of network preservation since larger networks tend to be more conserved due to their size alone. We observed that NAc$_{darkorange}$ and NAc$_{purple}$ showed little to no network preservation ($Z_{summary}$ <2), NAc$_{skyblue}$, NAc$_{darkgreen}$, PFC$_{darkred}$, and PFC$_{pink}$ showed moderate levels of network preservation (2< $Z_{summary}$ <10), and NAc$_{greenyellow}$, NAc$_{magenta}$, and PFC$_{lightgreen}$ showed high levels of network preservation ($Z_{summary}$ >10) (**Figure 5A/B**). For detailed information about the individual density and connectivity statistics that were used to create the composite network preservation statistics, see the **Appendix III**.
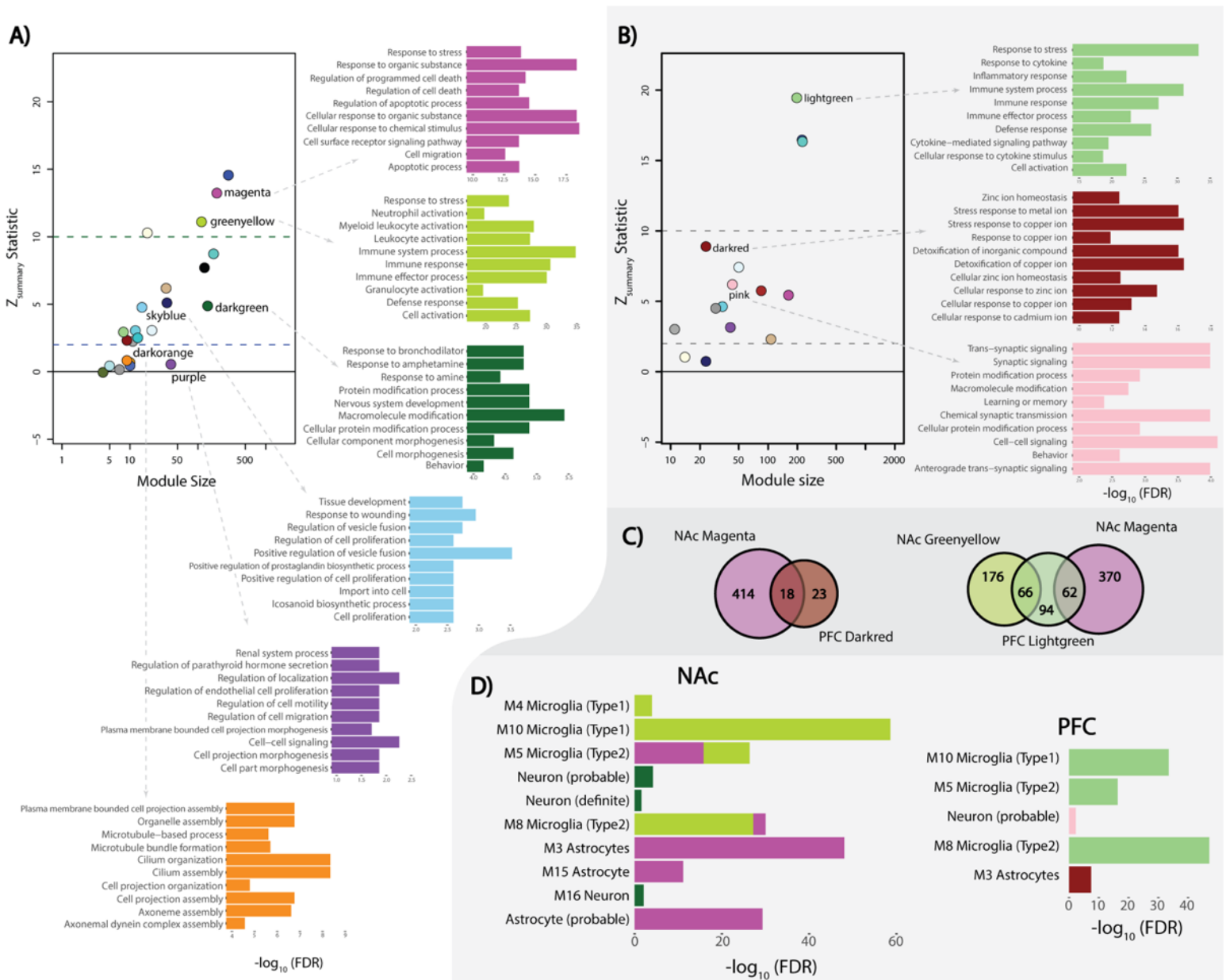
Figure 5: Network preservation and gene-set enrichment. *A)* NAc Z-summary statistic calculated as an aggregate of network preservation statistics (Preservation level: high = Z>10; moderate = 2<Z<10; low = Z<2) with color corresponded top-10 most significant (-$\log_{10}$(FDR) transformed) GO biological processes for significant AD associated modules. *B)* PFC Z-summary statistic and corresponding GO biological processes term (-$\log_{10}$(FDR) transformed). *C)* Venn-diagram of the shared transcripts from highly preserved NAc modules (NAc$_{magenta}$ and NAc$_{greenyellow}$) and their corresponding significant PFC modules (PFC$_{lightgreen}$ and PFC$_{darkred}$). *D)* Brain cell type gene-set enrichment from the NAc and PFC (-$\log_{10}$(FDR) transformed). Colors correspond with their respective modules (NAc$_{greenyellow}$, NAc$_{magenta}$, NAc$_{darkgreen}$, PFC$_{pink}$, PFC$_{darkred}$, and PFC$_{lightgreen}$) with single gene sets enriched in modules.

28

3.3.4) Biological Processes and Cell-type Enrichment

To gain perspective on the biological underpinnings of the significant gene networks from NAc and PFC, we performed a gene-set enrichment analysis, gene ontology (GO) biological processes annotation (ShineyGO ver.61) and neuronal cell type enrichment for the two regions. As one of our aims was to identify unique and shared gene networks associated with AD in NAc and PFC, we focused our analyzes on NAc modules that were highly (i.e., $NAc_{greenyellow}$ and $NAc_{magenta}$) and poorly (i.e., $NAc_{darkorange}$, and NAc_{purple}) preserved in PFC. $NAc_{greenyellow}$ and $NAc_{magenta}$ are primarily associated with the immune response process (FDR ≤0.05) believed to be a consequence of neurotoxicity caused by chronic alcohol abuse (***Figure 5A***). These modules are enriched among microglia and astrocyte cell types (FDR ≤0.05), which is expected based on the functional properties of the glial cells (***Figure 5D***). The poorly preserved NAc modules showed enrichment within gene-sets associated with cilia-based cell projection and cell morphogenesis (FDR≤0.05) (***Figure 5A***).

Corollary, we performed gene-set enrichment analysis on the PFC modules, which were highly and poorly preserved in NAc. (***Figure 5B***). Similar to the $NAc_{greenyellow}$ and $NAc_{magenta}$ modules, the highly preserved $PFC_{lightgreen}$ module was associated with immune response processes (FDR ≤0.05) and significant microglial cell type enrichment (FDR ≤0.05) (***Figure 5D***). $PFC_{darkred}$ and $NAc_{magenta}$, were moderately preserved with each other (***Figure 5C***) with $PFC_{darkred}$ showing astrocyte cell type enrichment (***Figure 5D***). Interestingly, a class of genes in one family of immune response proteins, metallothioneins (MTs), contained in both the $PFC_{darkred}$ and $NAc_{magenta}$ modules, were differentially expressed in both brain regions between cases and controls (***Figure 6***). Since hubs are considered the most important genes for preserving the network's integrity, when these analyses

were further limited only to the hub genes, not surprisingly, we captured the same GO terms and

biological process that we observed from the entire module gene lists.
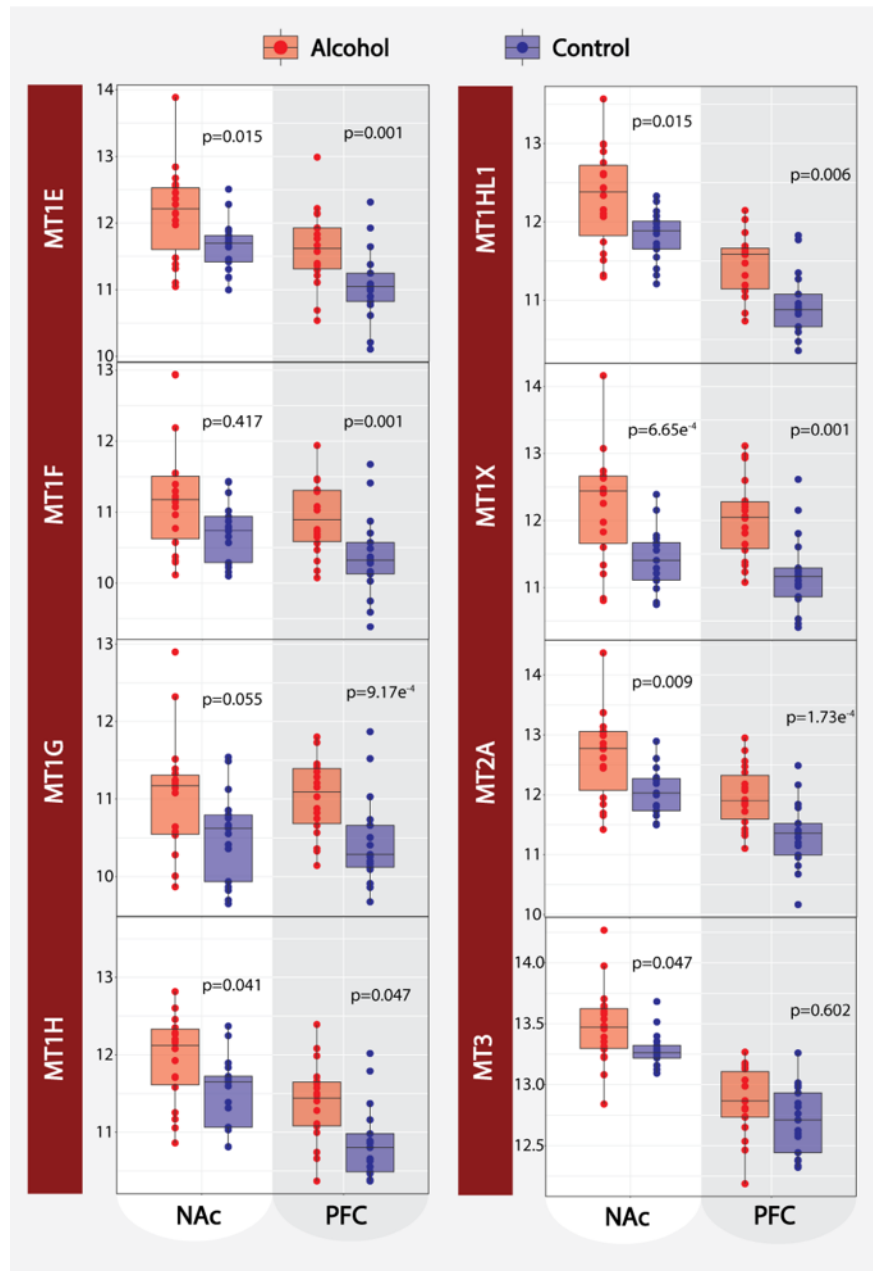
Figure 6: Metallothionein gene expression. Relative expression of 8 metallothionein cluster genes (MT1E, MT1F, MT1G, MT1H, MT1HL1, MT1X, MT2A, and MT3) comparing AD case to controls for both the NAc and PFC. P-values presented for each transcript are based on our bidirectional stepwise regression.

3.3.5) **Hub Genes of Potential Biological Significance**

To identify candidate hub genes of potential biological significance, we focused on the relationship between intramodular connectivity (i.e., MM) and gene significance (GS) to AD case status. Of the 459 genes from the 3 significant PFC modules and the 6 significant modules in NAc, we identified 99 and 433 unique hub genes with MM ≥ 0.80, respectively (*Figure 7*). We focus on the hub genes due to their biological relevance to AD and predicted role as drivers of expression for the entire module [70].
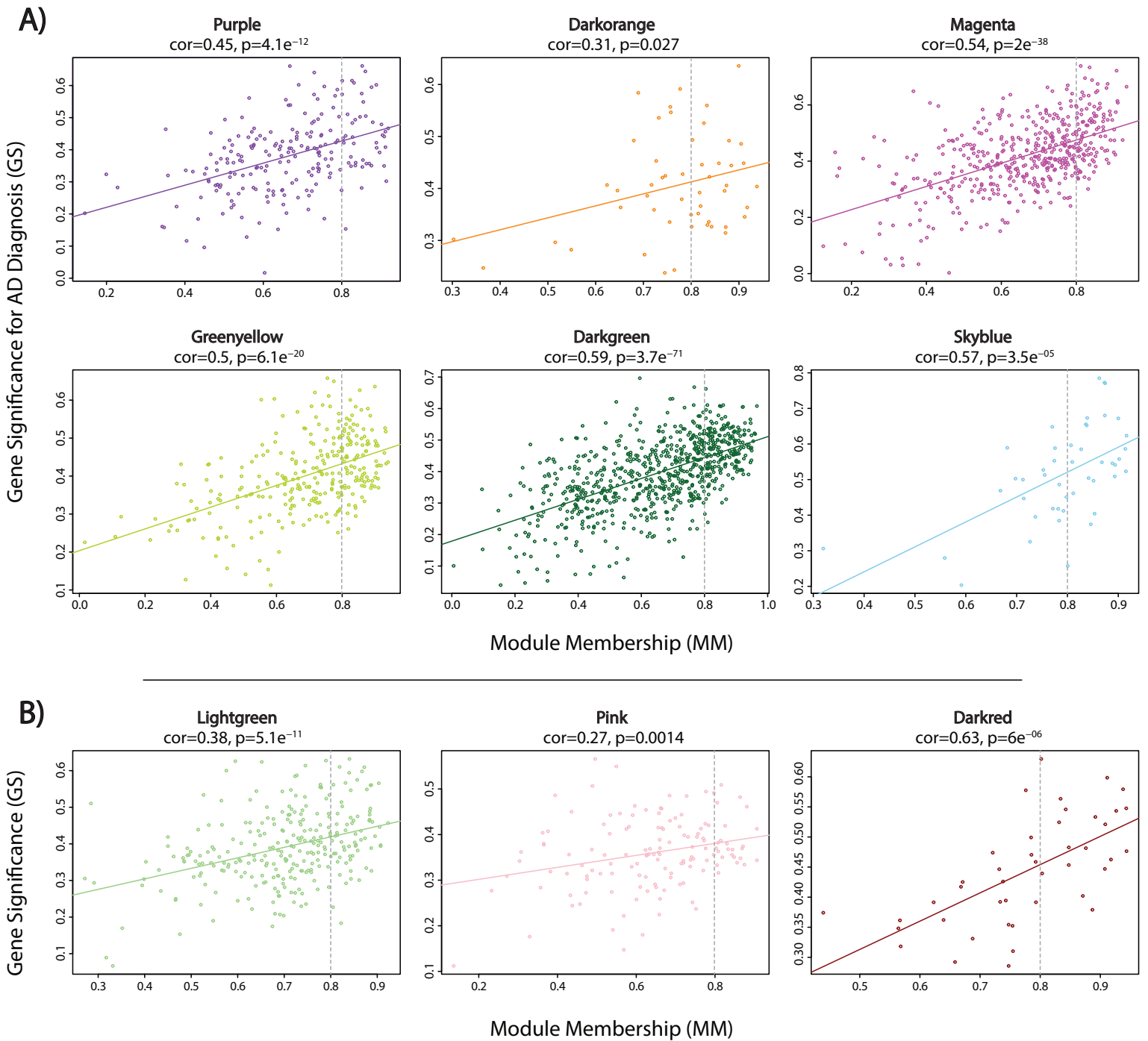
Figure 7: Hub gene prioritization based on module membership (MM) and gene significance (GS) for AD. *A)* Our analysis of the 1,843 transcripts within the six AD correlated modules from the NAc revealed a total of 433 unique candidate hub genes (MM ≥ 0.80). *B)* The three AD correlated modules from the PFC include 459 transcripts and 99 hub genes (MM ≥ 0.80).

3.3.6) Detection of miRNA Gene Network Modules in NAc and PFC

In NAc and PFC, we identified miRNA modules with varying levels of significant correlation to AD case status. The NAc miRNA data revealed 430 nominally significant loci, which clustered in 5 modules ranging from 18 (NAcmi$_{green}$) to 259 (NAcmi$_{turquoise}$) loci in size, of which, at Bonferroni adjusted p ≤0.05, three miRNA modules remained significantly correlated to AD (NAcmi$_{yellow}$, NAcmi$_{brown}$, and NAcmi$_{turquoise}$). Of these, NAcmi$_{yellow}$ and NAcmi$_{brown}$ were negatively correlated, whereas NAcmi$_{turquoise}$ was positively correlated within AD (**Figure 9A**). The 170 miRNA transcripts from the PFC clustered into 6 modules ranging in size from 9 (PFCmi$_{red}$) to 55 miRNA transcripts (PFCmi$_{turquoise}$), of which PFCmi$_{yellow}$ and PFCmi$_{red}$, remain significant at Bonferroni adjusted p ≤0.05; both miRNA modules were negatively correlated with AD (**Figure 9D**).
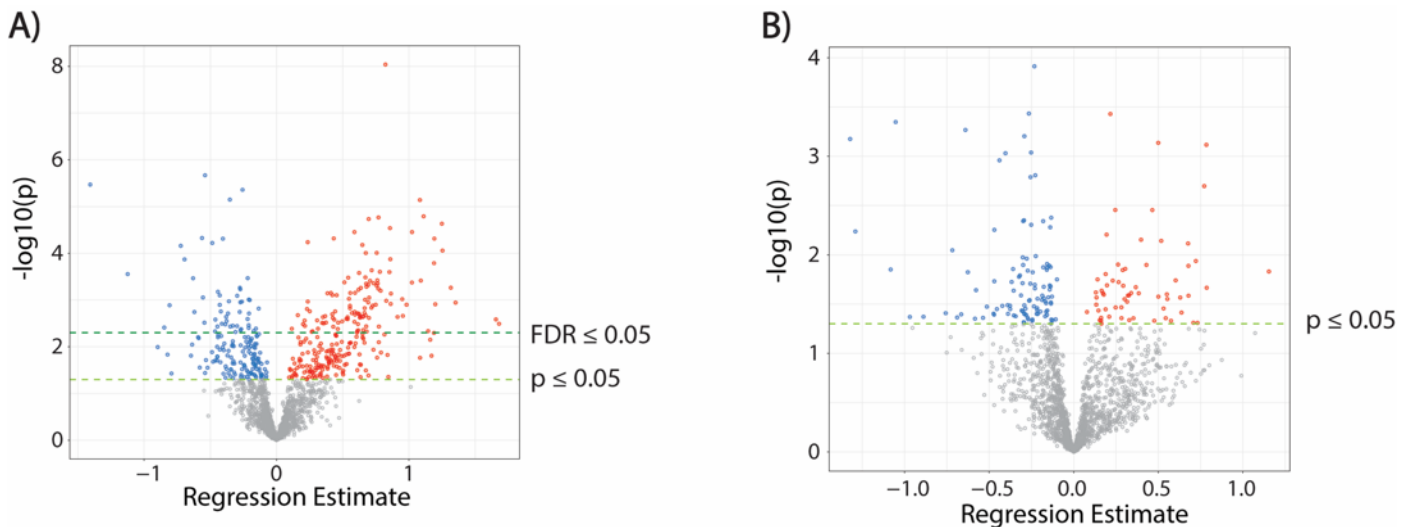
Figure 8: Volcano plots of differentially expressed mRNA from NAc and PFC. *A)* NAc regression analysis reveals 430 differentially expressed miRNA at the nominal p≤0.05which were used for downstream analyses. *B)* PFC regression shows 170 differentially expressed miRNA at p≤0.05.

3.3.7) **MiRNA Networks Show Unique Patterns of Regulation**

In an attempt to identify a higher order system, network levels of interactions, existing between the AD significant mRNA and miRNA modules we correlated their respective module MEs. From the NAc, we identified 2 significant positive mRNA/miRNA ME correlations and 4 negative ME correlations at Bonferroni adjusted p ≤0.05 (***Figure 9B***). To better understand the biological function of miRNA/mRNA interacting networks at specific loci, we honed on the interaction between individual miRNA/gene pairs. After correlating individual mRNA hubs and miRNA, we identified 1,801 significant mRNA/miRNA interactions (FDR ≤0.10) spanning 318 genes and 68 miRNA loci (*S9 Table*). Interestingly, we observed 97% (35/36) of the purple mRNA module hub genes to be negatively correlated with either mir-449a or mir-449b from NAcmi$_{brown}$ (***Figure 9C***). In PFC, we identified one positive mRNA/miRNA ME correlation and 3 negative correlations at Bonferroni adjusted p≤0.05 (***Figure 9E***). Individual mRNA/miRNA interaction analysis from the PFC revealed 6 mRNA/miRNA interactions (FDR of ≤0.10) spanning 6 genes and one miRNA transcript, mir-485-5p.
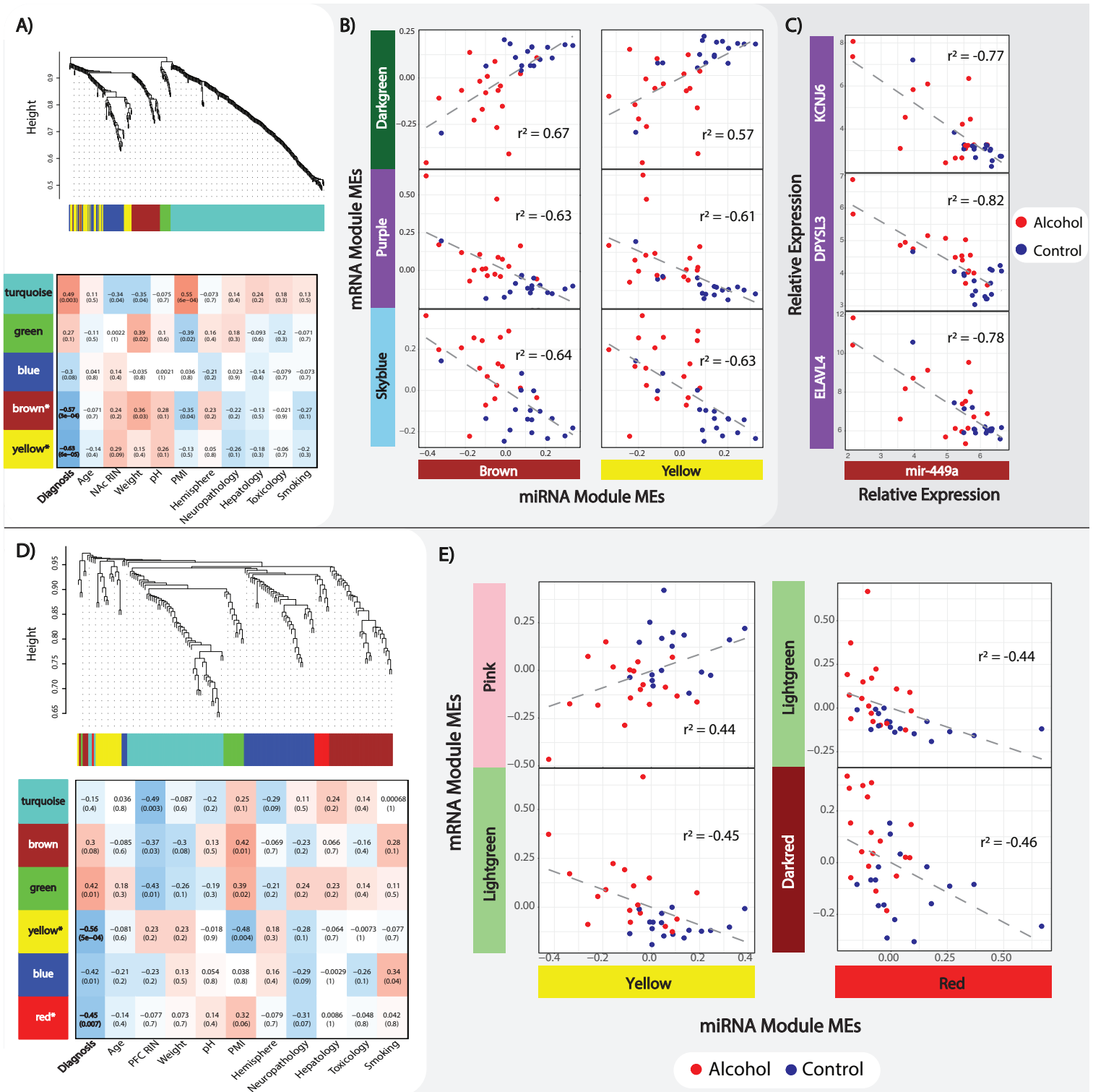
Figure 9: MiRNA WGCNA and mRNA:miRNA interaction. *A)* NAc miRNA cluster dendrogram and module assignment with module-trait relationship heatmap, both as previously described in *Figure 3*. *B)* Bonferroni adjusted significant (p≤0.05) NAc mRNA/miRNA module ME correlations (Pearson's). Alcohol and control groups are separated by color to emphasize sample clustering. *C)* Significant (FDR≤0.05) correlation (Pearson's) between mir-449a and selected mRNA transcripts from the low network preserved NAc$_{purple}$ module. D) PFC miRNA cluster dendrogram module assignment along with module-trait relationship heatmap. E) Bonferroni adjusted significant (p≤0.05) NAc mRNA:miRNA module ME correlations (Pearson's).

3.3.8) Brain Region Specific eQTL Regulation of Differential Gene Expression

In NAc, we detected a total of 36 mRNA eQTLs spanning 17 unique genes and 9 miRNA eQTLs covering 4 different miRNA (FDR ≤0.10). Of the 17 hubs with significant eQTLs, 7 are from NAc$_{darkgreen}$ (*VRK1, INPP4A, HMP19, DKK3, PCDH8, RNF34,* and *RASGRP1*), 4 from NAc$_{greenyellow}$ (*FCGR3A, CTSS, AASS,* and *RNASE4*), 3 from NAc$_{darkorange}$ (*DNALI1, CCDC81,* and *SPAG6*), 2 from NAc$_{purple}$ (*HIVEP1* and *GNAS*), and one from NAc$_{magenta}$ (*VAMP5*). Within the PFC we identified 34 eQTLs spanning 16 unique genes and 18 miRNA covering 7 different miRNA transcripts (FDR ≤0.10). Of these, 11 genes are from PFC$_{lightgreen}$ (*SERPINH1, CDKN1A, PNP, EMP1, FKBP5, IL4R, TNFRSF10B, RTEL1/TNFRSF6B, SERPINA1, MAFF,* and *SERPINA2*) and 5 from PFC$_{pink}$ (*GAD2, ACTL6B, KCNF1, SEZ6L,* and *EFNB3*). Among our significant eQTLs, we highlight two examples: *FCGR3A*:rs12087446 (NAc p= 3.24E-07; PFC p= 0.002) from the highly conserved NAc$_{greenyellow}$ module and *DNALI1*:rs12119598 (NAc p= 1.94E-09; PFC p=0.150) from the poorly conserved NAc$_{darkorange}$ module. The brain region specific eQTL impact on the expression of these two genes suggests that different genetic mechanisms are likely at play in NAc and PFC that may further shed light on the different behavioral measures encoded by the two brain regions (***Figure 10***). For the full list of cis-eQTL, please refer see ***Appendix IV***. To highlight the potential clinical importance of our findings and provide functional support for previous genetic studies, we also tested for enrichment of our clinically relevant eQTLs (i.e., testing only SNPs that showed a significant (SNP x AD) interaction term) and previously published GWAS of addiction phenotypes. While the overlap did not reach formal significance, likely due to the smaller GWAS sample size, we nevertheless observed suggestive enrichment, i.e., GWAS & Sequencing Consortium of Alcohol and Nicotine Use (GSCAN) drinks per week p=0.195; GSCAN smoking initiation p=0.251;

36

GSCAN smoking cessation p=0.147; and Collaborative Study on the Genetics of Alcoholism (COGA)+Irish p=0.299. Finally, we attempted to replicate all eQTLs in our study, irrespective of their potential disease relevance, in the GTEx database using the Fisher's exact test. Interestingly, we observed a significant overlap between our eQTLs detected in the PFC (n=2,368, 6.6% of eQTLs tested, p=0.003), but not in the NAc (n=5,436, 3.4% of eQTL tested, p=1).
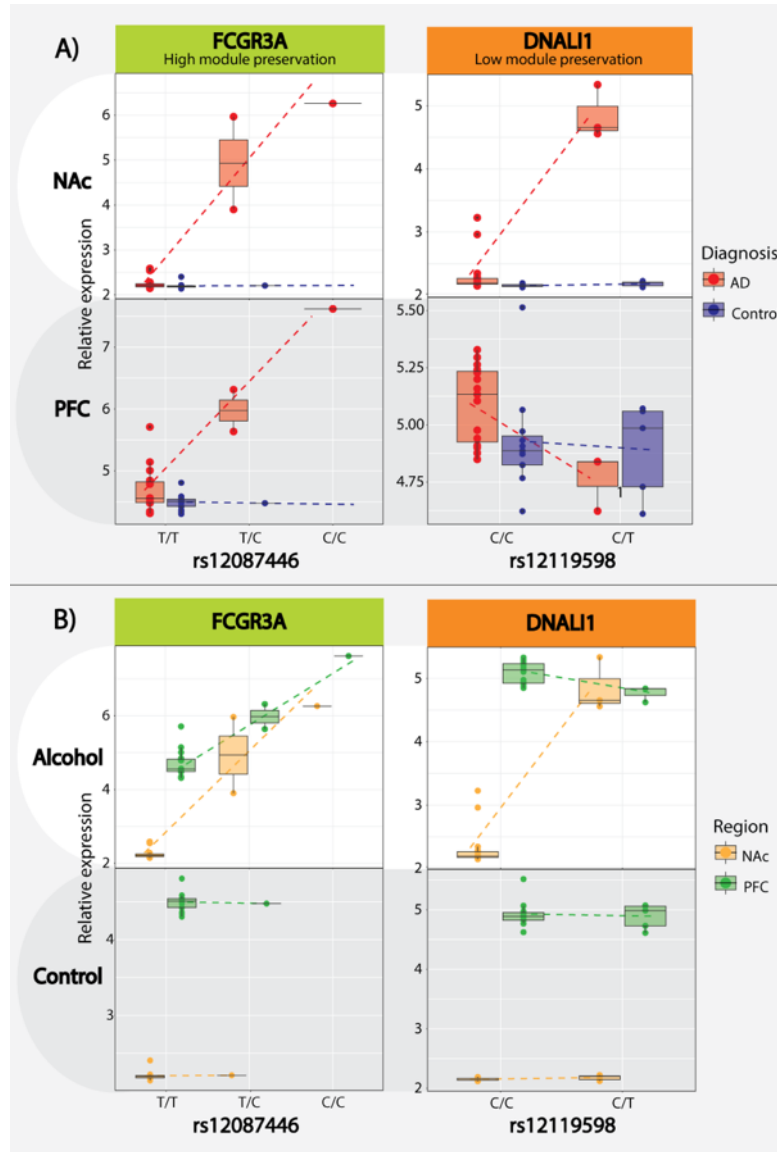
Figure 10: Cis-eQTL analysis. *A)* Cis-eQTL boxplot directly comparing AD case/control designation with the FCGR3A:rs12087446 eQTL from the high network preservation NAc$_{greenyellow}$/PFC$_{lightgreen}$ module and the DNALI1:rs12119598 eQTL from the low preservation NAC$_{darkorange}$ module, the relative expression is presented on the y-axis and SNP/genotype on the x-axis. *B)* Alternative boxplot visualization of the same cis-eQTL directly comparing differences between brain regions.

3.4) DISCUSSION

AUD continues to be a growing public health concern with a complex and poorly understood etiology as recreational alcohol use becomes habitual and problematic. The broad goal of this study is to identify the neurobiological processes associated with chronic alcohol use via analyzing brain region-specific gene networks from the NAc and PFC. To understand the human behavior leading to addiction, it is important to investigate how chronic alcohol use impacts expression changes in the evolutionarily newer cortical areas, in contrast to the older, more evolutionarily conserved subcortical brain regions [132]. Here, we attempt to understand the neurobiological underpinnings of alcohol specific reward conditioning in the NAc and disruption of executive function within PFC [18] through identifying gene networks and biological processes associated with AD that are conserved or unique to each brain region. Additionally, we assessed the relationship between the miRNA and mRNA networks significantly correlated to AD based on the miRNA functions to induce mRNA degradation and/or translational inhibition. Finally, we tested the impact of genetic variants on gene expression in a disease dependent manner via AD-mediated eQTL analysis.

Our network analyses are consistent with previously published reports by others and us, showing the upregulation of immune response mechanisms among AD cases as a byproduct of alcohol's neurotoxic effects [8]. The immune-related modules show significant enrichment for both astrocyte and microglial cell types, which has been validated by previous alcohol studies and the known immune functions of astrocyte and microglia in the brain [133, 134]. More importantly, we observed generalized up-regulation of immune response mechanisms within both the PFC and NAc, suggesting that the neurotoxic response to chronic alcohol use is ubiquitous across cortical and subcortical brain regions. Interestingly, in both brain regions, we further identified DEGs in

the MT cluster (*MT1HL1, MT1H, MT1X, MT1E, MT1G, MT1F, MT2A,* and *MT3*). The MT cluster is primarily responsible for maintaining the cellular homeostasis of zinc and copper while also regulating oxidative stress [135]. Zinc is an essential catalytic cofactor for alcohol metabolism via alcohol dehydrogenase [136]. Free or "chelated" zinc ions (Zn^{2+}) are seen in abundance in the brain, specifically at ionotropic glutamate receptors such as the NMDA receptor family. The interaction between Zn^{2+} and NMDAR activity has shown to be an important contributor to synaptic plasticity through regulating postsynaptic density assembly [47]. It is well understood that chronic alcohol abuse leads to varying degrees of organ-wide zinc deficiency [138]; however, the neurobiological consequences of how zinc deficiency in the brain contributes to AD neuropathology is poorly understood. We believe this interaction between chronic alcohol abuse, MT expression, zinc deficiency, and synaptic plasticity is an important avenue for future research that should be explored.

In addition to identifying dysregulated immune response mechanisms, we validate recent studies showing differential expression among signaling and neurodevelopmental processes within AD cases [74–76, 117]. However, these processes are less conserved between cortical and subcortical regions, likely due to the different neuronal composition and functional properties of the PFC and NAc [139]. Interestingly, two NAc modules that primarily associate with cilium assembly (NAc*darkorange*) and cellular localization/morphogenesis (NAc*purple*) show limited network preservation within the PFC. There has been increasing evidence suggesting primary cilia aid in facilitating extrasynaptic signaling during adult neurogenesis [140, 141], an important aspect of addiction related extracellular membrane plasticity [142]. For example, *GRP88*, a g-protein coupled receptor and primary cilia enriched gene [143], was linked to increased alcohol seeking behaviors in knock out (KO) mice models [144], further reinforcing the importance of primary cilia in AUD etiopathology. The cilium assembly genes enriched in NAc*darkorange*, were shown to be

associated with axonemal dynein assembly (*DNAAF1*, *DNAI2*, and *DNALI1*). A recent gene expression study in adolescent rat hippocampus identified increased expression of two dynein associated genes (*dnai1* and *dnah5*) [145]. One explanation for increased expression of primary cilia associated genes in the NAc relative to the PFC is related to potential discrepancies in adult neurogenesis between subcortical vs cortical brain regions. It is well understood that most adult neuronal stem cells originate in the ventricular–subventricular zones (V-SVZ) and migrate to adjacent cortical and subcortical brain regions as neuroblasts to promote neurogenesis [146]. A recent study showed increased adult neurogenesis of medium spiny neurons within the NAc and that the migration and incorporation of new neurons was experience-based [147]. We believe that the increased expression of genes that encode for the cilia assembly complex may reflective of experience mediated neurogenesis of medium spiny neurons in NAc, except being driven by chronic alcohol consumption instead of pain. These new neurons formed in response to alcohol use may play an important role in the reward response deficits we often associate with addiction and AUD [111].

Other interesting findings arise from our mRNA/miRNA interactions, e.g., when correlating the MEs from mRNA and miRNA modules, we see distinct patterns between cases and controls within both brain regions. Based on the known function of miRNAs in regulating the expression of target mRNAs [148] we can infer these significant miRNA networks may serve as a driving contributor for differential network expression between AD cases and controls. Specifically, 97% (35/36) of the hub genes from the NAc$_{purple}$ module were significantly negatively correlated with either mir-449a or mir-449b. Mir-449a/b have primarily been studied in the context of spermatogenesis and cellular proliferation in cancer [149–151]. Based on the mRNA-miRNA correlations, our study suggests that mir-449a/b cluster has additional functions related to cellular proliferation in the brain. Among the genes correlated with mir-449a in the NAc, *ELAVL4*,

DPYSL3, and *KCNJ6* have shown significant associations with AD in other expression, and genetic association studies [119, 152, 153], as well as being implicated in other SUDs [154–157].

In an attempt to understand the causal nature of the gene networks associated with AD, we integrated genetic information via eQTL analysis. We were able to detect a significant number of mRNA and miRNA cis-eQTLs from both brain regions. We selected highly significant eQTLs (*FCGR3A* (Fc fragment of IgG receptor IIIa):*rs12087446* and *DNALI1* (dynein axonemal light intermediate chain 1):*rs12119598*) based on *FCGR3A* and *DNALI1*'s role as network hubs to highlight the interaction between AD case status and eQTL while also demonstrating brain region-specific eQTL variation. *FCGR3A* is one of the low-affinity Fc receptor genes important for NK cell-mediated antibody-dependent cytotoxicity [158] and a hub gene from our highly conserved NAc$_{greenyellow}$ and PFC$_{lightgreen}$ modules. The consistent effect of *rs12087446* on *FCGR3A* expression between both brain regions suggests the genetic impact on immune response processes might also be ubiquitous across the brain of chronic alcohol users. Differential FCGR3A expression was recently shown to be associated with both alcohol preference and binge-like behaviors in the VTA of rats [159]. In contrast, *DNALI1,* a hub gene in the cilium assembly enriched NAc$_{darkorange}$ module, is under the genetic control of specific eQTL only in NAc but not in PFC, suggesting that changes to cilia organization due to alcohol abuse might be under different genetic control between the two brain regions. We observed suggestive evidence for enrichment between our eQTLs and previously published GWAS of alcohol or other addiction phenotypes, such as smoking. We believe this is primarily due to three factors: 1) low statistical power within our sample to detect genetic signals that would otherwise appear in large-scale GWAS studies, 2) our selective study design focusing only on potentially clinically relevant eQTLs, and 3) the presence of variants with a lower minor allele frequency (MAF) in the GWAS potentially not detectable in our dataset. We further successfully replicated our eQTLs in the GTEx database for PFC, but not NAc. One possible

explanation is that the increased number of DEG in the NAc relative to PFC with the fact GTEx does not include AD diagnosed brains in their analyses [160] effectively limits our ability to replicate GTEx eQTLs based on significant and potentially subtle non-significant expression changes among AD cases.

3.5) CONCLUSION

The strength of this study lies in our ability to compare and contrast expression changes between subjects with AD and controls within two different brain regions. We successfully identified gene networks and biological processes from both brain regions that were validated by previous AD studies as well implicated a novel biological process (cilia assembly) and gene family (MT cluster) as potentially important for the development of AD. Our mRNA/miRNA interaction analysis pinpointed mir-449a/b cluster as an important regulator of DEGs between AD cases and controls. Finally, via our eQTL analysis, we provided evidence that mRNA and miRNA expression differences between AD cases and controls might be under brain region specific genetic control. While our sample size could be perceived as a limitation, we mitigated this by utilizing WGCNA to aggregate DEGs into biologically relevant modules with single expression values, effectively increasing our power to detect significant AD associations within a multivariate framework. Additionally, to increase the power of our study, considering the more prevalent and heavier drinking patterns in men, we assessed the molecular processes of alcohol drinking in male subjects only. While we recognize the importance of comparing the molecular pathology of drinking between the two sexes, we would like to highlight observations from genetic epidemiological studies showing male and female subjects to have a similar genetic predisposition to alcohol abuse [161]. We further recognize that a number of our significant AD associated modules in PFC were also

nominally correlated to neuropathology (p≤0.05). This is not entirely unexpected, given the known neuropathological impact of chronic alcohol abuse [162]. Finally, while we understand that the lower RINs from the PFC can be seen as confounding factor, studies have suggested that reliable data can still be obtained from postmortem brain tissue even with suboptimal RNA quality . However, our careful analytical design to adjust for the impact of RIN on gene expression maintains the robustness of our results even in the presence of lower RINs.

Overall, the broader impact of our findings is the understanding that chronic alcohol consumption can reinforce addiction behaviors through dysregulating different biological process across various brain regions. This information could potentially lead to more focused therapies for AUD by targeting important brain regions specific neurobiological pathways involved in the development of alcohol addiction. While our results point to certain biological processes that differentiate between the PFC and NAc, these findings require replication in an independent postmortem brain samples spanning other cortical and subcortical brain regions. Additional support for the postmortem brain findings presented here can also be obtained by studying ethanol activity in animal models or neuronal cell cultures. Increased research within the methodological framework of our study can help validate our findings and identify biological processes and genes that play the most significant role in the development of AUD.

CHAPTER 4

STUDY 2: *Identifying a novel biological mechanism for alcohol addiction associated with circRNA networks acting as potential miRNA sponges in the nucleus accumbens of chronic alcohol users.*

4.1) INTRODUCTION

Alcohol is among the most readily available and commonly abused recreational drugs worldwide with substantial socio-economic and public health implications [12]. The shift from recreational alcohol use to problematic drinking, resulting in AUD is dependent upon genetic and environmental factors [166]. AUD is moderately heritable (~49%) [110], however, the genetic mechanisms underlying this heritability are poorly understood. While the alcohol dehydrogenase cluster on chromosome 4 has been among the most consistently replicated genetic loci associated with AUD [167], molecular studies from the MCL of human postmortem brains and animal models have implicated additional AUD risk genes involved in neurosignalling, synaptogenesis, and immune response [75, 168]. The limited overlap between molecular and genetic studies [169] have hindered our understanding of the link between AUD associated genetic loci and gene expression changes in the brain. Broadly, the human transcriptome can be divided into coding and non-coding, with the non-coding transcriptome (represented by a large set of ncRNA species characterized by their minimal or complete lack of protein-coding abilities and gene regulatory functions [170, 171]) being a largely unexplored domain of the human genome with a potentially substantial impact on the neuropathology of AUD. Among these, a particular class of ncRNA,

termed circRNA have been implicated in the development of alcoholic hepatitis in mouse models [107, 108].

CircRNA are abundantly and dynamically expressed throughout the mammalian central nervous system (CNS) [103, 172]. They primarily arise from pre-mRNA splicing events in which the 5' and 3' ends of introns or alternatively spliced exons are covalently linked to form closed loop structures [173]. While several hypotheses have been proposed to explain the mechanisms by which circRNAs regulate gene expression [174], a commonly accepted one, based on experimental observations, is the miRNA-sponge hypothesis [175]. MiRNAs regulate gene expression mainly through binding to the 3' untranslated regions (UTRs) of their target genes, leading to translational repression and mRNA degradation [176]. CircRNAs serve as competitive RNAs for miRNA by competing with miRNA response elements (MREs) in the 3'UTRs of mRNA. This leads to miRNA sequestration by circRNA and decreased miRNA-target interactions, effectively increasing gene expression as a result [176].

With their varied spatio-temporal expression in the brain, circRNA were shown to be implicated in the etiology of neurodegenerative and neuropsychiatric disorders [103, 178, 179]. To test whether these recent observations also extend to AD, we assessed the genome-wide expression of circRNA, miRNA, and mRNA in NAc from subjects with AD followed by weighted gene co-expression network (WGCNA) and bioinformatic and statistical analyses (*Figure 11*). Finally, we applied an eQTL analysis to identify genetic elements affecting circRNA expression and ability to interact with miRNA and mRNA. With this study, our main goals were to identify the potential regulatory mechanisms by which circRNA affect the expression of risk AUD genes and provide a methodological framework for exploring circRNA, miRNA, and mRNA interactions in future postmortem brain studies. To the best of our knowledge, this is the first study

to specifically examine the effect of circRNA on mRNA expression via miRNA sponge interactions in NAc from chronic alcohol abusers.
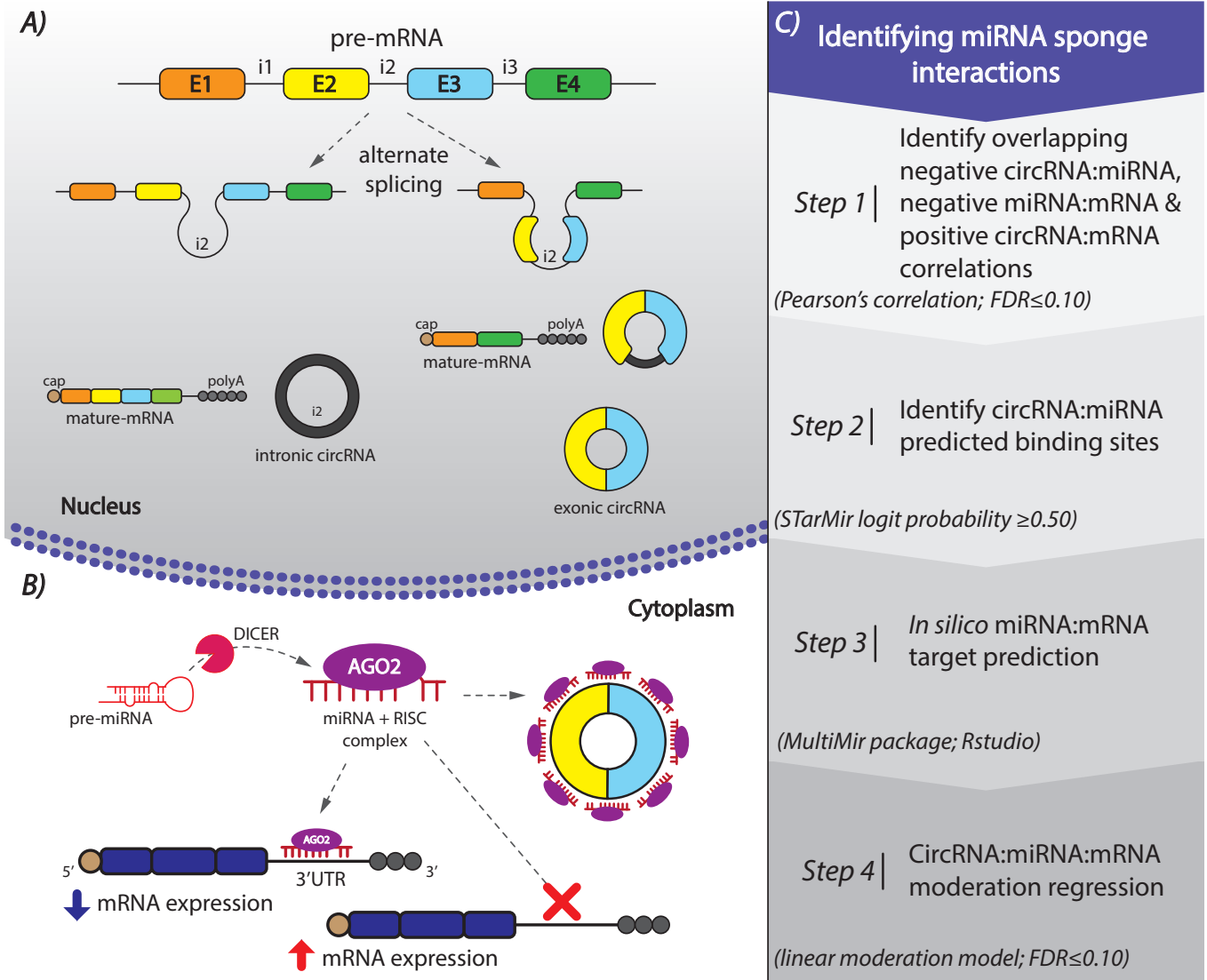
Figure 11: Framework for circRNAs as miRNA sponges and study design flowchart. *A)* CircRNAs are primarily formed through back splicing of unspliced transcripts in which, introns or a combination of exons and introns have their 3', and 5' ends covalently bonded to form closed-end loops. *B)* Under normal circumstance miRNA will bind to 3' UTR of mature mRNAs leading to mRNA degradation or translational repression, however, in the presence of circRNA with complementary sequences, miRNA are sequestered away from their target mRNAs leading to increased gene expression. *C)* Flowchart depicting the steps and analyses used to determine significant circRNA:miRNA:mRNA interactions in this study.

4.2) MATERIALS AND METHODS

4.2.1) Tissue Processing and RNA Extraction

Postmortem NAc from 42 AD cases and 42 controls was provided by the Australian Brain Donor Programs of NSW TRC under the support of The University of Sydney, National Health and Medical Research Council of Australia, Schizophrenia Research Institute, National Institute of Alcohol Abuse and Alcoholism, and the New South Wales Department of Health [113]. As part of a previous study [74], several criteria were used to exclude samples with (1) agonal state, (2) substantial brain damage, (3) history of infectious disease and (4) post-mortem interval >48 hours (**Appendix I**). Samples were further matched for RIN (mean=6.9, ±0.84), sex (all male), ethnicity (100% Caucasian), brain pH, and PMI, to minimize covariates' effect on expression, resulting in 18 matched case-control pairs (n=36). Total RNA from flash-frozen NAc was extracted and purified via mirVANA-PARIS kit (Life Technologies, Carlsbad, CA) following the manufacturer's protocol. RNA integrity (RIN) and concentrations were assessed via Agilent 2100 Bioanalyzer (Agilent Technologies, Inc., Santa Clara, CA) and Quant-iT Broad Range RNA Assay kit (Life Technologies) respectively.

4.2.1) Microarrays and Expression Normalization

Genome-wide circRNA, miRNA, and mRNA expression was assessed on three different platforms: (1) Arraystar Human Circular RNA Array spanning 13,617 circRNA probes, (2) Affymetrix GeneChip miRNA 3.0 Array spanning 1733 mature miRNAs, and (3) Affymetrix GeneChip Human Genome U133A 2.0 array containing 22,214 probe sets spanning ~ 18,400 unique mRNAs. Raw expression data from each assay were background corrected, $\log_2$ transformed, and quantile normalized via Partek Genomics Suite v6.23 (PGS; Partek Inc., St.

Louis, MO) and the limma package (version 4.0) in R. To exclude outliers that could impact downstream analyses, 3 samples were removed from the circRNA normalized dataset, leaving 17 cases and 16 controls (n=33), and one sample was removed from both the miRNA and mRNA normalized datasets, resulting in 17 cases and 18 controls (n=35). Since the mRNA and miRNA expression arrays were validated previously [74], here we validate only the circRNA array by assessing the expression of 3 randomly selected circRNA at the Arraystar facilities via quantitative PCR (qPCR). The assessed genes showed a high mean correlation (Kendall tau r=0.87 (SD±0.021)) between the two platforms (*Figure 12*).
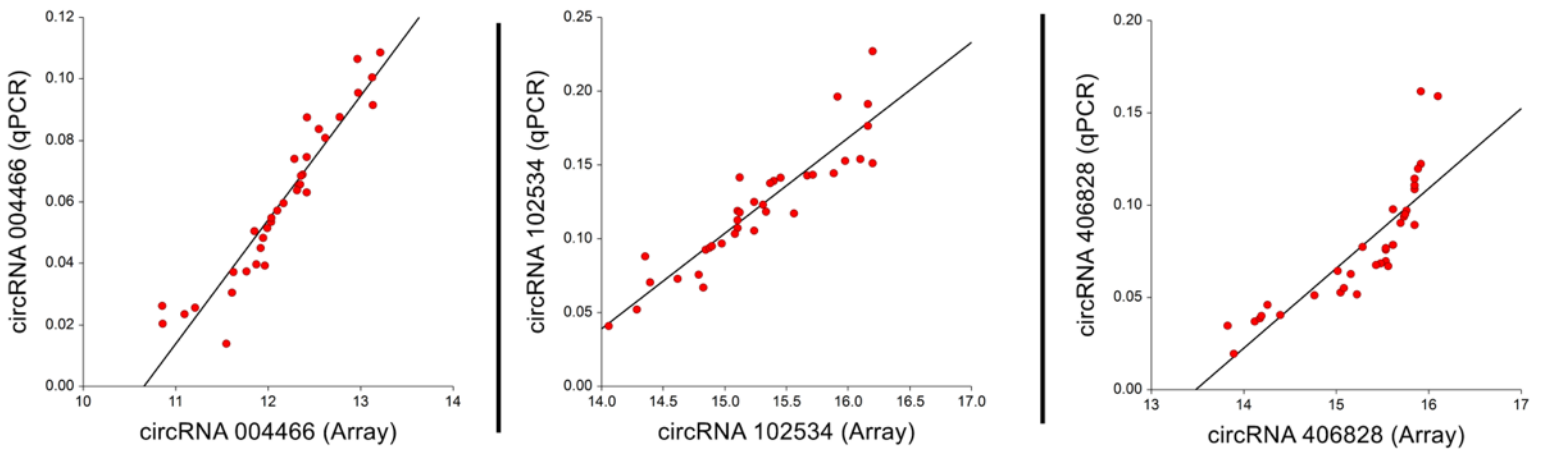
Figure 12: Validation of circRNA microarray via qPCR. The validity of the Arraystar Human Circular RNA Array was assessed by performing qPCR on 3 randomly selected circRNA. Overall, we identify a high mean correlation (Kendall tau r=0.87 (SD±0.021)) between the two platforms.

4.2.3) Identifying Differential Transcript Expression

We assessed the relationship between transcript expression and AD case status via two different regression analysis in RStudio (ver. 1.2.1335). Differentially expressed miRNA and mRNA were identified via a bidirectional stepwise regression elsewhere [168] using the Stats package (v.3.6.1) adjusting for demographic and postmortem covariates. Differential circRNA

expression was assessed via robust linear regression via the MASS package (v.7.351.5) with smoking and RIN included as covariates in the model [180] as these have been shown to have a greater impact on circRNA expression [181, 182], compared to other demographic and postmortem covariates [183].

4.2.4) Weighted Gene Co-expressed Network Analysis

The network analysis was performed on the nominally significant differentially expressed circRNAs (p≤0.05) using the WGCNA package in RStudio (v.1.69). Our selection criteria to include nominally significant genes were based on retaining genes with (i) smaller effect sizes, albeit true positive signals, (ii) exclude genes not likely associated with AD, and (iii) provide a sufficient number of genes for the network analysis. In the WGCNA, our similarity matrix was raised to a power ($\beta = 8$) to approximate the scale-free topography of the adjacency matrix, in which stronger correlations are emphasized over weaker ones. Transcript interconnectedness was determined from the calculated topological overlay measure (TOM). The default, unsupervised hierarchical clustering method was used to partition modules at specified dendrogram branch cut sites using the Dynamic Tree Cut method. Highly correlated modules were then merged based on minimum merge height of $r^2 = .8$ and minimum module size of 15. We used M1-M10 to categorically label co-expressed networks and the sum of relative expression within each module is represented as a MEs and used for downstream phenotypic analysis. MEs were then correlated to AD case-status and available demographic/biological covariates. To further validate the gene networks associated with AD in WGCNA, we also performed a bootstrap based resampling of 100 iterations with replacement (*Figure 13*).
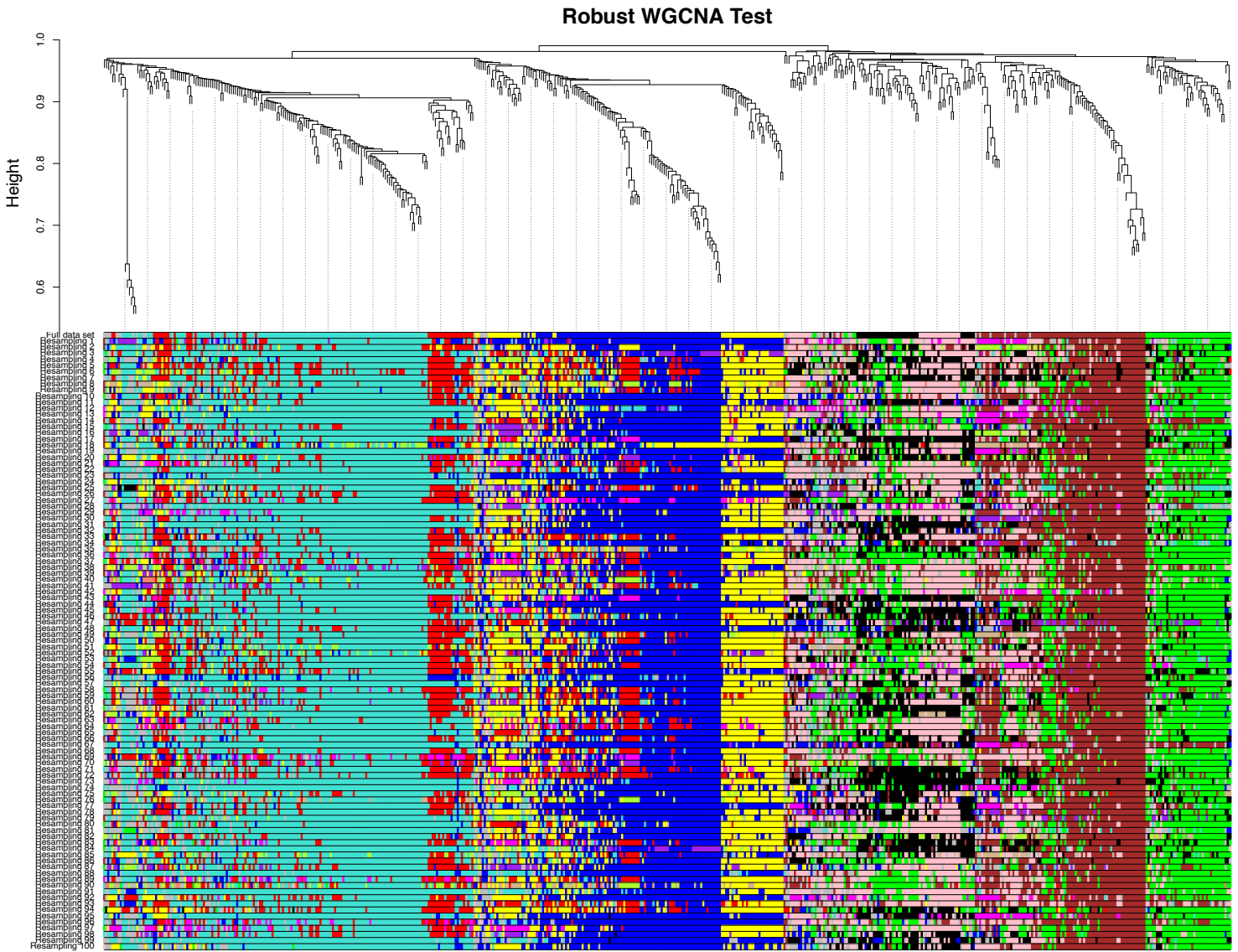
Figure 13: CircRNA robust WGCNA dendrogram module clustering. To ensure network robustness and minimize the potential effect of outlier samples on network structure, we used the robust 'bootstrapped' version of WGCNA as described in *Figure 4*.

4.2.5) **CircRNA Hub Gene Prioritization**

CircRNA hubs were identified from the absolute value of the Pearson's correlation coefficient between MEs and individual gene expression. This value of intramodular connectedness denoted as module MM was used to define circRNA hubs as transcripts significantly correlated to AD (p≤0.05) and a MM≥0.70 within the significant AD modules.

4.2.6) **Correlations Analysis between circRNA, miRNA, and mRNA**

We used only subjects with complete data across all three expression platforms (i.e., 17 AD cases and 15 controls). The circRNA:mRNA:mRNA correlations were based on Pearson's product moment generated in the miRLAB package (ver. 1.14.3) in RStudio. All significant negative circRNA:miRNA, negative miRNA:mRNA, and positive circRNA:mRNA correlations, respectively, were extracted at a FDR of 10% and retained for follow up analyses.

4.2.7) **Computational Prediction of circRNA:miRNA Interactions**

The circRNA-miRNA correlations were supplemented with computational predictions using STarMir in the Sfold application suite (http://sfold.wadsworth.org/cgi-bin/index.pl) [184]. STarMir calculates probability scores for binding predictions of shared seed sequences between circRNA and miRNA [185] based on logistic regression models developed from crosslinking immunoprecipitation (CLIP) studies [186]. Based on STarMir's recommendations, probability scores ≥0.50 were considered significant [184].

4.2.8) **Prediction of miRNA:mRNA Target Interactions**

Similarly, the miRNA:mRNA correlations were complemented with miRNA target predictions from the multiMiR package (v.1.6.0) in Rstudio. MultiMiR is a curated database of miRNA:mRNA target predictions which integrates both computational prediction algorithms (DIANA-microT-CDS, ElMMo, MicroCosm, miRanda, miRDB, PicTar, PITA, and TargetScan) and experimentally validated miRNA-target interactions (miRecords, miRTarBase, and TarBase) [187].

4.2.9) Moderation Analysis

The test for moderation, i.e., whether miRNA expression moderates the relationship between circRNA and target mRNAs, we utilized the Stats package in RStudio. The following linear regression model was used to test the impact the circRNA x miRNA interaction term on mRNA: $y = \beta0 + \beta1 + \beta2 + \beta3 + \beta4 + \beta5 + \beta4 * \beta5 + \varepsilon$. In this model y is mRNA expression, $\beta1$ is AD diagnosis, $\beta2$ is RIN, $\beta3$ is smoking history, $\beta4$ is circRNA expression, $\beta5$ is miRNA expression, $\beta4 * \beta5$ is our circRNA-miRNA interaction of interest, and ε is the error term. Significance was based on an FDR ≤0.10 threshold.

4.2.10) Gene-set Enrichment Analyses

We performed a GO biological processes gene-set enrichment via ShinyGO (v.0.61) at each stage in our analyses on mRNAs participating in significant circRNA:miRNA:mRNA interactions. ShinyGo utilizes a hypergeometric distribution to determine significant enrichment at a FDR ≤0.10 [188].

4.2.11) CircRNA eQTL Analysis and Enrichment in GWAS of Substance Abuse

The postmortem sample was genotyped as part of a larger GWAS study [74]. Monomorphic SNPs and those with excessive missingness (>20%) were filtered out. Only local, cis-eQTLs within 500kb of each circRNA hub's start/stop position were mapped, and variants in LD ($R^2 \geq 0.7$) were subsequently pruned via Plink v1.9 [189]. We utilized the MatrixEQTL package (ver. 2.3) in RStudio using a linear regression model adjusting for relevant covariates to detect cis-eQTL. The overlap (i.e., enrichment) was tested between our eQTLs and recent GWAS of substance abuse, including alcohol and smoking, using two mutually complementing tests (Cauchy Combination and Simes [130, 190]) adjusting for multiple testing and LD ($R^2 \geq 0.50$). For more details, see (***Appendix II***).

4.3) RESULTS

4.3.1) CircRNA are organized in networks associated with AD.

At the nominal $p \leq 0.05$, our gene expression analysis revealed 542 differentially expressed circRNAs between AD cases and controls (***Figure 14A***), with none of them achieving significance at FDR≤0.10. The nominally significant circRNAs clustered into 9 modules significantly correlated to AD (Bonferroni adj. $p \leq 0.05$) (***Figure 14B***), of which M1, M2, M4, and M5 were positively correlated, whereas M6-M10 were negatively correlated to AD status. From these modules, we identified 137 hub genes, which were selected for downstream statistical and bioinformatic analyses against mRNA (n=3,575) and miRNA (n=264) significantly associated with AD at a FDR≤0.10 as a part of a previous study on the same subjects (***Figure 14A***) [169]. See ***Appendix V*** for hub circRNA annotations, regression coefficients, and MM.
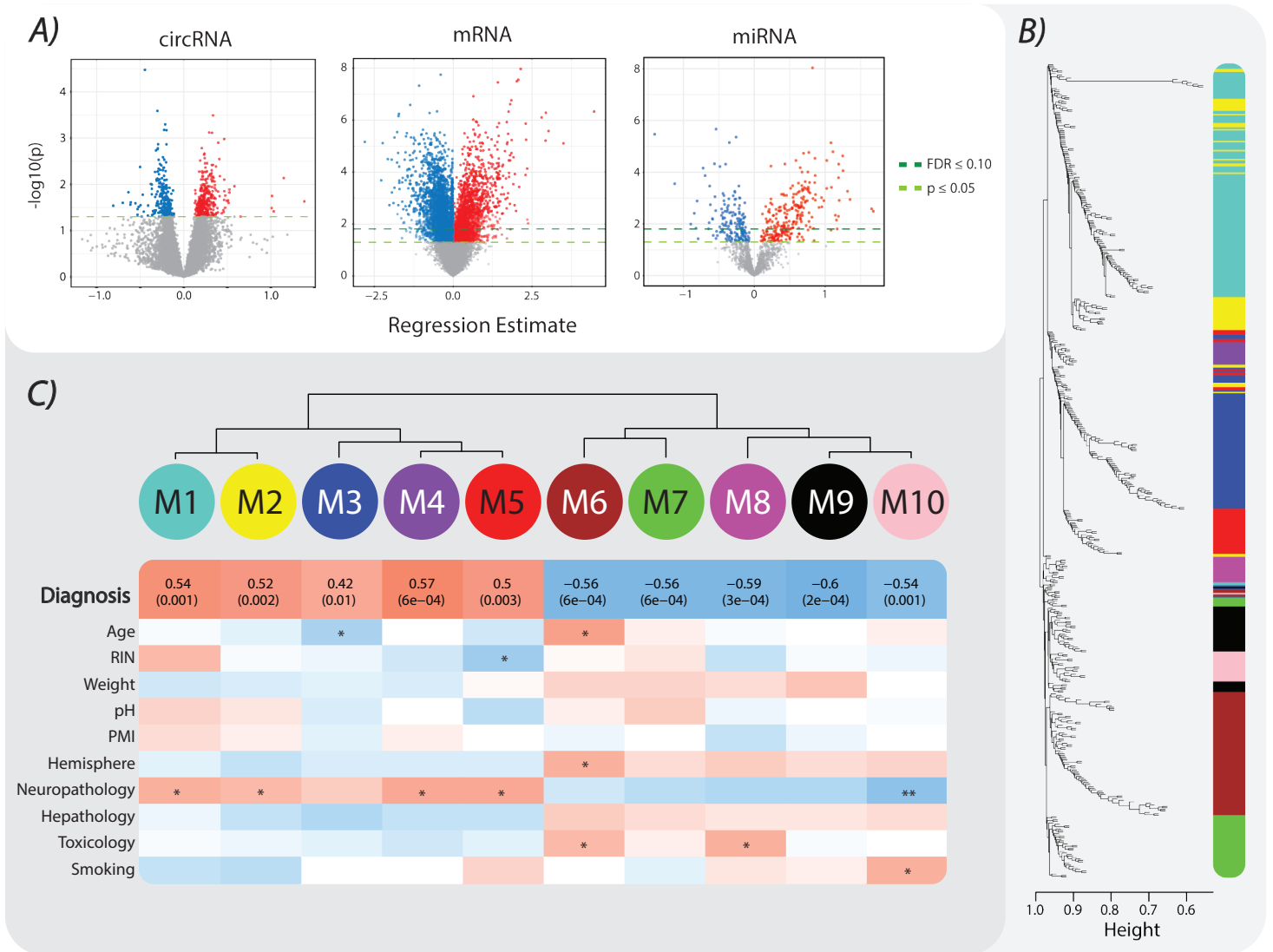
Figure 14: Differentially expressed transcripts and circRNA WGCNA results. *A)* Volcano-plots describing the relationship between regression estimates and -log$_{10}$(p) for each transcript level in our analysis (circRNA, miRNA, and mRNA). Dashed lines correspond with the significance threshold of p≤0.05 and FDR≤0.10. *B)* WGCNA module clustering dendrogram from our nominally AD significant (p≤0.05) circRNA transcripts *C)* Heat plot comparing the correlation (Pearson's) of our identified circRNA module MEs to AD diagnosis and all other available covariates. In respect to AD diagnosis, the top value represents the correlation coefficient, and the bottom value represents uncorrected p-values. For covariates: * = p ≤0.05 and ** = p≤0.005.

4.3.2) CircRNA, miRNA and mRNA show complex interaction patterns associated with AD.

We tested the circRNA ability to interact with miRNA and thus indirectly affect the miRNA target's expression in a disease dependent manner. Assuming circRNA act as miRNA sponges to impact mRNA expression, we posit that the most relevant downstream biological interactions will be represented by negative miRNA:mRNA and positive circRNA:mRNA correlations. Thus, we first performed three independent correlation analyses (circRNA:miRNA, miRNA:mRNA, and circRNA:mRNA) followed by tests to identify the intersection between these interactions at FDR of 10%. In the circRNA:miRNA (circRNA n=137; miRNA n=264) analysis, we identified 48 significant negative circRNA:miRNA correlations. The miRNA:mRNA (miRNA n=264; mRNA n=3,575) analysis revealed 46,501 significant negative correlations. Finally, the circRNA:mRNA (circRNA n=137; mRNA n=3,575) analysis revealed 2,221 significant positive correlations. From the intersection of these analyses, we identified a total of 2,480 overlapping correlations, which were then used in all subsequent follow-up analyses.

4.3.3) Binding predictions supplement intersecting circRNA, miRNA, and mRNA correlations.

To reinforce and complement our correlation analyses, the 2,480 overlapping circRNA:miRNA:mRNA correlations were further screened computationally to identify predicted circRNA:miRNA and miRNA:mRNA interacting pairs. Based on the STarMir's algorithm, no circRNA:miRNA binding predictions with a score greater than our significance threshold (logit probability≥0.50) were detected when circRNA:miRNA correlations were considered in isolation. However, by expanding the circRNA:miRNA binding predictions to include circRNA:miRNA

pairs correlated to the same mRNA, we identified 365 circRNA:miRNA:mRNA trios with intersecting negative miRNA:mRNA correlations, positive circRNA:mRNA correlations, and predicted circRNA:miRNA binding. We further narrow down these 365 interactions via a selection of the best miRNA:mRNA target predictions to identify the most robust 47 circRNA, miRNA, and mRNA participating in a three-way interaction.

4.3.4) Moderation analysis reveals circRNA x miRNA interactions impact mRNA expression.

The impact of miRNA sequestration on mRNA expression from these 47 circRNA, miRNA, and mRNA was formally tested in a linear regression model adjusting for AD status and controlling for covariate effects (RIN and smoking history). In the model, the miRNA sequestration by circRNA was assessed by introducing a (circRNA x miRNA) interaction term. At FDR≤0.10, we identified 23 interactions that show significant moderation effect on mRNA expression (*Table 1*). Interestingly, among these 23 interactions, circRNA-406702:miR-1200 stood out by affecting the expression of the largest set of mRNA (n=17) four of which (*HRAS, PRKCB, HOMER1*, and *PCLO*) are highlighted in *Figure 15*. For full moderation regression coefficients, see *Appendix VI*.

circRNA:miRNA:mRNA Interactions			miRNA:mRNA Cor		circRNA:mRNA Cor		circRNA:miRNA Binding		miRNA:mRNA target Predic		Circ X mi Interaction	
circRNA	miRNA	mRNA	Coef	FDR	Coef	FDR	Logit Prob	Seed	Predicted	Experimental	Estimate	FDR
circRNA-406742	hsa-miR-1200	ACTR2	-0.4251	0.0909	0.5044	0.0998	0.6955	offset-6mer		X	0.8127	0.0898
circRNA-406742	hsa-miR-1200	ASTN1	-0.5425	0.0260	0.5057	0.0987	0.6955	offset-6mer		X	2.0620	0.0070
circRNA-406742	hsa-miR-1200	ATP2B2	-0.5330	0.0293	0.6079	0.0440	0.6955	offset-6mer		X	2.5879	0.0077
circRNA-406742	hsa-miR-1200	E2F3	-0.5165	0.0361	0.5530	0.0708	0.6955	offset-6mer	X		0.9043	0.0913
circRNA-406742	hsa-miR-1200	HOMER1	-0.5717	0.0169	0.6755	0.0237	0.6955	offset-6mer	X		1.7868	0.0077
circRNA-406742	hsa-miR-1200	HRAS	-0.4523	0.0715	0.6014	0.0470	0.6955	offset-6mer	X		1.8261	0.0077
circRNA-406742	hsa-miR-1200	IMP4	-0.5091	0.0394	0.5483	0.0739	0.6955	offset-6mer		X	1.5305	0.0008
circRNA-406742	hsa-miR-1200	IPCEF1	-0.5550	0.0218	0.5356	0.0801	0.6955	offset-6mer	X		2.0946	0.0086
circRNA-406742	hsa-miR-1200	LDB2	-0.4212	0.0939	0.6082	0.0440	0.6955	offset-6mer	X		3.5155	0.0086
circRNA-406742	hsa-miR-1200	NDST3	-0.5663	0.0185	0.5400	0.0779	0.6955	offset-6mer	X		2.7353	0.0096
circRNA-406742	hsa-miR-1200	OSBPL8	-0.5532	0.0223	0.5434	0.0761	0.6955	offset-6mer	X		1.9161	0.0077
circRNA-406742	hsa-miR-1200	PCLO	-0.5141	0.0371	0.5592	0.0677	0.6955	offset-6mer	X		2.5603	0.0070
circRNA-406742	hsa-miR-1200	PRKCB	-0.5650	0.0188	0.5873	0.0535	0.6955	offset-6mer	X		5.3517	0.0009
circRNA-406742	hsa-miR-1200	RAB11FIP2	-0.5455	0.0250	0.5758	0.0583	0.6955	offset-6mer	X		0.9061	0.0104
circRNA-406742	hsa-miR-1200	RANBP2	-0.4977	0.0450	0.5858	0.0543	0.6955	offset-6mer		X	0.8803	0.0368
circRNA-406742	hsa-miR-1200	RFC2	-0.4256	0.0906	0.5162	0.0915	0.6955	offset-6mer		X	0.8356	0.0380
circRNA-406742	hsa-miR-1200	SSX2IP	-0.7589	0.0001	0.5269	0.0847	0.6955	offset-6mer	X		2.0238	0.0009
circRNA-000390	hsa-miR-361-5p	NEK7	-0.5016	0.0430	0.6356	0.0342	0.7444	offset-6mer	X	X	2.2585	0.0898
circRNA-065645	hsa-miR-571	NR3C1	-0.4644	0.0639	0.5547	0.0697	0.7044	offset-6mer		X	-1.5579	0.0550
circRNA-405170	hsa-miR-4310	CELF1	-0.4440	0.0773	0.5324	0.0812	0.7029	7mer-m8	X	X	0.6517	0.0898
circRNA-101134	hsa-miR-665	MLEC	-0.5167	0.0361	0.5433	0.0762	0.6796	6mer	X		-0.6227	0.0134
circRNA-001072	hsa-miR-3187-3p	GPD2	-0.5295	0.0307	0.5681	0.0622	0.6087	7mer-A1	X		-0.7690	0.0380

Table 2: Top circRNA:miRNA:mRNA interactions. Significant circRNA:miRNA:mRNA interactions that survive all of our bioinformatic and statistical tests (i.e. negative miRNA:mRNA correlation, positive circRNA:mRNA correlation, circRNA:miRNA predicted binding, miRNA:mRNA target prediction, and moderation regression).
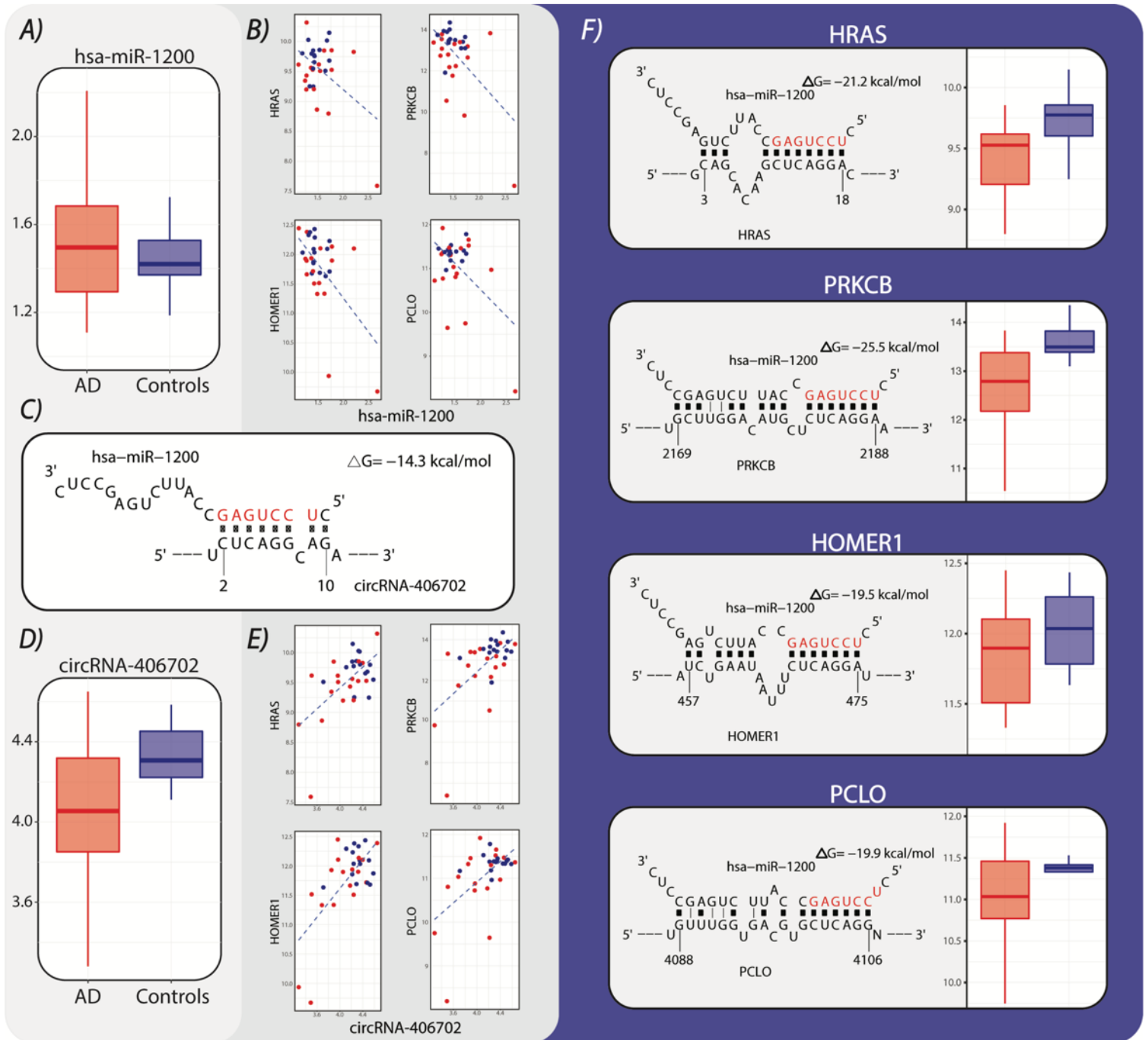
Figure 15: CircRNA-406702:miR-1200 interacting trans-synaptic signaling associated genes. *A)* Boxplot showing relative expression differences between AD cases and controls for miR-1200. *B)* Diagram of predicted binding loci between circRNA-406702 and miR-1200. *C)* Boxplot showing relative expression differences between AD cases and controls for circRNA-406702. *D)* Correlation plots displaying the significant negative relationship between miR-1200 and interacting trans-synaptic signaling associated genes (HRAS r^2=-0.45; PRKCB r^2=-0.57; HOMER1 r^2=-0.57; PCLO r^2=-0.51) *E)* Correlation plot displaying significant positive relationship between circRNA-406702 and select genes HRAS r^2=0.61; PRKCB r^2=0.59; HOMER1 r^2= 0.68; PCLO r^2=0.56). *F)* Boxplots for differential mRNA expression between AD cases and controls and diagram of miRNA predicted binding to the 3'UTR of target genes.

4.3.5) CircRNA interact with genes associated with neuronal function.

At each stage of our analyses, we consistently identified significant enrichment (FDR≤0.10) of genes involved in cellular localization, synaptic transmission, neural development, and response to organic stimuli gene-sets (*Figure 16*). The 23 circRNA:miRNA:mRNA interactions also revealed significant enrichment (FDR≤0.10) for GO biological processes associated with regulation of DNA metabolism, anatomical structure homeostasis, regulation of biosynthesis, dendritic spine organization, and anterograde trans-synaptic signaling.

4.3.6) Genetic variants potentially impact circRNA expression.

Our eQTL analysis revealed 3 significant circRNA-eQTLs at an FDR≤0.10 (*Figure 17A*). When we repeated the eQTL analysis taking into consideration the interaction (AD x genotype) term, we detect 7 additional significant eQTLs (FDR≤0.10), which were associated with one circRNA (circRNA-080252). After expanding our eQTL analysis to incorporate results at a more relaxed significance threshold, (unadj. p≤0.002), we identified additional 96 eQTLs that were used in the downstream enrichment analysis. Among these, we identified multiple circRNA that participated in significant circRNA:miRNA:mRNA interactions at various stages in our multi-step analyses (*Figure 17B/C*). For full eQTL results, *Appendix VII*.
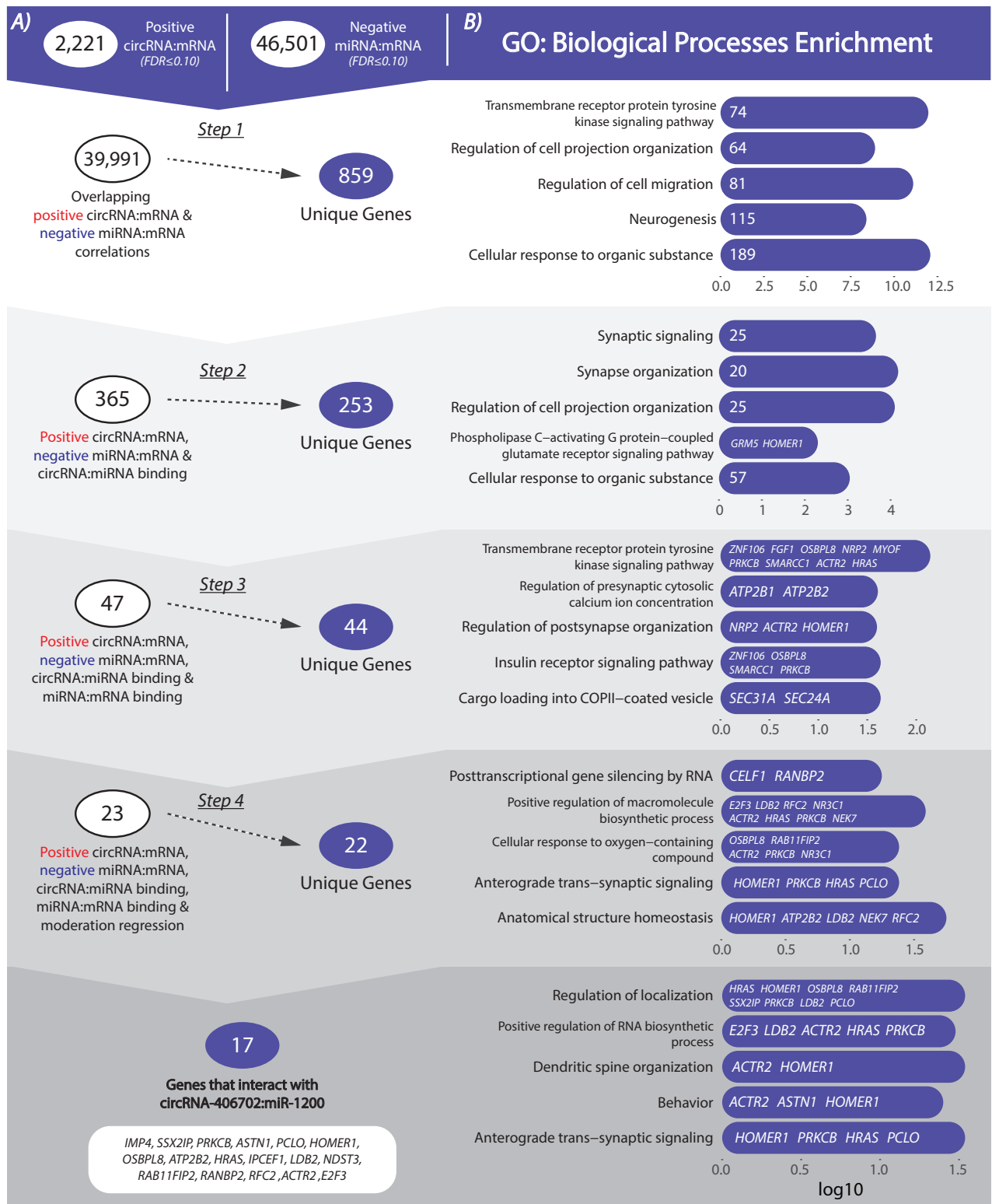
Figure 16: Identification of significant circRNA:miRNA:mRNA interactions and GO biological processes enrichment. *A)* Breakdown of the number of significant circRNA:miRNA:mRNA interactions and unique genes each step in our analysis beginning with positive circRNA:mRNA and negative miRNA:mRNA correlations and ending with circRNA-406702:miR-1200 interacting mRNA. *B)* GO biological processes enrichment for each set of unique genes at each step in our analysis. The genes or the number of genes from our list are presented within each histogram of the associated gene-set.
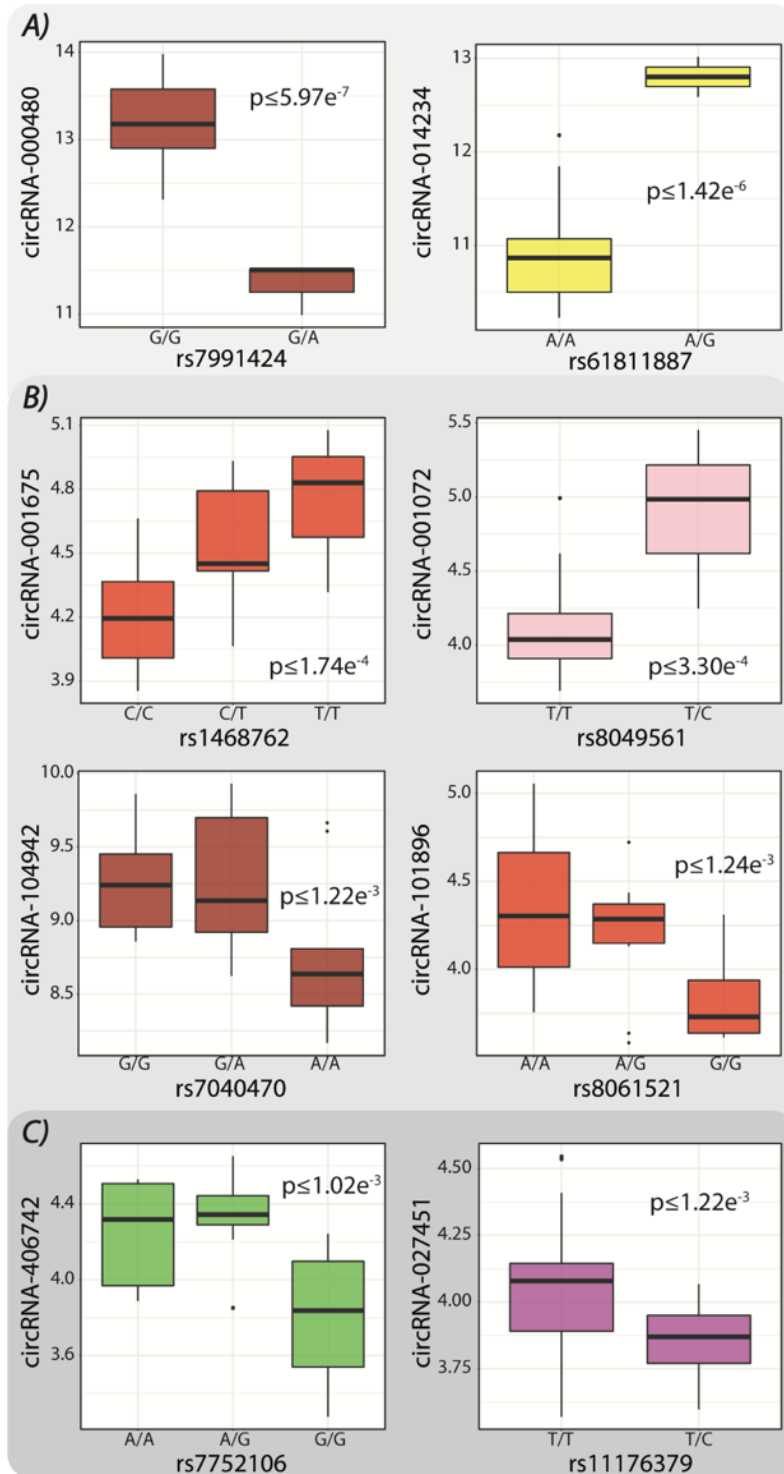
Figure 17: Significant circRNA cis-eQTLs. *A)* eQTLs that survive FDR ≤0.10 significance threshold. *B)* eQTLs from circRNA:miRNA:mRNA trios with negatively correlated miRNA:mRNA, positively correlated miRNA:mRNA, predicted circRNA:miRNA binding, and miRNA:mRNA predicted interactions. *C)* eQTLs for circRNA that participate in circRNA:miRNA:mRNA interactions that survive all our bioinformatics and statistical tests.

4.3.7) CircRNA associated SNPs are enriched within AUD and smoking GWAS.

We employed the Cauchy Combination (CC) and Simes [130, 190] tests to detect eQTLs (n=96) and SNPs in LD with them ($r^2 \geq 0.50$; n=1,558) that were enriched among the significant (p≤5E-4) loci from recent GWAS of AUD and smoking [128] and Psychiatric Genetics Consortium (PGC) AUD GWAS [29]). Adjusting for multiple testing and background enrichment, we observed significant enrichment for our eQTLs in GSCAN cigarettes per day, GSCAN smoking initiation and PGC-AUD European ancestry (*Table 3*).

Study	CC p-value	Simes p-value
GSCAN drinks per week	1	0.2139
GSCAN smoking initiation	0.024*	0.053^
PGC AUD Europeans	0.034*	0.058^
COGA+Irish AUD meta-analysis	0.044*	0.086^
GSCAN cigarettes per day	1.41E-05**	2.74E-05**
GSCAN smoking cessation	1	0.564

Table 3: CircRNA hub eQTL enrichment within addiction GWAS. We observe significant enrichment when comparing eQTLs associated with circRNA hubs from our analysis against recent GWAS of AUD and smoking. ^= p≤0.10, * = p≤0.05, and ** = p≤0.005.

4.4) DISCUSSION

In recent years, studies on AUD have attempted to identify the underlying molecular mechanisms for the development of problematic and addictive drinking behaviors. Much of the functional neurobiological work has been performed in animal models [192], whereas large-scale GWAS have attempted to identify heritable genetic variants associated with AUD and other addictive behaviors [192, 193]. The translation of findings from human genetic studies to functional animal studies, however, has been limited [194]. This is most likely due to the complex non-linear relationships between environmental and genetic factors in humans that are difficult to

recapitulate in animal models of AD. Thus, to address this interaction between environmental and genetic factors we decided to explore the transcriptome (mRNA, miRNA, and circRNA) as the functional endophenotype between genetic variation and molecular processes in human postmortem brain tissue from subjects with AD.

Our group has identified miRNA and mRNA networks associated with AD, assigned biological function to these networks, tested their preservation between cortical and subcortical brain regions and assessed the impact of genetic variation on specific network hub expression [74, 168]. Here, we were interested in complementing these earlier studies to determine the impact of circRNA on the molecular processes underlying the neuropathology of AUD, within the framework of the miRNA sponge hypothesis. Network approaches have the added benefit of aggregating transcripts with small effect sizes into clusters that, when analyzed as a single expression unit, increase power to detect significant results [120]. Additionally, we limit our downstream analyses to the identified circRNA hubs based on their high intramodular connectivity and predicted role as drivers of expression changes for entire modules, effectively increasing their biological relevance to AD [70].

Our study relied upon a series of experimental, statistical and bioinformatics tests to narrow down well over a billion possible interactions between circRNA, miRNA, and mRNA to highly specific three-way interactions within the miRNA sponge hypothesis that survive several layers of correction for multiple testing. Among our most significant circRNA:miRNA interacting pairs, (i.e., circRNA-406702:miR-1200), we observed a unique set of genes negatively correlated with miR-1200 and positively correlated with circRNA-406702. Some of these (such as *HRAS*, *PRKCB*, *HOMER1*, *PCLO*, *ASTN1*, and *ATP2B2*) are enriched within gene-sets associated with synaptic transmission/development, highlighting their potential importance to the neuropathology of AD [195]. HRAS, a small GTP-binding protein, interacts with downstream PI3K, AKT, and

mTORC1 as part of a neurosignalling pathway ("Go" pathway) believed to be important for promoting neuroadaptations associated with excessive alcohol consumption and relapse [196]. This is supported by studies showing *HRAS* expression is increased among mice strains consuming alcohol in high quantities [197], as well as in the NAc of rats with an extended history of excessive consumption followed by periods of abstinence [198]. However, in contrast to the animal-based studies, in our sample, we observed decreased *HRAS* expression in AD subjects. A possible explanation would be that the ligand-gated ion channels mediating HRAS activity become desensitized due to chronic receptor activation after years of alcohol abuse which cannot be easily replicated in animal models [199, 200]. *PRKCB* (protein kinase C beta), another gene implicated in our study, is an isoform of the protein kinase C (PKC) family. This set of proteins is shown to be essential for the development of AD through their interaction with CREB-BDNF neurosignalling pathway, which was reported to be associated with synaptic plasticity . More importantly, genetic variants nearby *PRKCB* have been significantly associated with comorbid bipolar disorder, SUD [204], and alcohol cue-elicited brain activation [203].

Among the other genes interacting with circRNA-406702:miR-1200 are *HOMER1* and *PCLO*, which encode for proteins playing an important role at the synapse. *HOMER1* encodes for one of the Homer scaffolding proteins (Homer1/2), which link metabotropic glutamate receptors (mGlu1-5) to the postsynaptic density [205]. Both HOMER1 and one of the mGlu receptor, GRM5, have been consistently implicated as potential therapeutic targets for the treatment of AD due to their role in regulating alcohol facilitated neuroplasticity [81, 206]. Additionally, it has been shown that a polymorphism (rs7713917) in the regulatory region of *HOMER1* can help predict increased alcohol consumption in adolescents years later [207]. *PCLO* codes for the Piccolo protein, a scaffolding protein at the active zone of the presynaptic cytomatrix, an area where neurotransmitters are released [208]. Intronic SNPs within the *PCLO* gene have been one of the

most studied genetic variants associated with major depressive disorder [209]. Functional studies have suggested that these polymorphisms may play an active role in emotional memory processing [210, 211] and previous research has indicated that deficits in emotional processing is a hallmark of AD [212]. This deficit then may lead to enhanced emotional reactivity to positive and negative stimuli during periods of drinking and periods of withdrawal, effectively reinforcing continued alcohol abuse [213, 214]. Importantly, *PLCO*, along with *HOMER1* have both been implicated as differentially expressed in multiple gene expression studies of AD [215–219]. Finally, *ASTN1* (Astrotactin 1) is a gene that codes for a protein receptor important for glial-guided neuron migration [220]. In the context of AD, a family-based linkage study has shown *ASTN1* is significantly associated with AD in multiplex families. Overall, the results from our study provide further support for research suggesting circRNA play an important, yet still underexplored, role in neuronal function [221].

Some of the miRNAs implicated at various steps in our circRNA analysis, while not all of them directly associated with AD, show significant associations with alcoholic liver disease, brain function, and neuropsychiatric disorders. Among the several miRNA identified from our significant circRNA:miRNA interactions, miR-665 is significantly upregulated in the PFC of alcoholics [96], and miR-361-5p shows increased expression in the PFC of early stage AD mouse models [222]. The maternal expression of another miRNA from our study (miR-3119) was shown to increase following alcohol consumption during pregnancy [223]. Two other miRNAs (miR-1200, and miR-3187-3p) have been implicated in various neurobiological processes relevant to AD etiology. Of these, miR-1200 has been predicted to regulate neuronal connexins 36, 45, and 57 in humans, mice and rats [224]. Connexins (Cx) are essential for gap junction function at electrical synapses, with Cx36 shown to be associated with various rewarding effects of alcohol intoxication in knock-out (KO) mice [225]. Another report has suggested miR-3187-3p expression changes

modify the neuronal cell response to oxidative stress [226]. Increased oxidative stress is a well-known consequence of alcohol's neurotoxic effects in the brain [227] with multiple studies from our group and others identifying increased expression of immune and stress response genes in the postmortem brains of chronic alcohol users [77, 168, 228]. Finally, miR-571 has shown to be an important biomarker for alcohol related liver disease [229]. We further show that miR-571 interacts significantly with *NR3C1*, a highly pleiotropic glucocorticoid receptor, necessary for stress response and reported to be significantly associated with AD [230, 231].

In respect to our cis-eQTL analysis, we identify genetic variants that impact the expression of our circRNA hubs. While no specific polymorphisms at the genome-wide significance level (p≤5E-8) in GWAS of AUD were replicated among our eQTLs, we observed significant enrichment at a lower significance threshold (p≤5e-4) using two separate genomic enrichment tests using recent GWAS of AUD and smoking [29, 128]. Possible explanations for this observation are the limited power of our postmortem brain sample and GWAS of AUD that are still underpowered [232]. However, most likely with increased postmortem brain sample sizes [233] and deep-phenotyping of subjects with chronic alcohol abuse [234], we may begin to see a meaningful overlap between the results from these two methods. Nevertheless, the importance of identifying eQTL enrichment among GWAS signals from our eQTL analysis is two-fold: first, help validate the clinical relevance of these large association studies by providing a functional explanation for AUD associated GWAS signals, and second reinforce such identified eQTLs and SNPs in LD as likely candidates for future, more targeted, follow up analyses. Our study also highlights a potentially novel neurobiological mechanism of alcohol addiction by demonstrating that alcohol abuse may impact the expression of known AD risk genes through altering circRNA expression and circRNA's ability to act as miRNA sponges. Our circRNA eQTL study further suggests that we must be careful when interpreting GWAS signals given that genetic variants impacting the

expression of proximal circRNA can alter the expression of distal genes through the epistatic interaction between circRNA and miRNA.

Our study does also have a few limitations. First, it is possible that by focusing solely on the circRNA and miRNA interactions, we may have overlooked other molecular mechanisms (i.e. epigenetic factors) that potentially can also affect the functions of risk AD loci. Second, while the use of male subjects only can be perceived as a limitation, this was a deliberate choice in order to increase our statistical power by removing sex-based variability. Genetic epidemiological studies have shown that male and female subjects have a similar genetic predisposition with respect to alcohol abuse [161].

In summary, to the best of our knowledge, ours is the first to specifically investigate the effect of circRNA and miRNA interactions on gene expression in NAc from subjects with AD. We are confident that this pilot study opens the door for future studies that will corroborate our findings by experimentally validating these results and further exploring them in the context of increased and more diverse postmortem brain databases. Moreover, we believe that our study will be the steppingstone on which future studies will expand on our integrative analytical approach to incorporate other brain regions and psychiatric phenotypes.

CHAPTER 5

CONCLUSION

5.1) SUMMARY

The purpose of this dissertation was to identify biological processes associated with AUD via comparative transcriptomic analyses from the postmortem brains of chronic alcohol abusers. We also explored the regulatory mechanisms for significant differential expression through integrating ncRNA interactions and genotypic information. Overall, we identified DEG networks associated with AD that displayed either high or low levels of network preservation between areas of the MCL, while also providing a novel mechanism for the regulation of AUD associated genes in the form of circRNA:miRNA:mRNA interactions.

In *Study 1*, we validate previous research that shows immune/stress response upregulation is associated with AD, which is believed to be the neurotoxic consequence of chronic ethanol exposure in the brain. More specifically, we implicate the differentially expressed MT cluster as an oxidative stress response mechanism that can impact synaptic plasticity through regulating extracellular Zn^{2+}, an important cofactor for neurotransmission [137, 138, 235]. When we examine biological processes that show little to no conservation between brain regions, we observe that genes associated with cilia based cell projection appear to be disproportionately dysregulated within the NAc of chronic alcohol abusers. This could be representative of experience-based adult neurogenesis of medium spiny neurons facilitated by alcohol consumption and intoxication [147]. These findings set the framework for looking at biological processes that underlie specific addiction reinforcing behaviors based on functional specialization and the differences in gene dysregulation between cortical and subcortical brain regions. In a broad sense, we hope investigating specific

brain regions within the context of AUD can inform more focused therapeutic interventions to target neurobiological processes that impact addiction in a brain-region specific manner.

Study 2 serves as a pilot study for assessing circRNA expression changes in the postmortem brain of chronic alcohol abusers while also providing the analytical framework for investigating miRNA sponge interactions *in silico*. Our integrative statistical and bioinformatic approach which included correlation, ncRNA target prediction, and moderation regression, allowed us to identify significant circRNA:miRNA:mRNA interactions associated with AD. More importantly, these findings revealed significant circRNA interacting genes that are associated with trans-synaptic signaling and neuroplasticity, meaningful biological processes in respect to the development of addictive behaviors [195]. Additionally, we identified significant cis-eQTLs for differentially expressed circRNA that also show overlap with recent GWAS of AUD and smoking. By highlighting GWAS enriched SNPs associated with circRNA that participate in significant miRNA sponge interactions, we provide a functional explanation for previous GWAS where interpretation has been notoriously challenging [236, 237]. These findings also highlight additional issues when interpreting GWAS. Significant hits are often inherently associated with the genes at proximal loci or the genes in which they are embedded [238]. When we consider circRNA, there is the possibility a local SNP may impact the expression of an intronic/exonic circRNA rather than the expression of its host gene, leading to functional expression changes at distal loci due to circRNA:miRNA:mRNA interactions.

The results from these two studies highlight the utility of postmortem brains and transcriptomic profiling for the study of AUD and other SUDs. We reveal novel neurobiological processes of particular relevance to the development of AUD within the framework of the cycle of addiction. We also provide the first account of circRNA as important molecular moderators for expression changes of previously identified AUD risk genes through their role as miRNA sponges.

5.2) **LIMITATIONS**

Like most research, this dissertation is not without its own set of limitations. Most notably is our decreased statistical power to detect significant results due to limited samples sizes. To combat this, we utilized robust statistical analyses in which cases and controls were matched for biological and technical covariates in an effort to control for potential confounds. In most cases we still identified substantial effect sizes for DEG that can be deemed significant even after FDR correction. This is unfortunately a limitation that is shared across all postmortem brain studies given the limited availability of useable tissue [180]. As brain banks worldwide continue to expand their repositories, the scientific impact of postmortem brain studies will continue to increase as sample sizes increase. Additionally, in an effort to limit the effect of confounding factors, we made the conscious decision to only utilize male tissue. Therefore, it is important to acknowledge that the findings presented here can only be interpreted within the context of people assigned male at birth. Finally, as mentioned in Chapter 1, we have to be careful when making causal inferences from our results, given that cases represent chronic alcohol abusers diagnosed with severe AD. For this reason, it is difficult to determine if these results are indicative of biological processes dysregulated in response to chronic alcohol consumption or if they represent predictive risk factors that cause AUD. Like other neuropsychiatric disorders, AD risk is determined based on a combination of environmental and genetic factors [161, 166]. Interestingly for AUD, the act of consuming alcohol serves as an environmental risk factor in itself, creating a feedback loop for continued abuse due to positive or negative reinforcement and conditioning during periods of intoxication followed by withdrawal. So, while we acknowledge that determining the causal relationship between our data and the development of AUD is limited, we do reveal biological

process and gene regulatory mechanisms that can still serve as useful biomarkers for predicting and potentially treating AUD.

5.3) FUTURE DIRECTION

The research presented in this dissertation provides the framework for future molecular genetic studies of AUD and other neuropsychiatric disorders. Most notably is the need to replicate and validate these findings in both expanded postmortem brain studies and experimental studies using proven animal and cell models as proxies for human brain tissue. Ideally, future research can utilize the computational framework presented to investigate DEG networks associated with AUD that are shared or unique to other brain regions believed important for addiction (i.e. the VTA, hippocampus, and amygdala). Additionally, we believe our study design for both comparing the transcriptomic profiles between different brain regions and assessing disease associated circRNA:miRNA:mRNA interactions can be easily translated to the study of other neuropsychiatric and neurodegenerative disorders. Experimental validation of *Study 2* results will be key for determining if our *in silico* predictions of circRNA acting as miRNA sponges accurately represent what is occurring *in vivo*. One possibility would be performing a luciferase reporter experiment [239] on a circRNA:miRNA:mRNA trio to assess the ability of miRNA to attenuate the expression of the target gene in the presence of circRNA expressed in different quantities. When the miRNA is overexpressed, it is expected to observe decreased mRNA expression, but when circRNA is spiked-in, the effect of miRNA on mRNA expression will be weakened as miRNA preferentially interacts with the overexpressed circRNA instead. Additionally, it would be possible to perform knockout and knockdown experiments on animal models in which the expression of miRNA and circRNA are manipulated to explore the mediating effect of circRNA:miRNA

interactions on mRNA expression. In a broader sense, the findings presented here and in follow up studies should be explored within the context of identifying targeted therapeutics for ethanol sensitive biological processes to help prevent and protect against the development of severe debilitating AUD.

REFERENCES

[1] Boffetta P, Lowenfels AB, Burns H, Brawley O, Rehm J. *Alcohol: Science, Policy and Public Health*. OUP Oxford, 2013.

[2] Rehm J. The Risks Associated With Alcohol Use and Alcoholism. *Alcohol Research & Health* 2011; 34: 135–143.

[3] Corrao G, Rubbiati L, Bagnardi V, Zambon A, Poikolainen K. Alcohol and coronary heart disease: a meta-analysis. *Addiction* 2000; 95: 1505–1523.

[4] Diehl AM. Liver disease in alcohol abusers: clinical perspective. *Alcohol* 2002; 27: 7–11.

[5] Clapp P, Bhave SV, Hoffman PL. How Adaptation of the Brain to Alcohol Leads to Dependence. *Alcohol Res Health* 2008; 31: 310–339.

[6] Dawson DA, Goldstein RB, Grant BF. Differences in the Profiles of DSM-IV and DSM-5 Alcohol Use Disorders: Implications for Clinicians. *Alcohol Clin Exp Res* 2013; 37: E305–E313.

[7] Koob GF, Volkow ND. Neurocircuitry of Addiction. *Neuropsychopharmacology* 2010; 35: 217–238.

[8] Montesinos J, Alfonso-Loeches S, Guerri C. Impact of the Innate Immune Response in the Actions of Ethanol on the Central Nervous System. *Alcoholism: Clinical and Experimental Research* 2016; 40: 2260–2270.

[9] Nery S, Fishell G, Corbin JG. The caudal ganglionic eminence is a source of distinct cortical and subcortical cell populations. *Nature Neuroscience* 2002; 5: 1279–1287.

[10] Sekar S, Liang WS. Circular RNA expression and function in the brain. *Noncoding RNA Res* 2019; 4: 23–29.

[11] Organization WH. *Global Status Report on Alcohol and Health 2018*. World Health Organization, 2019.

[12] Rehm J, Mathers C, Popova S, Thavorncharoensap M, Teerawattananon Y, Patra J. Global burden of disease and injury and economic cost attributable to alcohol use and alcohol-use disorders. *Lancet* 2009; 373: 2223–2233.

[13] Association AP. *Diagnostic and Statistical Manual of Mental Disorders (DSM-5®)*. American Psychiatric Pub, 2013.

[14] Room R, Babor T, Rehm J. Alcohol and public health. *The Lancet* 2005; 365: 519–530.

[15] Koob GF, Volkow ND. Neurobiology of addiction: a neurocircuitry analysis. *Lancet Psychiatry* 2016; 3: 760–773.

[16]   Abernathy K, Chandler LJ, Woodward JJ. ALCOHOL AND THE PREFRONTAL CORTEX. *Int Rev Neurobiol* 2010; 91: 289–320.

[17]   Quintero GC. Role of nucleus accumbens glutamatergic plasticity in drug addiction. *Neuropsychiatr Dis Treat* 2013; 9: 1499–1512.

[18]   Koob GF, Volkow ND. Neurocircuitry of Addiction. *Neuropsychopharmacology* 2010; 35: 217–238.

[19]   Ponnappa BC, Rubin E. Modeling Alcohol's Effects on Organs in Animal Models. *Alcohol Research & Health* 2000; 24: 93.

[20]   Alasmari F, Goodwani S, McCullumsmith RE, Sari Y. Role of glutamatergic system and mesocorticolimbic circuits in alcohol dependence. *Prog Neurobiol* 2018; 171: 32–49.

[21]   Weiss F, Porrino LJ. Behavioral Neurobiology of Alcohol Addiction: Recent Advances and Challenges. *J Neurosci* 2002; 22: 3332–3337.

[22]   Di Nicola M, Tedeschi D, De Risio L, Pettorruso M, Martinotti G, Ruggeri F, et al. Co-occurrence of alcohol use disorder and behavioral addictions: relevance of impulsivity and craving. *Drug and Alcohol Dependence* 2015; 148: 118–125.

[23]   Creed M, Kaufling J, Fois GR, Jalabert M, Yuan T, Lüscher C, et al. Cocaine Exposure Enhances the Activity of Ventral Tegmental Area Dopamine Neurons via Calcium-Impermeable NMDARs. *J Neurosci* 2016; 36: 10759–10768.

[24]   Myrick H, Anton RF, Li X, Henderson S, Drobes D, Voronin K, et al. Differential Brain Activity in Alcoholics and Social Drinkers to Alcohol Cues: Relationship to Craving. *Neuropsychopharmacology* 2004; 29: 393.

[25]   Abrahao KP, Salinas AG, Lovinger DM. Alcohol and the Brain: Neuronal Molecular Targets, Synapses, and Circuits. *Neuron* 2017; 96: 1223.

[26]   Harris RA, Trudell JR, Mihic SJ. Ethanol's Molecular Targets. *Sci Signal* 2008; 1: re7–re7.

[27]   Beisswenger TB, Holmquist B, Vallee BL. chi-ADH is the sole alcohol dehydrogenase isozyme of mammalian brains: implications and inferences. *Proc Natl Acad Sci U S A* 1985; 82: 8369–8373.

[28]   Heit C, Dong H, Chen Y, Thompson DC, Deitrich RA, Vasiliou V. The Role of CYP2E1 in Alcohol Metabolism and Sensitivity in the Central Nervous System. *Subcell Biochem* 2013; 67: 235–247.

[29]   Walters RK, Polimanti R, Johnson EC, McClintick JN, Adams MJ, Adkins AE, et al. Transancestral GWAS of alcohol dependence reveals common genetic underpinnings with psychiatric disorders. *Nature Neuroscience* 2018; 21: 1656–1669.

[30]   Tawa EA, Hall SD, Lohoff FW. Overview of the Genetics of Alcohol Use Disorder. *Alcohol Alcohol* 2016; 51: 507–514.

[31]   Kranzler HR, Zhou H, Kember RL, Vickers Smith R, Justice AC, Damrauer S, et al. Genome-wide association study of alcohol consumption and use disorder in 274,424 individuals from multiple populations. *Nature Communications* 2019; 10: 1499.

[32]   Park BL, Kim JW, Cheong HS, Kim LH, Lee BC, Seo CH, et al. Extended genetic effects of ADH cluster genes on the risk of alcohol dependence: from GWAS to replication. *Hum Genet* 2013; 132: 657–668.

[33]   Ron D, Berger A. Targeting the intracellular signaling "STOP" and "GO" pathways for the treatment of alcohol use disorders. *Psychopharmacology* 2018; 235: 1727–1743.

[34]   Ron D, Barak S. Molecular mechanisms underlying alcohol-drinking behaviours. *Nat Rev Neurosci* 2016; 17: 576–591.

[35]   Coultrap SJ, Bayer KU. CaMKII regulation in information processing and storage. *Trends Neurosci* 2012; 35: 607–618.

[36]   Wang J, Lanfranco MF, Gibb SL, Yowell QV, Carnicella S, Ron D. Long-lasting adaptations of the NR2B-containing NMDA receptors in the dorsomedial striatum play a crucial role in alcohol consumption and relapse. *J Neurosci* 2010; 30: 10187–10198.

[37]   Ohnishi H, Murata Y, Okazawa H, Matozaki T. Src family kinases: modulators of neurotransmitter receptor function and behavior. *Trends Neurosci* 2011; 34: 629–637.

[38]   Ben Hamida S, Neasta J, Lasek AW, Kharazia V, Zou M, Carnicella S, et al. The small G protein H-Ras in the mesolimbic system is a molecular gateway to alcohol-seeking and excessive drinking behaviors. *J Neurosci* 2012; 32: 15849–15858.

[39]   Baouz S, Jacquet E, Accorsi K, Hountondji C, Balestrini M, Zippel R, et al. Sites of phosphorylation by protein kinase A in CDC25Mm/GRF1, a guanine nucleotide exchange factor for Ras. *J Biol Chem* 2001; 276: 1742–1749.

[40]   McGough NNH, He D-Y, Logrip ML, Jeanblanc J, Phamluong K, Luong K, et al. RACK1 and brain-derived neurotrophic factor: a homeostatic pathway that regulates alcohol addiction. *J Neurosci* 2004; 24: 10542–10552.

[41]   Logrip ML, Janak PH, Ron D. Escalating ethanol intake is associated with altered corticostriatal BDNF expression. *J Neurochem* 2009; 109: 1459–1468.

[42]   Logrip ML, Barak S, Warnault V, Ron D. Corticostriatal BDNF and alcohol addiction. *Brain Res* 2015; 1628: 60–67.

[43]   Hensler JG, Ladenheim EE, Lyons WE. Ethanol consumption and serotonin-1A (5-HT1A) receptor function in heterozygous BDNF (+/-) mice. *J Neurochem* 2003; 85: 1139–1147.

[44] Gorka SM, Teppen T, Radoman M, Phan KL, Pandey SC. Human Plasma BDNF Is Associated With Amygdala-Prefrontal Cortex Functional Connectivity and Problem Drinking Behaviors. *Int J Neuropsychopharmacol* 2020; 23: 1–11.

[45] de la Grange P, Gratadou L, Delord M, Dutertre M, Auboeuf D. Splicing factor and exon profiling across human tissues. *Nucleic Acids Res* 2010; 38: 2825–2838.

[46] Ramsköld D, Wang ET, Burge CB, Sandberg R. An Abundance of Ubiquitously Expressed Genes Revealed by Tissue Transcriptome Sequence Data. *PLOS Computational Biology* 2009; 5: e1000598.

[47] Cáceres M, Lachuer J, Zapala MA, Redmond JC, Kudo L, Geschwind DH, et al. Elevated gene expression levels distinguish human from non-human primate brains. *Proc Natl Acad Sci USA* 2003; 100: 13030–13035.

[48] Enard W, Khaitovich P, Klose J, Zöllner S, Heissig F, Giavalisco P, et al. Intra- and interspecific variation in primate gene expression patterns. *Science* 2002; 296: 340–343.

[49] Khaitovich P, Muetzel B, She X, Lachmann M, Hellmann I, Dietzsch J, et al. Regional patterns of gene expression in human and chimpanzee brains. *Genome Res* 2004; 14: 1462–1473.

[50] Lin S, Lin Y, Nery JR, Urich MA, Breschi A, Davis CA, et al. Comparison of the transcriptional landscapes between human and mouse tissues. *PNAS* 2014; 111: 17224–17229.

[51] Mortazavi A, Williams BA, McCue K, Schaeffer L, Wold B. Mapping and quantifying mammalian transcriptomes by RNA-Seq. *Nature Methods* 2008; 5: 621–628.

[52] Wang ET, Sandberg R, Luo S, Khrebtukova I, Zhang L, Mayr C, et al. Alternative isoform regulation in human tissue transcriptomes. *Nature* 2008; 456: 470–476.

[53] Yeo G, Holste D, Kreiman G, Burge CB. Variation in alternative splicing across human tissues. *Genome Biol* 2004; 5: R74.

[54] Nestler EJ, Hyman SE. Animal models of neuropsychiatric disorders. *Nature Neuroscience* 2010; 13: 1161–1169.

[55] Goltseker K, Hopf FW, Barak S. Advances in behavioral animal models of alcohol use disorder. *Alcohol* 2019; 74: 73–82.

[56] Blanchard RJ, McKittrick CR, Blanchard DC. Animal models of social stress: effects on behavior and brain neurochemical systems. *Physiology & Behavior* 2001; 73: 261–271.

[57] Cryan JF, Holmes A. Model organisms: The ascent of mouse: advances in modelling human depression and anxiety. *Nature Reviews Drug Discovery* 2005; 4: 775–790.

[58]   Lister RG. Ethologically-based animal models of anxiety disorders. *Pharmacology & Therapeutics* 1990; 46: 321–340.

[59]   Glantz MD. Addiction Models and the Challenge of Having Impact. *Alcoholism: Clinical and Experimental Research* 2019; 43: 1823–1828.

[60]   Castillo-Carniglia A, Keyes KM, Hasin DS, Cerdá M. Psychiatric comorbidities in alcohol use disorder. *The Lancet Psychiatry* 2019; 6: 1068–1080.

[61]   Field M, Kersbergen I. Are animal models of addiction useful? *Addiction* 2020; 115: 6–12.

[62]   Harper C, Garrick T, Matsumoto I, Pfefferbaum A, Adalsteinsson E, Sullivan E, et al. How Important Are Brain Banks for Alcohol Research? *Alcoholism: Clinical and Experimental Research* 2003; 27: 310–323.

[63]   Jordan B. Historical background and anticipated developments. *Ann N Y Acad Sci* 2002; 975: 24–32.

[64]   VanGuilder HD, Vrana KE, Freeman WM. Twenty-five years of quantitative PCR for gene expression analysis. *BioTechniques* 2008; 44: 619–626.

[65]   Dheda K, Huggett JF, Bustin SA, Johnson MA, Rook G, Zumla A. Validation of housekeeping genes for normalizing RNA expression in real-time PCR. *BioTechniques* 2004; 37: 112–119.

[66]   Schena M, Shalon D, Davis RW, Brown PO. Quantitative Monitoring of Gene Expression Patterns with a Complementary DNA Microarray. *Science* 1995; 270: 467–470.

[67]   Barabási A-L, Gulbahce N, Loscalzo J. Network medicine: a network-based approach to human disease. *Nature Reviews Genetics* 2011; 12: 56–68.

[68]   Langfelder P, Horvath S. WGCNA: an R package for weighted correlation network analysis. *BMC Bioinformatics* 2008; 9: 559.

[69]   Subramanian A, Tamayo P, Mootha VK, Mukherjee S, Ebert BL, Gillette MA, et al. Gene set enrichment analysis: A knowledge-based approach for interpreting genome-wide expression profiles. *PNAS* 2005; 102: 15545–15550.

[70]   Langfelder P, Mischel PS, Horvath S. When Is Hub Gene Selection Better than Standard Meta-Analysis? *PLOS ONE* 2013; 8: e61505.

[71]   Gilad Y, Rifkin SA, Pritchard JK. Revealing the architecture of gene regulation: the promise of eQTL studies. *Trends in Genetics* 2008; 24: 408–415.

[72]   Bryois J, Buil A, Evans DM, Kemp JP, Montgomery SB, Conrad DF, et al. Cis and Trans Effects of Human Genomic Variants on Gene Expression. *PLOS Genetics* 2014; 10: e1004461.

[73] Liu J, Lewohl JM, Harris RA, Iyer VR, Dodd PR, Randall PK, et al. Patterns of Gene Expression in the Frontal Cortex Discriminate Alcoholic from Nonalcoholic Individuals. *Neuropsychopharmacology* 2006; 31: 1574–1582.

[74] Mamdani M, Williamson V, McMichael GO, Blevins T, Aliev F, Adkins A, et al. Integrating mRNA and miRNA Weighted Gene Co-Expression Networks with eQTLs in the Nucleus Accumbens of Subjects with Alcohol Dependence. *PLOS ONE* 2015; 10: e0137671.

[75] Farris SP, Arasappan D, Hunicke-Smith S, Harris RA, Mayfield RD. Transcriptome Organization for Chronic Alcohol Abuse in Human Brain. *Mol Psychiatry* 2015; 20: 1438–1447.

[76] Warden AS, Mayfield RD. Gene expression profiling in the human alcoholic brain. *Neuropharmacology* 2017; 122: 161–174.

[77] Kapoor M, Wang J-C, Farris SP, Liu Y, McClintick J, Gupta I, et al. Analysis of whole genome-transcriptomic organization in brain to identify genes associated with alcoholism. *Translational Psychiatry* 2019; 9: 1–11.

[78] Zhou Z, Yuan Q, Mash DC, Goldman D. Substance-specific and shared transcription and epigenetic changes in the human hippocampus chronically exposed to cocaine and alcohol. *PNAS* 2011; 108: 6626–6631.

[79] Farris SP, Dayne Mayfield R. Chapter Eleven - RNA-Seq Reveals Novel Transcriptional Reorganization in Human Alcoholic Brain. In: Hitzemann R, Mcweeney S (eds) *International Review of Neurobiology*. Academic Press, pp. 275–300.

[80] Koob GF. A role for GABA mechanisms in the motivational effects of alcohol. *Biochemical Pharmacology* 2004; 68: 1515–1525.

[81] Goodwani S, Saternos H, Alasmari F, Sari Y. Metabotropic and ionotropic glutamate receptors as potential targets for the treatment of alcohol use disorder. *Neuroscience & Biobehavioral Reviews* 2017; 77: 14–31.

[82] Ponomarev I, Wang S, Zhang L, Harris RA, Mayfield RD. Gene Coexpression Networks in Human Brain Identify Epigenetic Modifications in Alcohol Dependence. *J Neurosci* 2012; 32: 1884–1897.

[83] Jurd R, Thornton C, Wang J, Luong K, Phamluong K, Kharazia V, et al. Mind Bomb-2 Is an E3 Ligase That Ubiquitinates the N-Methyl-d-aspartate Receptor NR2B Subunit in a Phosphorylation-dependent Manner. *J Biol Chem* 2008; 283: 301–310.

[84] Yi Z, Petralia RS, Fu Z, Swanwick CC, Wang Y-X, Prybylowski K, et al. The Role of the PDZ Protein GIPC in Regulating NMDA Receptor Trafficking. *J Neurosci* 2007; 27: 11663–11675.

[85] Eisenhardt M, Leixner S, Luján R, Spanagel R, Bilbao A. Glutamate Receptors within the Mesolimbic Dopamine System Mediate Alcohol Relapse Behavior. *J Neurosci* 2015; 35: 15523–15538.

[86] Bartel DP. MicroRNAs: Genomics, Biogenesis, Mechanism, and Function. *Cell* 2004; 116: 281–297.

[87] Diederichs S, Haber DA. Dual role for argonautes in microRNA processing and posttranscriptional regulation of microRNA expression. *Cell* 2007; 131: 1097–1108.

[88] Ritchie W, Flamant S, Rasko JEJ. Predicting microRNA targets and functions: traps for the unwary. *Nature Methods* 2009; 6: 397–398.

[89] John B, Enright AJ, Aravin A, Tuschl T, Sander C, Marks DS. Human MicroRNA Targets. *PLOS Biology* 2004; 2: e363.

[90] Lewis BP, Burge CB, Bartel DP. Conserved seed pairing, often flanked by adenosines, indicates that thousands of human genes are microRNA targets. *Cell* 2005; 120: 15–20.

[91] Kertesz M, Iovino N, Unnerstall U, Gaul U, Segal E. The role of site accessibility in microRNA target recognition. *Nature Genetics* 2007; 39: 1278–1284.

[92] Stappert L, Roese-Koerner B, Brüstle O. The role of microRNAs in human neural stem cells, neuronal differentiation and subtype specification. *Cell Tissue Res* 2015; 359: 47–64.

[93] Ludwig N, Leidinger P, Becker K, Backes C, Fehlmann T, Pallasch C, et al. Distribution of miRNA expression across human tissues. *Nucleic Acids Res* 2016; 44: 3865–3877.

[94] Issler O, Chen A. Determining the role of microRNAs in psychiatric disorders. *Nature Reviews Neuroscience* 2015; 16: 201–212.

[95] Most D, Leiter C, Blednov YA, Harris RA, Mayfield RD. Synaptic microRNAs Coordinately Regulate Synaptic mRNAs: Perturbation by Chronic Alcohol Consumption. *Neuropsychopharmacology* 2016; 41: 538–548.

[96] Lewohl JM, Nunez YO, Dodd PR, Tiwari GR, Harris RA, Mayfield RD. Up-Regulation of MicroRNAs in Brain of Human Alcoholics. *Alcoholism: Clinical and Experimental Research* 2011; 35: 1928–1937.

[97] Miranda RC, Pietrzykowski AZ, Tang Y, Sathyan P, Mayfield D, Keshavarzian A, et al. MicroRNAs: master regulators of ethanol abuse and toxicity? *Alcohol Clin Exp Res* 2010; 34: 575–587.

[98] Most D, Workman E, Harris RA. Synaptic adaptations by alcohol and drugs of abuse: changes in microRNA expression and mRNA regulation. *Front Mol Neurosci* 2014; 7: 85.

[99] Li Y, Zheng Q, Bao C, Li S, Guo W, Zhao J, et al. Circular RNA is enriched and stable in exosomes: a promising biomarker for cancer diagnosis. *Cell Research* 2015; 25: 981–984.

[100] Chen L-L, Yang L. Regulation of circRNA biogenesis. *RNA Biology* 2015; 12: 381–388.

[101] Eulalio A, Huntzinger E, Izaurralde E. Getting to the root of miRNA-mediated gene silencing. *Cell* 2008; 132: 9–14.

[102] Panda AC. Circular RNAs Act as miRNA Sponges. In: Xiao J (ed) *Circular RNAs: Biogenesis and Functions*. Singapore: Springer, pp. 67–79.

[103] Mehta SL, Dempsey RJ, Vemuganti R. Role of circular RNAs in brain development and CNS diseases. *Progress in Neurobiology* 2020; 186: 101746.

[104] Maass PG, Glažar P, Memczak S, Dittmar G, Hollfinger I, Schreyer L, et al. A map of human circular RNAs in clinically relevant tissues. *J Mol Med* 2017; 95: 1179–1189.

[105] Rodd ZA, Kimpel MW, Edenberg HJ, Bell RL, Strother WN, McClintick JN, et al. Differential gene expression in the nucleus accumbens with ethanol self-administration in inbred alcohol-preferring rats. *Pharmacology Biochemistry and Behavior* 2008; 89: 481–498.

[106] Xu K, Anderson TR, Neyer KM, Lamparella N, Jenkins G, Zhou Z, et al. Nucleotide sequence variation within the human tyrosine kinase B neurotrophin receptor gene: association with antisocial alcohol dependence. *The Pharmacogenomics Journal* 2007; 7: 368–379.

[107] Dou X, Feng L, Ying N, Ding Q, Song Q, Jiang F, et al. RNA Sequencing Reveals a Comprehensive Circular RNA Expression Profile in a Mouse Model of Alcoholic Liver Disease. *Alcoholism: Clinical and Experimental Research* 2020; 44: 415–422.

[108] Meng H, Wang L, You H, Huang C, Li J. Circular RNA expression profile of liver tissues in an EtOH-induced mouse model of alcoholic hepatitis. *European Journal of Pharmacology* 2019; 862: 172642.

[109] Yang Y, Chen H, Ding N, Wang S, Duan Z, Birnbaum Y, et al. Expression Profiling of Circular RNAs and Micrornas in Heart Tissue of Mice with Alcoholic Cardiomyopathy. *CPB* 2018; 46: 2284–2296.

[110] Verhulst B, Neale MC, Kendler KS. The heritability of alcohol use disorders: a meta-analysis of twin and adoption studies. *Psychological medicine* 2015; 45: 1061.

[111] Koob GF, Moal ML. Plasticity of reward neurocircuitry and the 'dark side' of drug addiction. *Nat Neurosci* 2005; 8: 1442–1444.

[112] Gilpin NW, Koob GF. Neurobiology of Alcohol Dependence: Focus on Motivational Mechanisms. *Alcohol Research & Health* 2008; 31: 185.

[113] Harper C, Dixon G, Sheedy D, Garrick T. Neuropathological alterations in alcoholic brains. Studies arising from the New South Wales Tissue Resource Centre. *Progress in Neuro-Psychopharmacology and Biological Psychiatry* 2003; 27: 951–961.

[114] Sutherland GT, Sheedy D, Kril JJ. Using autopsy brain tissue to study alcohol-related brain damage in the genomic age. *Alcohol Clin Exp Res* 2014; 38: 1–8.

[115] Alasmari F, Goodwani S, McCullumsmith RE, Sari Y. Role of glutamatergic system and mesocorticolimbic circuits in alcohol dependence. *Prog Neurobiol* 2018; 171: 32–49.

[116] McMichael GO, Drake J, Vornholt ES, Cresswell K, Williamson V, Chatzinakos C, et al. Assessing the role of long-noncoding RNA in nucleus accumbens in subjects with alcohol dependence. *bioRxiv* 2019; 583203.

[117] Flatscher-Bader T, van der Brug M, Hwang JW, Gochee PA, Matsumoto I, Niwa S, et al. Alcohol-responsive genes in the frontal cortex and nucleus accumbens of human alcoholics. *Journal of Neurochemistry* 2005; 93: 359–370.

[118] Liu J, Lewohl JM, Harris RA, Iyer VR, Dodd PR, Randall PK, et al. Patterns of gene expression in the frontal cortex discriminate alcoholic from nonalcoholic individuals. *Neuropsychopharmacology* 2006; 31: 1574–1582.

[119] Luo J, Xu P, Cao P, Wan H, Lv X, Xu S, et al. Integrating Genetic and Gene Co-expression Analysis Identifies Gene Networks Involved in Alcohol and Stress Responses. *Front Mol Neurosci*; 11. Epub ahead of print 2018. DOI: 10.3389/fnmol.2018.00102.

[120] Zhang B, Horvath S. A general framework for weighted gene co-expression network analysis. *Stat Appl Genet Mol Biol* 2005; 4: Article17.

[121] Schadt EE, Lamb J, Yang X, Zhu J, Edwards S, GuhaThakurta D, et al. An integrative genomics approach to infer causal associations between gene expression and disease. *Nat Genet* 2005; 37: 710–717.

[122] Weis S, Llenos IC, Dulay JR, Elashoff M, Martínez-Murillo F, Miller CL. Quality control for microarray analysis of human brain samples: The impact of postmortem factors, RNA characteristics, and histopathology. *J Neurosci Methods* 2007; 165: 198–209.

[123] Irizarry RA, Bolstad BM, Collin F, Cope LM, Hobbs B, Speed TP. Summaries of Affymetrix GeneChip probe level data. *Nucleic Acids Res* 2003; 31: e15–e15.

[124] Osterndorff-Kahanek EA, Becker HC, Lopez MF, Farris SP, Tiwari GR, Nunez YO, et al. Chronic Ethanol Exposure Produces Time- and Brain Region-Dependent Changes in Gene Coexpression Networks. *PLOS ONE* 2015; 10: e0121522.

[125] Hoffman GE, Schadt EE. variancePartition: interpreting drivers of variation in complex gene expression studies. *BMC Bioinformatics* 2016; 17: 483.

[126] Langfelder P, Luo R, Oldham MC, Horvath S. Is My Network Module Preserved and Reproducible? *PLOS Computational Biology* 2011; 7: e1001057.

[127] Ge SX, Jung D. ShinyGO: a graphical enrichment tool for ani-mals and plants. *bioRxiv* 2018; 315150.

[128] Chang L-H, Couvy-Duchesne B, Liu M, Medland SE, Verhulst B, Benotsch EG, et al. Association between polygenic risk for tobacco or alcohol consumption and liability to licit and illicit substance use in young Australian adults. *Drug and Alcohol Dependence* 2019; 197: 271–279.

[129] Edenberg HJ. The Collaborative Study on the Genetics of Alcoholism: An Update. *Alcohol Research & Health* 2002; 26: 214–218.

[130] Li M-X, Gui H-S, Kwan JSH, Sham PC. GATES: a rapid and powerful gene-based association test using extended Simes procedure. *Am J Hum Genet* 2011; 88: 283–293.

[131] GTEx Consortium. The Genotype-Tissue Expression (GTEx) project. *Nat Genet* 2013; 45: 580–585.

[132] Teffer K, Semendeferi K. Chapter 9 - Human prefrontal cortex: Evolution, development, and pathology. In: Hofman MA, Falk D (eds) *Progress in Brain Research*. Elsevier, pp. 191–218.

[133] Colton CA. Heterogeneity of Microglial Activation in the Innate Immune Response in the Brain. *J Neuroimmune Pharmacol* 2009; 4: 399–418.

[134] Farina C, Aloisi F, Meinl E. Astrocytes are active players in cerebral innate immunity. *Trends in Immunology* 2007; 28: 138–145.

[135] Vallee BL. The function of metallothionein. *Neurochem Int* 1995; 27: 23–33.

[136] Jörnvall H, Persson B, Jeffery J. Characteristics of alcohol/polyol dehydrogenases. *European Journal of Biochemistry* 1987; 167: 195–201.

[137] Paoletti P, Vergnano AM, Barbour B, Casado M. Zinc at glutamatergic synapses. *Neuroscience* 2009; 158: 126–136.

[138] Skalny AV, Skalnaya MG, Grabeklis AR, Skalnaya AA, Tinkov AA. Zinc deficiency as a mediator of toxic effects of alcohol abuse. *Eur J Nutr* 2018; 57: 2313–2322.

[139] Nery S, Fishell G, Corbin JG. The caudal ganglionic eminence is a source of distinct cortical and subcortical cell populations. *Nat Neurosci* 2002; 5: 1279–1287.

[140] Whitfield JF. The neuronal primary cilium—an extrasynaptic signaling device. *Cellular Signalling* 2004; 16: 763–767.

[141] Guemez-Gamboa A, Coufal NG, Gleeson JG. Primary cilia in the developing and mature brain. *Neuron* 2014; 82: 511–521.

[142] Smith ACW, Scofield MD, Kalivas PW. The tetrapartite synapse: Extracellular matrix remodeling contributes to corticoaccumbens plasticity underlying drug addiction. *Brain Research* 2015; 1628: 29–39.

[143] Ehrlich AT, Semache M, Bailly J, Wojcik S, Arefin TM, Colley C, et al. Mapping GPR88-Venus illuminates a novel role for GPR88 in sensory processing. *Brain Struct Funct* 2018; 223: 1275–1296.

[144] Ben Hamida S, Mendonça-Netto S, Arefin TM, Nasseef MT, Boulos L-J, McNicholas M, et al. Increased Alcohol Seeking in Mice Lacking Gpr88 Involves Dysfunctional Mesocorticolimbic Networks. *Biol Psychiatry* 2018; 84: 202–212.

[145] Choi MR, Han JS, Chai YG, Jin Y-B, Lee S-R, Kim D-J. Gene expression profiling in the hippocampus of adolescent rats after chronic alcohol administration. *Basic & Clinical Pharmacology & Toxicology*. Epub ahead of print 19 October 2019. DOI: 10.1111/bcpt.13342.

[146] Zhao C, Deng W, Gage FH. Mechanisms and Functional Implications of Adult Neurogenesis. *Cell* 2008; 132: 645–660.

[147] García-González D, Dumitru I, Zuccotti A, Yen T-Y, Herranz-Pérez V, Tan LL, et al. Neurogenesis of medium spiny neurons in the nucleus accumbens continues into adulthood and is enhanced by pathological pain. *Molecular Psychiatry* 2020; 1–17.

[148] Eulalio A, Huntzinger E, Izaurralde E. Getting to the root of miRNA-mediated gene silencing. *Cell* 2008; 132: 9–14.

[149] Fang Y, Gu X, Li Z, Xiang J, Chen Z. miR-449b inhibits the proliferation of SW1116 colon cancer stem cells through downregulation of CCND1 and E2F3 expression. *Oncology Reports* 2013; 30: 399–406.

[150] Noonan EJ, Place RF, Pookot D, Basak S, Whitson JM, Hirata H, et al. miR-449a targets HDAC-1 and induces growth arrest in prostate cancer. *Oncogene* 2009; 28: 1714–1724.

[151] Wu J, Bao J, Kim M, Yuan S, Tang C, Zheng H, et al. Two miRNA clusters, miR-34b/c and miR-449, are essential for normal brain development, motile ciliogenesis, and spermatogenesis. *PNAS* 2014; 111: E2851–E2857.

[152] Evangelou E, Gao H, Chu C, Ntritsos G, Blakeley P, Butts AR, et al. New alcohol-related genes suggest shared genetic mechanisms with neuropsychiatric disorders. *Nat Hum Behav* 2019; 3: 950–961.

[153] Kamarajan C, Pandey AK, Chorlian DB, Manz N, Stimus AT, Edenberg HJ, et al. A KCNJ6 gene polymorphism modulates theta oscillations during reward processing. *Int J Psychophysiol* 2017; 115: 13–23.

[154] Benowitz NL. Pharmacology of Nicotine: Addiction, Smoking-Induced Disease, and Therapeutics. *Annual Review of Pharmacology and Toxicology* 2009; 49: 57–71.

[155] Simmler LD, Anacker AMJ, Levin MH, Vaswani NM, Gresch PJ, Nackenoff AG, et al. Blockade of the 5-HT transporter contributes to the behavioural, neuronal and molecular effects of cocaine. *British Journal of Pharmacology* 2017; 174: 2716–2738.

[156] Lehrmann E, Oyler J, Vawter MP, Hyde TM, Kolachana B, Kleinman JE, et al. Transcriptional profiling in the human prefrontal cortex: evidence for two activational states associated with cocaine abuse. *The Pharmacogenomics Journal* 2003; 3: 27–40.

[157] Bryant CD, Yazdani N. RNA-binding proteins, neural development and the addictions. *Genes, Brain and Behavior* 2016; 15: 169–186.

[158] Mahaweni NM, Olieslagers TI, Rivas IO, Molenbroeck SJJ, Groeneweg M, Bos GMJ, et al. A comprehensive overview of FCGR3A gene variability by full-length gene sequencing including the identification of V158F polymorphism. *Scientific Reports* 2018; 8: 1–11.

[159] McBride WJ, Kimpel MW, McClintick JN, Ding Z-M, Hauser SR, Edenberg HJ, et al. Changes in Gene Expression within the Ventral Tegmental Area Following Repeated Excessive Binge-Like Alcohol Drinking by Alcohol-Preferring (P) Rats. *Alcohol (Fayetteville, NY)* 2013; 47: 367.

[160] Lonsdale J, Thomas J, Salvatore M, Phillips R, Lo E, Shad S, et al. The Genotype-Tissue Expression (GTEx) project. *Nature Genetics* 2013; 45: 580–585.

[161] Kendler KS, Prescott CA, Myers J, Neale MC. The Structure of Genetic and Environmental Risk Factors for Common Psychiatric and Substance Use Disorders in Men and Women. *Arch Gen Psychiatry* 2003; 60: 929–937.

[162] Harper C. The Neuropathology of Alcohol-Related Brain Damage. *Alcohol Alcohol* 2009; 44: 136–140.

[163] Jung M, Schaefer A, Steiner I, Kempkensteffen C, Stephan C, Erbersdobler A, et al. Robust MicroRNA Stability in Degraded RNA Preparations from Human Tissue and Cell Samples. *Clin Chem* 2010; 56: 998–1006.

[164] Weis S, Llenos IC, Dulay JR, Elashoff M, Martínez-Murillo F, Miller CL. Quality control for microarray analysis of human brain samples: The impact of postmortem factors, RNA characteristics, and histopathology. *Journal of Neuroscience Methods* 2007; 165: 198–209.

[165] Stan AD, Ghose S, Gao X-M, Roberts RC, Lewis-Amezcua K, Hatanpaa KJ, et al. Human postmortem tissue: What quality markers matter? *Brain Research* 2006; 1123: 1–11.

[166] Heath AC, Bucholz KK, Madden P a. F, Dinwiddie SH, Slutske WS, Bierut LJ, et al. Genetic and environmental contributions to alcohol dependence risk in a national twin sample: consistency of findings in women and men. *Psychological Medicine* 1997; 27: 1381–1396.

[167] Tawa EA, Hall SD, Lohoff FW. Overview of the Genetics of Alcohol Use Disorder. *Alcohol Alcohol* 2016; 51: 507–514.

[168] Vornholt E, Mamdani M, Drake J, McMichael G, Taylor ZN, Bacanu S-A, et al. Network Preservation Reveals Shared and Unique Biological Processes Associated with Chronic Alcohol Abuse in NAc and PFC. *bioRxiv* 2020; 2020.05.21.108621.

[169] Hart AB, Kranzler HR. Alcohol Dependence Genetics: Lessons Learned From Genome-Wide Association Studies (GWAS) and Post-GWAS Analyses. *Alcoholism: Clinical and Experimental Research* 2015; 39: 1312–1327.

[170] Fabbri M, Girnita L, Varani G, Calin GA. Decrypting noncoding RNA interactions, structures, and functional networks. *Genome Res* 2019; 29: 1377–1388.

[171] Mayfield RD. Emerging roles for ncRNAs in alcohol use disorders. *Alcohol* 2017; 60: 31–39.

[172] Qu S, Yang X, Li X, Wang J, Gao Y, Shang R, et al. Circular RNA: A new star of noncoding RNAs. *Cancer Letters* 2015; 365: 141–148.

[173] Ebbesen KK, Hansen TB, Kjems J. Insights into circular RNA biology. *RNA Biology* 2017; 14: 1035–1045.

[174] Han B, Chao J, Yao H. Circular RNA and its mechanisms in disease: From the bench to the clinic. *Pharmacology & Therapeutics* 2018; 187: 31–44.

[175] Salzman J. Circular RNA Expression: Its Potential Regulation and Function. *Trends in Genetics* 2016; 32: 309–316.

[176] Lai EC. Micro RNAs are complementary to 3′UTR sequence motifs that mediate negative post-transcriptional regulation. *Nature Genetics* 2002; 30: 363–364.

[177] Hansen TB, Jensen TI, Clausen BH, Bramsen JB, Finsen B, Damgaard CK, et al. Natural RNA circles function as efficient microRNA sponges. *Nature* 2013; 495: 384–388.

[178] Lukiw W. Circular RNA (circRNA) in Alzheimer's disease (AD). *Front Genet*; 4. Epub ahead of print 2013. DOI: 10.3389/fgene.2013.00307.

[179] Zimmerman AJ, Hafez AK, Amoah SK, Rodriguez BA, Dell'Orco M, Lozano E, et al. A psychiatric disease-related circular RNA controls synaptic gene expression and cognition. *Molecular Psychiatry* 2020; 1–16.

[180] Vornholt E, Luo D, Qiu W, McMichael GO, Liu Y, Gillespie N, et al. Postmortem brain tissue as an underutilized resource to study the molecular pathology of neuropsychiatric disorders across different ethnic populations. *Neuroscience & Biobehavioral Reviews* 2019; 102: 195–207.

[181] Rochow H, Franz A, Jung M, Weickmann S, Ralla B, Kilic E, et al. Instability of circular RNAs in clinical tissue samples impairs their reliable expression analysis using RT-qPCR: from the myth of their advantage as biomarkers to reality. *Theranostics* 2020; 10: 9268.

[182] Zeng N, Wang T, Chen M, Yuan Z, Qin J, Wu Y, et al. Cigarette smoke extract alters genome-wide profiles of circular RNAs and mRNAs in primary human small airway epithelial cells. *Journal of Cellular and Molecular Medicine* 2019; 23: 5532–5541.

[183] Liu Z, Ran Y, Tao C, Li S, Chen J, Yang E. Detection of circular RNA expression and related quantitative trait loci in the human dorsolateral prefrontal cortex. *Genome Biology* 2019; 20: 99.

[184] Rennie W, Liu C, Carmack CS, Wolenc A, Kanoria S, Lu J, et al. STarMir: a web server for prediction of microRNA binding sites. *Nucleic Acids Res* 2014; 42: W114-118.

[185] Riffo-Campos ÁL, Riquelme I, Brebi-Mieville P. Tools for Sequence-Based miRNA Target Prediction: What to Choose? *Int J Mol Sci*; 17. Epub ahead of print 9 December 2016. DOI: 10.3390/ijms17121987.

[186] Liu C, Mallick B, Long D, Rennie WA, Wolenc A, Carmack CS, et al. CLIP-based prediction of mammalian microRNA binding sites. *Nucleic Acids Res* 2013; 41: e138–e138.

[187] Ru Y, Kechris KJ, Tabakoff B, Hoffman P, Radcliffe RA, Bowler R, et al. The multiMiR R package and database: integration of microRNA–target interactions along with their disease and drug associations. *Nucleic Acids Res* 2014; 42: e133–e133.

[188] Ge SX, Jung D, Yao R. ShinyGO: a graphical gene-set enrichment tool for animals and plants. *Bioinformatics* 2020; 36: 2628–2629.

[189] Purcell S, Neale B, Todd-Brown K, Thomas L, Ferreira MAR, Bender D, et al. PLINK: A Tool Set for Whole-Genome Association and Population-Based Linkage Analyses. *Am J Hum Genet* 2007; 81: 559–575.

[190] Liu Y, Xie J. Cauchy Combination Test: A Powerful Test With Analytic p-Value Calculation Under Arbitrary Dependency Structures. *null* 2020; 115: 393–402.

[191] Goltseker K, Hopf FW, Barak S. Advances in behavioral animal models of alcohol use disorder. *Alcohol* 2019; 74: 73–82.

[192] Gelernter J, Kranzler HR, Sherva R, Almasy L, Koesterer R, Smith AH, et al. Genome-wide association study of alcohol dependence:significant findings in African- and European-Americans including novel risk loci. *Molecular Psychiatry* 2014; 19: 41–49.

[193] Walters RK, Adams MJ, Adkins AE, Aliev F, Bacanu S-A, Batzler A, et al. Trans-ancestral GWAS of alcohol dependence reveals common genetic underpinnings with psychiatric disorders. *bioRxiv* 2018; 257311.

[194] Barkley-Levenson AM, Crabbe JC. Bridging Animal and Human Models: Translating From (and to) Animal Genetics. *Alcohol Research : Current Reviews* 2012; 34: 325.

[195] Roberto M, Varodayan FP. Synaptic targets: Chronic alcohol actions. *Neuropharmacology* 2017; 122: 85–99.

[196] Ron D, Barak S. Molecular mechanisms underlying alcohol-drinking behaviours. *Nature Reviews Neuroscience* 2016; 17: 576–591.

[197] Mulligan MK, Ponomarev I, Hitzemann RJ, Belknap JK, Tabakoff B, Harris RA, et al. Toward understanding the genetics of alcohol drinking through transcriptome meta-analysis. *Proceedings of the National Academy of Sciences of the United States of America* 2006; 103: 6368–6373.

[198] Ben Hamida S, Neasta J, Lasek AW, Kharazia V, Zou M, Carnicella S, et al. The small G protein H-Ras in the mesolimbic system is a molecular gateway to alcohol-seeking and excessive drinking behaviors. *The Journal of Neuroscience: The Official Journal of the Society for Neuroscience* 2012; 32: 15849–15858.

[199] Jin Z, Bhandage AK, Bazov I, Kononenko O, Bakalkin G, Korpi ER, et al. Expression of specific ionotropic glutamate and GABA-A receptor subunits is decreased in central amygdala of alcoholics. *Front Cell Neurosci*; 8. Epub ahead of print 2014. DOI: 10.3389/fncel.2014.00288.

[200] Dopico AM, Lovinger DM. Acute Alcohol Action and Desensitization of Ligand-Gated Ion Channels. *Pharmacol Rev* 2009; 61: 98–114.

[201] Trudell JR, Messing RO, Mayfield J, Harris RA. Alcohol dependence: molecular and behavioral evidence. *Trends Pharmacol Sci* 2014; 35: 317–323.

[202] Newton PM, Ron D. Protein kinase C and alcohol addiction. *Pharmacological Research* 2007; 55: 570–577.

[203] Chen J, Hutchison KE, Calhoun VD, Claus ED, Turner JA, Sui J, et al. CREB-BDNF pathway influences alcohol cue-elicited activation in drinkers. *Human Brain Mapping* 2015; 36: 3007–3019.

[204] Dalvie S, Fabbri C, Ramesar R, Serretti A, Stein DJ. Glutamatergic and HPA-axis pathway genes in bipolar disorder comorbid with alcohol- and substance use disorders. *Metab Brain Dis* 2016; 31: 183–189.

[205] Castelli V, Brancato A, Cavallaro A, Lavanco G, Cannizzaro C. Homer2 and Alcohol: A Mutual Interaction. *Front Psychiatry*; 8. Epub ahead of print 2017. DOI: 10.3389/fpsyt.2017.00268.

[206] Meyers JL, Salling MC, Almli LM, Ratanatharathorn A, Uddin M, Galea S, et al. Frequency of alcohol consumption in humans; the role of metabotropic glutamate receptors and downstream signaling pathways. *Translational Psychiatry* 2015; 5: e586–e586.

[207] Heinrich A, Müller KU, Banaschewski T, Barker GJ, Bokde ALW, Bromberg U, et al. Prediction of alcohol drinking in adolescents: Personality-traits, behavior, brain responses, and genetic variations in the context of reward sensitivity. *Biological Psychology* 2016; 118: 79–87.

[208] Fenster SD, Chung WJ, Zhai R, Cases-Langhoff C, Voss B, Garner AM, et al. Piccolo, a Presynaptic Zinc Finger Protein Structurally Related to Bassoon. *Neuron* 2000; 25: 203–214.

[209] Sullivan PF, de Geus EJC, Willemsen G, James MR, Smit JH, Zandbelt T, et al. Genome-wide association for major depressive disorder: a possible role for the presynaptic protein piccolo. *Molecular Psychiatry* 2009; 14: 359–375.

[210] Woudstra S, Tol M-J van, Bochdanovits Z, Wee NJ van der, Zitman FG, Buchem MA van, et al. Modulatory Effects of the Piccolo Genotype on Emotional Memory in Health and Depression. *PLOS ONE* 2013; 8: e61494.

[211] Woudstra S, Bochdanovits Z, van Tol M-J, Veltman DJ, Zitman FG, van Buchem MA, et al. Piccolo genotype modulates neural correlates of emotion processing but not executive functioning. *Translational Psychiatry* 2012; 2: e99–e99.

[212] Dvorak RD, Sargent EM, Kilwein TM, Stevenson BL, Kuvaas NJ, Williams TJ. Alcohol use and alcohol-related consequences: associations with emotion regulation difficulties. *The American Journal of Drug and Alcohol Abuse* 2014; 40: 125–130.

[213] Curtin JJ, Patrick CJ, Lang AR, Cacioppo JT, Birbaumer N. Alcohol Affects Emotion Through Cognition. *Psychol Sci* 2001; 12: 527–531.

[214] Volkow ND, Wang G-J, Fowler JS, Tomasi D. Addiction Circuitry in the Human Brain. *Annu Rev Pharmacol Toxicol* 2012; 52: 321–336.

[215] Tapocik JD, Solomon M, Flanigan M, Meinhardt M, Barbier E, Schank JR, et al. Coordinated dysregulation of mRNAs and microRNAs in the rat medial prefrontal cortex following a history of alcohol dependence. *The Pharmacogenomics Journal* 2013; 13: 286–296.

[216] McBride WJ. Chapter 11 - Gene Expression in CNS Regions of Genetic Rat Models of Alcohol Abuse. In: Watson RR, Zibadi S (eds) *Addictive Substances and Neurological Disease*. Academic Press, pp. 89–102.

[217] McBride WJ, Kimpel MW, Schultz JA, McClintick JN, Edenberg HJ, Bell RL. Changes in gene expression in regions of the extended amygdala of alcohol-preferring rats after binge-like alcohol drinking. *Alcohol* 2010; 44: 171–183.

[218] Rodd ZA, Kimpel MW, Edenberg HJ, Bell RL, Strother WN, McClintick JN, et al. Differential gene expression in the nucleus accumbens with ethanol self-administration in inbred alcohol-preferring rats. *Pharmacology Biochemistry and Behavior* 2008; 89: 481–498.

[219] McBride WJ, Kimpel MW, McClintick JN, Ding Z-M, Hyytia P, Colombo G, et al. Gene expression in the ventral tegmental area of 5 pairs of rat lines selectively bred for high or low ethanol consumption. *Pharmacology Biochemistry and Behavior* 2012; 102: 275–285.

[220] Wilson PM, Fryer RH, Fang Y, Hatten ME. Astn2, A Novel Member of the Astrotactin Gene Family, Regulates the Trafficking of ASTN1 during Glial-Guided Neuronal Migration. *J Neurosci* 2010; 30: 8529–8540.

[221] Hill SY, Weeks DE, Jones BL, Zezza N, Stiffler S. ASTN1 and alcohol dependence: Family-based association analysis in multiplex alcohol dependence families. *American Journal of Medical Genetics Part B: Neuropsychiatric Genetics* 2012; 159B: 445–455.

[222] Nunez YO, Truitt JM, Gorini G, Ponomareva ON, Blednov YA, Harris RA, et al. Positively correlated miRNA-mRNA regulatory networks in mouse frontal cortex during early stages of alcohol dependence. *BMC Genomics* 2013; 14: 725.

[223] Gardiner AS, Gutierrez HL, Luo L, Davies S, Savage DD, Bakhireva LN, et al. Alcohol Use During Pregnancy is Associated with Specific Alterations in MicroRNA Levels in Maternal Serum. *Alcoholism: Clinical and Experimental Research* 2016; 40: 826–837.

[224] Higa GSV, Sousa E de, Walter LT, Kinjo ER, Resende RR, Kihara AH. MicroRNAs in Neuronal Communication. *Mol Neurobiol* 2014; 49: 1309–1326.

[225] Steffensen SC, Bradley KD, Hansen DM, Wilcox JD, Wilcox RS, Allison DW, et al. THE ROLE OF CONNEXIN-36 GAP JUNCTIONS IN ALCOHOL INTOXICATION AND CONSUMPTION. *Synapse (New York, NY)*; 65. Epub ahead of print August 2011. DOI: 10.1002/syn.20885.

[226] Pallarès-Albanell J, Zomeño-Abellán MT, Escaramís G, Pantano L, Soriano A, Segura MF, et al. A High-Throughput Screening Identifies MicroRNA Inhibitors That Influence Neuronal Maintenance and/or Response to Oxidative Stress. *Molecular Therapy - Nucleic Acids* 2019; 17: 374–387.

[227] Haorah J, Ramirez SH, Floreani N, Gorantla S, Morsey B, Persidsky Y. Mechanism of alcohol-induced oxidative stress and neuronal injury. *Free radical biology & medicine* 2008; 45: 1542.

[228] McClintick JN, Xuei X, Tischfield JA, Goate A, Foroud T, Wetherill L, et al. Stress–response pathways are altered in the hippocampus of chronic alcoholics. *Alcohol* 2013; 47: 505–515.

[229] Roderburg C, Mollnow T, Bongaerts B, Elfimova N, Cardenas DV, Berger K, et al. Micro-RNA Profiling in Human Serum Reveals Compartment-Specific Roles of miR-571 and miR-652 in Liver Cirrhosis. *PLOS ONE* 2012; 7: e32999.

[230] Desrivières S, Lourdusamy A, Müller C, Ducci F, Wong CP, Kaakinen M, et al. Glucocorticoid receptor (NR3C1) gene polymorphisms and onset of alcohol abuse in adolescents. *Addiction Biology* 2011; 16: 510–513.

[231] Gatta E, Grayson DR, Auta J, Saudagar V, Dong E, Chen Y, et al. Genome-wide methylation in alcohol use disorder subjects: implications for an epigenetic regulation of the cortico-limbic glucocorticoid receptors (NR3C1). *Molecular Psychiatry* 2019; 1–13.

[232] Salvatore JE, Han S, Farris SP, Mignogna KM, Miles MF, Agrawal A. Beyond genome-wide significance: integrative approaches to the interpretation and extension of GWAS findings for alcohol use disorder. *Addiction Biology* 2019; 24: 275–289.

[233] Gibson G. Hints of hidden heritability in GWAS. *Nature Genetics* 2010; 42: 558–560.

[234] Asif H, Alliey-Rodriguez N, Keedy S, Tamminga CA, Sweeney JA, Pearlson G, et al. GWAS significance thresholds for deep phenotyping studies can depend upon minor allele frequencies and sample size. *Molecular Psychiatry* 2020; 1–8.

[235] Ebadi M, Iversen PL, Hao R, Cerutis DR, Rojas P, Happe HK, et al. Expression and regulation of brain metallothionein. *Neurochem Int* 1995; 27: 1–22.

[236] Holmes MV, Davey Smith G. Problems in interpreting and using GWAS of conditional phenotypes illustrated by 'alcohol GWAS'. *Molecular Psychiatry* 2019; 24: 167–168.

[237] Moore JH, Asselbergs FW, Williams SM. Bioinformatics challenges for genome-wide association studies. *Bioinformatics* 2010; 26: 445–455.

[238] Watanabe K, Taskesen E, van Bochoven A, Posthuma D. Functional mapping and annotation of genetic associations with FUMA. *Nature Communications* 2017; 8: 1826.

[239] Kuhn DE, Martin MM, Feldman DS, Terry AV, Nuovo GJ, Elton TS. Experimental Validation of miRNA Targets. *Methods* 2008; 44: 47–54.

APPENDICES

Appendix I: Sample Demographics

ID	Diagnosis	Age	NAc RIN	PFC RIN	Weight (g)	pH	PMI	Hemisphere	Neuro.	Hepat.	Tox	Smoking
13	Alcohol	61	6.9	3.6	1340	6.93	21	0	0	1	2	1
18	Control	44	6.9	3.7	1220	6.6	50	0	0	0	9	2
20	Control	62	8.1	3.4	1480	6.56	37.5	1	0	1	9	9
24	Alcohol	56	6.4	2.1	1284	6.51	45	0	0	1	1	9
25	Control	63	7.3	5.2	1570	6.94	24	1	0	1	2	1
26	Alcohol	42	6.4	5.8	1400	6.5	41	0	1	1	2	0
27	Control	46	7	1.4	1490	6.65	25	1	0	1	0	9
30	Control	56	7.1	3.8	1510	6.76	37	1	0	1	9	1
33	Alcohol	52	6	2.8	1380	6.78	45.5	0	1	1	0	1
35	Control	43	8.3	2.9	1500	6.43	13	1	0	0	0	2
40	Alcohol	59	6.7	2.6	1520	6.57	24	0	0	1	0	0
42	Alcohol	56	8.2	2.5	1230	6.52	22	0	1	1	0	1
43	Alcohol	54	7.8	7.8	1340	6.41	17	0	0	1	1	1
45	Alcohol	46	8	2.9	1200	6.51	24	1	0	1	1	9
46	Alcohol	39	7.6	2.8	1360	6.56	24	0	0	1	9	1
48	Alcohol	73	8.5	5	1300	6.3	24	0	1	1	1	0
51	Control	56	7.8	7.2	1635	6.53	24	1	0	9	9	1
54	Control	50	7.3	7.9	1500	6.26	19	0	0	1	0	2
56	Alcohol	63	5.5	4.3	1616	6.21	25.5	1	1	1	0	1
57	Alcohol	50	6.2	3.6	1420	6.59	24	0	1	1	1	1
60	Alcohol	50	6.3	6.6	1520	6.3	17	0	1	1	9	9
61	Alcohol	51	6.4	2.2	1460	6.35	46	0	1	1	9	1
62	Alcohol	64	6.7	3.4	1370	6.76	39	1	1	1	1	1
64	Alcohol	55	6.9	7.2	1362	7.02	48	1	1	1	2	1
65	Control	55	6.7	8.3	1631	6.39	12	0	0	1	9	0
66	Control	47	6.5	3.1	1534	6.74	38	0	0	1	1	1
68	Control	50	6.7	7.4	1426	6.37	30	1	0	0	0	1
69	Control	55	6.3	4.4	1560	6.89	39	0	0	1	2	0
70	Alcohol	53	5.8	5	1340	6.75	57	1	1	1	9	1
73	Control	82	5.3	3.4	1300	6.24	36	0	0	9	9	0
74	Control	64	6.5	7.8	1390	6.94	9.5	1	1	1	9	1
76	Alcohol	73	6.8	8	1188	6.84	19	1	0	1	9	1
77	Control	73	6	3.2	1380	6.8	48	1	0	9	9	1
80	Control	57	7.7	3.1	1360	6.6	18	0	0	1	9	2
82	Control	59	5.3	3.6	1360	6.56	20	1	0	0	9	1

*Please refer to **Table 2** for dummy code reference for hemisphere, neuropathology (Neuro.), hepatology (Hepat.), Toxicology (Tox.), and smoking

Appendix II: Supplemental Methodology

AUD GWAS Enrichment:

To compare the overlap between our eQTL results with GWAS of other addiction phenotypes, such as for alcohol use and smoking. We began by first isolating all SNPs in LD (r2= 0.50) using the data available from the 1000 Genomes Project. We used Plink 1.9 to tag SNPs from the 1000 Genomes Project in LD (r2=0.5, -tag-kb=500kb) with significant SNPs from our eQTL analyses. Next, all SNPs from the curated list and those extracted from 1000Genomes were checked against our genotypic dataset to ensure that they are all present. The annotations for this expanded list of SNPs was extracted from dbSNP (https://www.ncbi.nlm.nih.gov/snp/), which also included SNPs mapped on different dbSNP build. This list of SNPs was compared to two different GWAS: i) *GWAS & Sequencing Consortium of Alcohol and Nicotine Use* (GSCAN), ii) *Psychiatric Genetics Consortium AUD GWAS* (PGC-AUD) (***only study 2*) and iii) *Collaborative Study on the Genetics of Alcoholism* (COGA) (**only study 1*). The enrichment analyses are based on two stages: i) to build competitive enrichment tests, recompute p-values to adjust for background enrichment, ii) use the adjusted p-values to build two enrichment statistics that are optimal in different parts of the parameter space. First, we adjust the p-values for background enrichment by recomputing the p-values under the realized non-centrality parameter of GWAS based $\chi_1^2 = Z^2$ (chi-square) statistics of each SNP, where Z is the Z-score of a GWAS SNP. Noncentrality parameter is estimated by the method of moments, i.e. we can estimate $\widehat{\lambda^2} = \max{(\overline{Z^2} - 1,0)}$, where $\overline{Z^2}$ is the mean squares of Z-scores of all measured SNPs in the genome scan. Second, we use adjusted p-values of eQTL SNPs to compute i) a Cauchy combination test for p-values [35] that is heuristically more powerful when there are numerous signals and ii) a Simes test that is likely to be most powerful when there are a few significant signals. The two enrichment statistics are likely to cover all scenarios of practical importance.

Replication in the GTEx Database:

We began by performing an independent eQTL analysis on the NAc and PFC from the entire 22,214 probeset and genome-wide SNP data while controlling for all available covariates using the *modelLinear* command within the MatrixEQTL package (ver. 2.2) in R. Next, we isolated significant eQTLs (at FDR ≤0.05) containing SNPs with available RS IDs (NAc=160,119, PFC=35,990) from our sample. This list of eQTLs was then compared to the significant (FDR≤0.05) list of eQTLs in NAc and PFC with available RS IDs and gene symbols (HGNC) (NAc=854,654, PFC=718,679) from GTEx. The overlap significance was tested via a Fisher's exact test (at p ≤0.05).

Appendix III: Network Preservation Supplemental *(Study 1)*.

NAc

	MedianRank.pres	MedianRank.qual	Zsummary.pres	Zsummary.qual
black	13	19.5	7.7	15
blue	11	21.5	15	19
cyan	7	16	3	4.1
darkgreen	19	19	4.9	14
darkgrey	11	3.5	2.3	6.8
darkolivegreen	22	6	-0.045	2.8
darkorange	18	12	0.83	4.7
darkred	6	7	2.3	6.4
darkturquoise	6	6	2.5	7.1
gold	18	24	20	0.096
greenyellow	8	12.5	11	21
grey60	21	23	0.15	1.3
lightcyan	14	12	3.1	7.9
lightgreen	2	15	2.9	3.2
lightyellow	1	6.5	10	9.2
magenta	9	16.5	13	21
midnightblue	10	3.5	5.1	12
orange	17	9	0.68	5.7
paleturquoise	16	15.5	0.43	2.3
purple	21	21	0.55	5.1
royalblue	21	3.5	0.45	7.1
skyblue	4	1	4.8	11
tan	7	9	6.2	11
turquoise	13	17	8.7	19
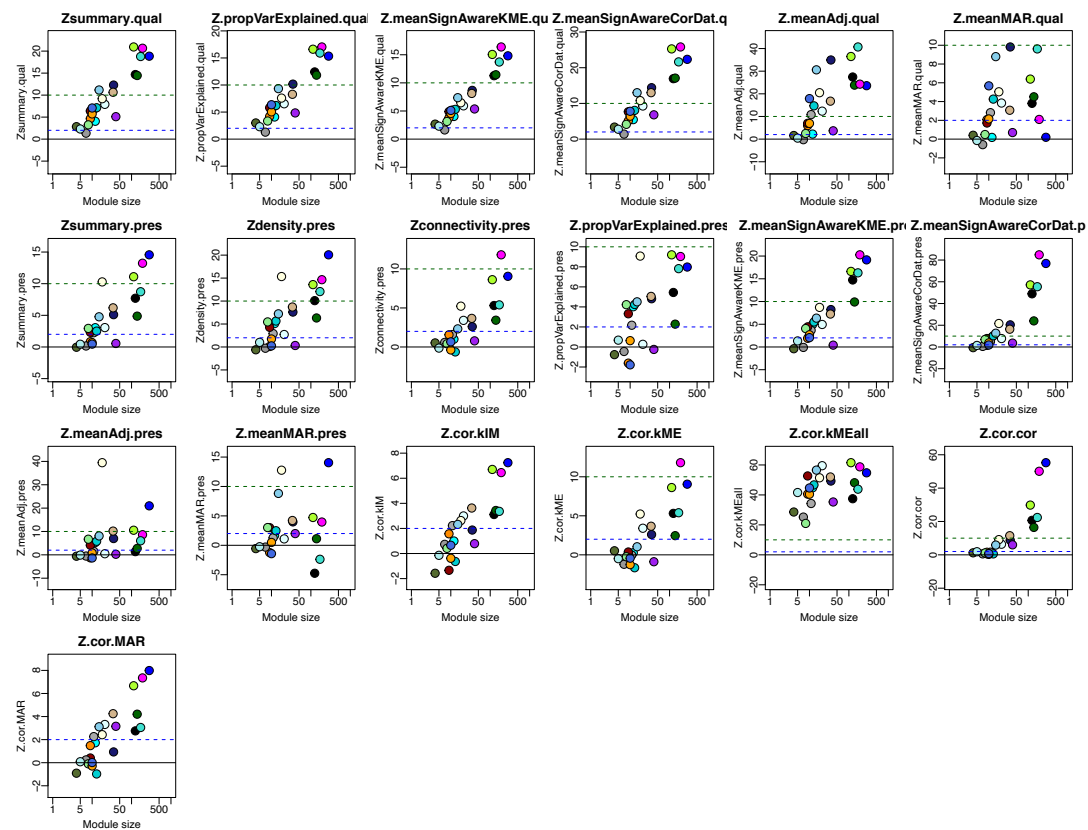
*Green indicates **high** network preservation Zsummary > 10*

*Red indicates **low/no** network preservation Zsummary < 2*

Only modules associated with AD are highlighted

PFC

	medianRank.pres	medianRank.qual	Zsummary.pres	Zsummary.qual
blue	7	12	16	21
brown	11	8.5	5.7	14
cyan	8	6.5	4.6	9.1
darkgreen	15	15	0.53	1.7
darkgrey	5	3	3	6
darkred	1	2	8.9	9.9
darkturquoise	2	2	1.7	3.9
gold	14	18	19	2.3
grey60	6	6.5	4.5	8.3
lightcyan	3	3	7.4	16
lightgreen	4	10	19	21
lightyellow	13	8.5	1	4.3
magenta	15	14	5.4	16
midnightblue	17	14.5	0.74	4.2
pink	8	16.5	6.2	5.6
purple	12	5	3.1	12
tan	16	11	2.3	14
turquoise	7	15	16	18
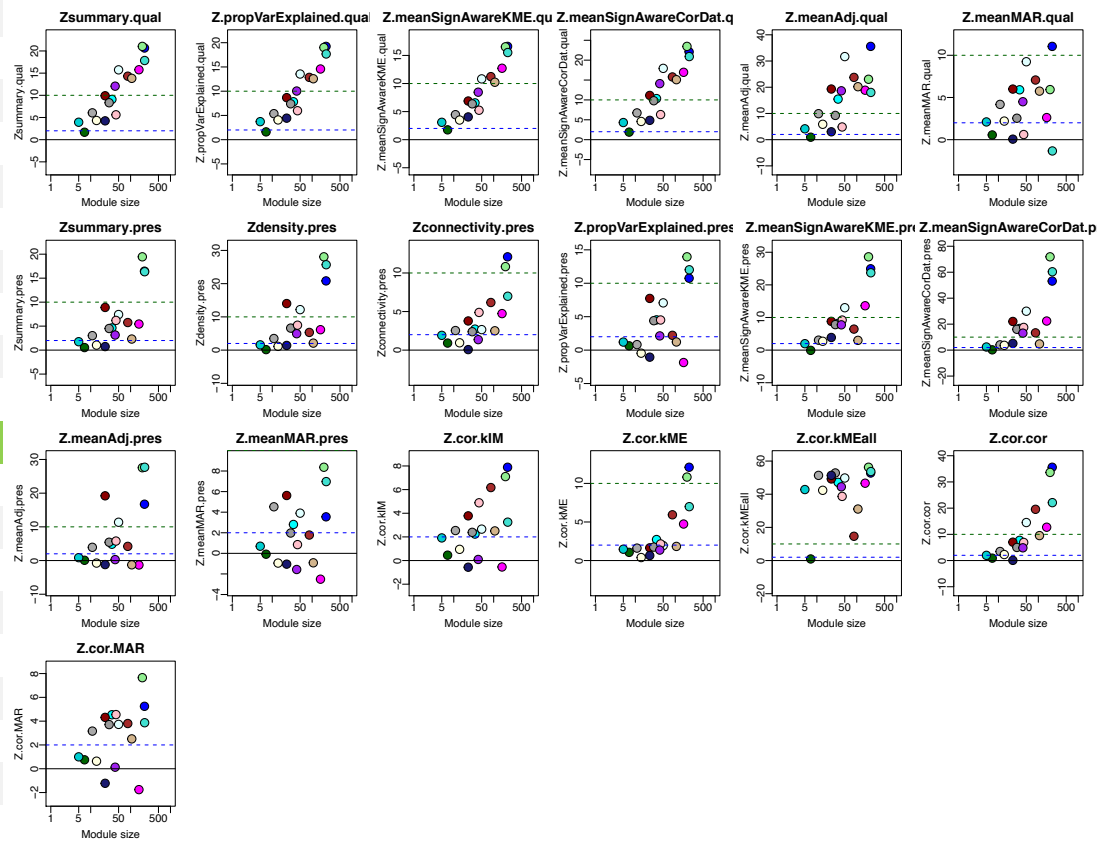
*Green indicates **high** network preservation Zsummary > 10*

*Red indicates **low/no** network preservation Zsummary < 2*

Only modules associated with AD are highlighted

Appendix IV: mRNA and miRNA eQTL results *(Study 1)*.

NAc mRNA

SNPs	Gene	Module Color	Beta	p-value	FDR
rs76383282	VRK1	darkgreen	-153.68	4.35E-10	4.19E-05
rs56315113	VRK1	darkgreen	-148.14	4.68E-10	4.19E-05
rs12119598	DNALI1	darkorange	2.61	1.94E-09	0.00011565
chr14:97060694:I	VRK1	darkgreen	-4.96	1.48E-08	0.00066179
rs113509630	VRK1	darkgreen	-4.36	3.96E-08	0.00141771
rs17095223	VRK1	darkgreen	-4.84	1.25E-07	0.00374452
rs12087446	FCGR3A	greenyellow	2.30	3.24E-07	0.00830005
chr11:86181489:D	CCDC81	darkorange	33.44	5.56E-07	0.01230765
rs72967925	CCDC81	darkorange	33.36	6.19E-07	0.01230765
rs72704613	CTSS	greenyellow	129.87	1.96E-06	0.03514187
rs12622681	INPP4A	darkgreen	-4.43	2.46E-06	0.03997544
rs62395648	HMP19	darkgreen	-4.23	2.91E-06	0.04129406
rs8009802	VRK1	darkgreen	-4.47	3.00E-06	0.04129406
rs3757534	AASS	greenyellow	28.11	3.50E-06	0.04476207
rs117564276	DKK3	darkgreen	-3.95	3.92E-06	0.0468016
rs112178835	PCDH8	darkgreen	-173.84	6.97E-06	0.07436284
rs184788948	RNF34	darkgreen	-25.62	7.06E-06	0.07436284
rs115559579	VAMP5	magenta	47.11	9.54E-06	0.08168067
rs61850597	SPAG6	darkorange	171.58	1.01E-05	0.08168067
rs148298758	SPAG6	darkorange	166.45	1.01E-05	0.08168067
rs2228035	RNASE4	greenyellow	1.36	1.06E-05	0.08168067
rs148394489	PCDH8	darkgreen	-170.84	1.09E-05	0.08168067
rs2929652	RASGRP1	darkgreen	2.65	1.10E-05	0.08168067
rs143242677	hivep1	purple	48.32	1.13E-05	0.08168067
rs72833730	hivep1	purple	1.77	1.17E-05	0.08168067
rs62395654	HMP19	darkgreen	-4.48	1.22E-05	0.08168067
rs144637086	CCDC81	darkorange	1.01	1.28E-05	0.08168067

PFC mRNA

SNPs	Gene	ModuleColor	Beta	p-value	FDR
rs35702714	SERPINH1	lightgreen	122.35	5.09E-08	0.00080759
rs150584068	SERPINH1	lightgreen	63.00	5.29E-08	0.00080759
rs139891301	SERPINH1	lightgreen	129.34	6.03E-08	0.00080759
rs2367888	GAD2	pink	3.62	2.26E-07	0.00227006
chr6:36894342:D	CDKN1A	lightgreen	47.95	4.85E-07	0.00385573
rs192839670	PNP	lightgreen	93.88	5.76E-07	0.00385573
chr12:13728631:D	EMP1	lightgreen	99.91	7.57E-07	0.00434306
chr7:100327516:I	ACTL6B	pink	-72.82	1.32E-06	0.00662345
rs113756971	SERPINH1	lightgreen	4.18	2.25E-06	0.01003246
chr10:26943627:D	GAD2	pink	-83.83	3.44E-06	0.01380103
rs190205726	KCNF1	pink	-54.79	4.57E-06	0.01667587
rs72671266	PNP	lightgreen	2.85	6.88E-06	0.02057311
chr2:11079640:D	KCNF1	pink	28.28	8.10E-06	0.02057311
rs73407374	ACTL6B	pink	-2.62	8.18E-06	0.02057311
rs76866975	SERPINH1	lightgreen	3.99	8.18E-06	0.02057311
rs16982145	SEZ6L	pink	-75.40	8.20E-06	0.02057311
rs75881054	ACTL6B	pink	-2.67	9.57E-06	0.02261546
chr14:20754346:I	PNP	lightgreen	2.70	1.16E-05	0.02332986
rs151115763	FKBP5	lightgreen	60.74	1.19E-05	0.02332986
chr14:20767963:D	PNP	lightgreen	3.21	1.22E-05	0.02332986
rs115498188	CDKN1A	lightgreen	3.40	1.22E-05	0.02332986
rs57851931	EFNB3	pink	-2.91	1.46E-05	0.02662338
rs77770867	IL4R	lightgreen	2.05	1.72E-05	0.02957634
rs150702181	ACTL6B	pink	-47.31	1.78E-05	0.02957634
rs139016292	ACTL6B	pink	-91.75	1.84E-05	0.02957634
rs62224198	SEZ6L	pink	-2.68	2.66E-05	0.04113376
rs143033493	TNFRSF10B	lightgreen	1.95	3.90E-05	0.05795623

rs78231083	CCDC81	darkorange	1.01	1.28E-05	0.08168067
rs1878584	INPP4A	darkgreen	-3.18	1.38E-05	0.08284902
rs4639245	HMP19	darkgreen	-65.27	1.39E-05	0.08284902
rs73216200	AASS	greenyellow	32.11	1.54E-05	0.08629573
rs73214170	AASS	greenyellow	33.20	1.54E-05	0.08629573
rs12797770	DKK3	darkgreen	-3.53	1.87E-05	0.09900247
rs56216438	GNAS	purple	2.21	1.91E-05	0.09900247
rs151055528	hivep1	purple	1.86	1.96E-05	0.09900247
rs28374830	HMP19	darkgreen	-4.18	1.99E-05	0.09900247

NAc miRNA

SNPs	miRNA	p-value	FDR	Beta
chr22:17808799:l	hsa-miR-3198_st	3.53E-09	0.00	6.20107223
rs62236483	hsa-miR-3198_st	6.14E-09	0.00	5.90474185
rs5749044	hsa-miR-3198_st	2.17E-07	0.01	5.85165973
rs117257865	hsa-miR-548w_st	6.72E-07	0.02	78.7667399
rs146187481	hsa-miR-554_st	1.81E-06	0.05	1.99215672
rs115847329	hsa-miR-554_st	2.73E-06	0.06	2.18207902
rs149333818	hsa-miR-554_st	4.27E-06	0.08	2.00689655
rs113728410	hsa-miR-662_st	4.91E-06	0.08	51.7990942
rs116330355	hsa-miR-554_st	5.79E-06	0.09	1.9284393

rs77378872	EMP1	lightgreen	3.04	4.25E-05	0.06097885
rs138327160	RTEL1-TNFRSF6B	lightgreen	63.60	4.60E-05	0.06368342
rs10459599	serpina1	lightgreen	64.20	5.37E-05	0.07185147
rs116446213	CDKN1A	lightgreen	3.26	6.44E-05	0.08341808
rs59750296	MAFF	lightgreen	-2.68	6.80E-05	0.08529648
rs7170633	serpina2	lightgreen	0.99	8.15E-05	0.09760694
rs7599293	KCNF1	pink	1.98	8.26E-05	0.09760694

PFC miRNA

SNPs	miRNA	p-value	FDR	Beta
chr2:102540036:l	hsa-miR-4772-3p_st	7.30E-08	0.00	-43.538731
chr2:102626208	hsa-miR-4772-3p_st	1.57E-07	0.00	-46.696133
rs148011441	hsa-miR-4772-3p_st	1.92E-07	0.00	-46.555537
rs12590216	hsa-miR-4504_st	2.79E-07	0.00	0.77615612
rs58467487	hsa-miR-483-3p_st	1.71E-06	0.01	-57.002932
rs12502106	hsa-miR-3139_st	1.75E-06	0.01	1.61852741
rs62454419	hsa-miR-550b_st	4.55E-06	0.03	-1.9033484
rs75825775	hsa-miR-1282_st	5.17E-06	0.03	48.9821879
rs77930061	hsa-miR-1282_st	6.30E-06	0.03	49.4686309
rs77604542	hsa-miR-483-3p_st	6.95E-06	0.03	-2.0565029
chr2:103387950:l	hsa-miR-4772-3p_st	8.41E-06	0.03	-1.4827998
rs12047264	hsa-miR-4258_st	1.08E-05	0.04	1.02110738
rs80021659	hsa-miR-550b_st	1.81E-05	0.05	-33.865258
rs60442281	hsa-miR-483-3p_st	2.42E-05	0.07	-2.0281147
rs11630961	hsa-miR-1282_st	2.91E-05	0.08	1.87410058
rs144850295	hsa-miR-550b_st	3.35E-05	0.08	-2.0630924
rs187535367	hsa-miR-550b_st	3.58E-05	0.08	-2.0944421
rs72724253	hsa-miR-1282_st	4.06E-05	0.09	1.46214249

Appendix V: CircRNA hub annotation, significance to AD, and MM *(Study 2)*.

	Hub circRNA annotations				AD significance			WGCNA results	
Probe ID	*circRNA*	*chr/strand*	*circRNA type*	*Host Gene*	*AD reg coef*	*Std. Error*	*p-value*	*Module*	*MM*
ASCRP3005798	hsa_circRNA_104238	chr6/+	exonic	TIAM2	0.35443566	0.15202303	0.02688424	M1	0.94221766
ASCRP3013231	hsa_circRNA_407198	chr9/-	intronic	ROR2	0.51011825	0.21113002	0.02221041	M1	0.91358434
ASCRP3004776	hsa_circRNA_406791	chr6/+	exonic	ZNF451	0.47500323	0.21098971	0.03211394	M1	0.8980134
ASCRP3013402	hsa_circRNA_101064	chr12/-	exonic	TFCP2	0.52462988	0.20298153	0.0150484	M1	0.89673576
ASCRP3009617	hsa_circRNA_405609	chr17/+	intronic	VMP1	0.47675388	0.18909361	0.01744529	M1	0.889519
ASCRP3004153	hsa_circRNA_400947	chr12/-	exonic	HDAC7	0.24319989	0.0765922	0.00353466	M1	0.86470334
ASCRP3012052	hsa_circRNA_006578	chr1/-	exonic	STK40	0.33280078	0.15698306	0.04268664	M1	0.86089489
ASCRP3004438	hsa_circRNA_102088	chr17/-	exonic	HDAC5	0.24577477	0.09132429	0.01169246	M1	0.85797797
ASCRP3007815	hsa_circRNA_102724	chr2/-	exonic	FANCL	0.33739302	0.16136414	0.04541244	M1	0.85241129
ASCRP3013243	hsa_circRNA_405786	chr19/+	intronic	AXL	0.32509416	0.15257405	0.04171694	M1	0.8494327
ASCRP3011731	hsa_circRNA_001952	chr13/+	antisense	DACH1	0.38640241	0.17227296	0.03270802	M1	0.84934091
ASCRP3010143	hsa_circRNA_000928	chr19/+	exonic	PROSER3	0.21977097	0.10627248	0.04766341	M1	0.84290986
ASCRP3013224	hsa_circRNA_403649	chr6/+	exonic	DOPEY1	0.35270831	0.14253645	0.01943426	M1	0.84080607
ASCRP3004117	hsa_circRNA_406138	chr21/-	intergenic		0.29684996	0.11587426	0.01587307	M1	0.83638201
ASCRP3007019	hsa_circRNA_104716	chr8/-	exonic	TSNARE1	0.28114238	0.13437958	0.04529021	M1	0.82540135
ASCRP3011336	hsa_circRNA_404433	chr1/+	exonic	KIF1B	0.31274942	0.14586749	0.04054152	M1	0.82260889
ASCRP3004513	hsa_circRNA_001109	chr2/-	sense overlapping	AFF3	0.26592524	0.11326323	0.02591503	M1	0.81991794
ASCRP3000686	hsa_circRNA_003627	chr17/+	exonic	RPA1	0.25669147	0.11420871	0.03237938	M1	0.81226741
ASCRP3011402	hsa_circRNA_000599	chr15/+	exonic	USP8	0.31723606	0.12878351	0.01994012	M1	0.80963714
ASCRP3012636	hsa_circRNA_402355	chr2/+	exonic	PTPN4	0.30953303	0.13940707	0.03436812	M1	0.80469802
ASCRP3003348	hsa_circRNA_101553	chr15/+	exonic	SNX1	0.45883161	0.21321919	0.03986267	M1	0.80302553
ASCRP3007718	hsa_circRNA_102066	chr17/+	exonic	CASC3	0.31495929	0.11000405	0.00771369	M1	0.80008902
ASCRP3000614	hsa_circRNA_066970	chr3/+	exonic	EAF2	0.35817045	0.13066026	0.01037176	M1	0.79926977
ASCRP3000325	hsa_circRNA_004145	chr5/-	sense overlapping	SKP1	0.27202296	0.1304037	0.04588373	M1	0.79923311
ASCRP3013140	hsa_circRNA_103131	chr21/-	exonic	BRWD1	0.33956506	0.15413413	0.0356893	M1	0.78504495
ASCRP3003195	hsa_circRNA_405845	chr2/+	exonic	CLIP4	0.32494803	0.12032928	0.01143664	M1	0.78271929
ASCRP3003221	hsa_circRNA_401450	chr15/+	exonic	GLCE	0.32306621	0.15614008	0.04755458	M1	0.78212412
ASCRP3003233	hsa_circRNA_068109	chr3/+	exonic	USP13	0.29547096	0.11394707	0.01475335	M1	0.77989862
ASCRP3001294	hsa_circRNA_002863	chr2/-	exonic	GFPT1	0.27170284	0.1121201	0.02185009	M1	0.77376144
ASCRP3011074	hsa_circRNA_100947	chr11/+	exonic	CUL5	0.24034022	0.07330821	0.0027133	M1	0.76727912
ASCRP3011384	hsa_circRNA_400057	chr2/+	intronic	RNU6-81P	0.28378008	0.13538257	0.04490908	M1	0.76330876

ASCRP3012980	hsa_circRNA_072473	chr5/+	exonic	SKIV2L2	0.43550153	0.20492988	0.04222006	M1	0.75602247
ASCRP3009543	hsa_circRNA_100927	chr11/-	exonic	PICALM	0.21553433	0.07223817	0.00572776	M1	0.75547759
ASCRP3003793	hsa_circRNA_083996	chr8/-	exonic	WHSC1L1	0.34778166	0.14139635	0.02011035	M1	0.75027107
ASCRP3007240	hsa_circRNA_072837	chr5/-	exonic	SMA5	0.3381052	0.14328295	0.02523416	M1	0.74487048
ASCRP3003607	hsa_circRNA_100472	chr1/+	exonic	SNAP47	0.22009696	0.0798228	0.00997751	M1	0.74479474
ASCRP3011338	hsa_circRNA_001206	chr22/+	exonic	CRKL	0.23732784	0.10282578	0.02832513	M1	0.74287095
ASCRP3002395	hsa_circRNA_104346	chr7/-	exonic	HERPUD2	0.36667831	0.1741731	0.0440474	M1	0.74254149
ASCRP3004033	hsa_circRNA_074217	chr5/-	exonic	ECSCR	0.18179942	0.07666611	0.02458294	M1	0.73873942
ASCRP3008271	hsa_circRNA_001869	chr9/-	exonic	ZCCHC6	0.30568469	0.10322203	0.00605333	M1	0.73857296
ASCRP3008173	hsa_circRNA_001382	chr15/-	sense overlapping	MYO5A	0.15322943	0.06816952	0.03236475	M1	0.73567313
ASCRP3007831	hsa_circRNA_102594	chr19/+	exonic	POLD1	0.18923428	0.08632104	0.03653948	M1	0.73126997
ASCRP3004112	hsa_circRNA_102593	chr19/+	exonic	POLD1	0.18983574	0.08494774	0.03330372	M1	0.72239186
ASCRP3005188	hsa_circRNA_100485	chr1/-	exonic	PCNXL2	0.21126124	0.10075211	0.04484169	M1	0.71499591
ASCRP3002658	hsa_circRNA_405472	chr16/+	exonic	RP11-467L24.1	0.23021737	0.09189787	0.01810873	M1	0.70957154
ASCRP3004770	hsa_circRNA_028241	chr12/-	exonic	ATXN2	0.33169726	0.16107141	0.04854237	M1	0.70881893
ASCRP3011126	hsa_circRNA_020515	chr10/-	exonic	TCERG1L	0.16891327	0.07753227	0.03763208	M1	0.70566561
ASCRP3010987	hsa_circRNA_008338	chr11/+	exonic	ZNF215	0.26646012	0.0882357	0.0052329	M2	0.87469856
ASCRP3003317	hsa_circRNA_016266	chr1/+	exonic	MAPKAPK2	0.3087154	0.12956967	0.02396353	M2	0.86188897
ASCRP3007546	hsa_circRNA_404836	chr11/-	intronic	NUP98	0.27121256	0.10522022	0.01529909	M2	0.85328554
ASCRP3011725	hsa_circRNA_104602	chr8/-	exonic	SLC20A2	0.1827308	0.08597594	0.0421978	M2	0.84535449
ASCRP3003107	hsa_circRNA_012173	chr1/+	exonic	RPS8	0.247996	0.11581063	0.04077473	M2	0.82605393
ASCRP3000643	hsa_circRNA_103700	chr4/+	exonic	HERC5	0.29145241	0.1289739	0.03152095	M2	0.82575969
ASCRP3012923	hsa_circRNA_056204	chr2/+	exonic	DDX18	0.26747828	0.08419095	0.0035186	M2	0.80364145
ASCRP3012903	hsa_circRNA_014234	chr1/-	exonic	S100A2	0.36336494	0.1748495	0.04665184	M2	0.76206174
ASCRP3005732	hsa_circRNA_001645	chr6/+	exonic	HECA	0.2351102	0.11091365	0.0427067	M2	0.75368353
ASCRP3010524	hsa_circRNA_000484	chr13/-	sense overlapping	RCBTB1	0.26922141	0.11083312	0.02156563	M2	0.73010011
ASCRP3012482	hsa_circRNA_025614	chr12/-	exonic	C2CD5	0.25960913	0.12268139	0.04303911	M2	0.72383444
ASCRP3001284	hsa_circRNA_406606	chr5/-	intronic	PDE4D	0.32490049	0.11534296	0.00863787	M2	0.71649793
ASCRP3011980	hsa_circRNA_405066	chr12/+	exonic	IFT81	0.20244031	0.08546224	0.02472435	M2	0.71466666
ASCRP3009946	hsa_circRNA_027691	chr12/+	exonic	TMTC3	0.28021105	0.11361564	0.01980422	M2	0.71443406
ASCRP3010884	hsa_circRNA_103569	chr3/+	exonic	LRCH3	0.22469484	0.09609202	0.0264741	M2	0.70186442
ASCRP3002957	hsa_circRNA_079387	chr7/+	exonic	C7orf26	0.18339509	0.07695239	0.02393067	M2	0.70178121
ASCRP3005003	hsa_circRNA_082089	chr7/-	exonic	POT1	0.21909642	0.09448697	0.02765523	M4	0.85868089
ASCRP3012301	hsa_circRNA_027451	chr12/-	exonic	GRIP1	0.19712131	0.08745133	0.03191965	M4	0.84205529
ASCRP3002168	hsa_circRNA_005843	chr2/-	sense overlapping	LINC01473	0.28006767	0.13359323	0.04488176	M4	0.82654505
ASCRP3010761	hsa_circRNA_002663	chr8/-	exonic	C8orf76	0.23763198	0.10557362	0.03214536	M4	0.7810837

98

ASCRP3005182	hsa_circRNA_100518	chr10/+	exonic	ZMYND11	0.20822005	0.08938427	0.02700275	M4	0.74731456
ASCRP3013237	hsa_circRNA_001785	chr10/+	sense overlapping	FAM208B	0.21924285	0.09867358	0.03425222	M4	0.720688
ASCRP3008151	hsa_circRNA_102203	chr17/+	exonic	SNHG20	0.17587906	0.07303328	0.02261427	M4	0.7194125
ASCRP3001569	hsa_circRNA_405886	chr2/+	exonic	PAPOLG	0.24799651	0.09710863	0.01617321	M4	0.71665054
ASCRP3008631	hsa_circRNA_400623	chr10/-	exonic	TLL2	0.28116629	0.10664684	0.01331936	M4	0.70848352
ASCRP3011641	hsa_circRNA_007290	chrX/-	sense overlapping	FUNDC1	0.23985978	0.10098358	0.02436647	M4	0.70504507
ASCRP3002274	hsa_circRNA_101342	chr14/-	exonic	SNX6	0.3750327	0.1760794	0.04179052	M5	0.87819052
ASCRP3012325	hsa_circRNA_000390	chr4/-	sense overlapping	PDS5A	0.23350004	0.10307318	0.03113406	M5	0.85683567
ASCRP3000049	hsa_circRNA_101915	chr16/-	exonic	FANCA	0.26286608	0.09422644	0.00922543	M5	0.82846255
ASCRP3004492	hsa_circRNA_104016	chr5/+	exonic	ERGIC1	0.23365789	0.10908668	0.04072624	M5	0.81875582
ASCRP3004943	hsa_circRNA_406001	chr2/+	sense overlapping	LOC101927156	0.22841652	0.10933782	0.04558504	M5	0.81835246
ASCRP3007335	hsa_circRNA_003223	chr15/-	exonic	MYO1E	0.20478554	0.08174458	0.01810687	M5	0.81575422
ASCRP3010857	hsa_circRNA_090302	chrX/-	exonic	CASK	0.28936389	0.11771578	0.02017805	M5	0.81411439
ASCRP3001147	hsa_circRNA_404886	chr11/+	exonic	PTPRJ	0.24349849	0.11594432	0.04452938	M5	0.80784965
ASCRP3001645	hsa_circRNA_100282	chr1/-	exonic	DNTTIP2	0.33144138	0.12683521	0.01407145	M5	0.79334849
ASCRP3007290	hsa_circRNA_402705	chr22/+	exonic	SPECC1L	0.2900758	0.12107844	0.02326126	M5	0.79297793
ASCRP3002043	hsa_circRNA_101896	chr16/-	exonic	ZCCHC14	0.26899917	0.12631672	0.04182144	M5	0.77642946
ASCRP3001686	hsa_circRNA_001675	chr7/+	sense overlapping	C1GALT1	0.2565116	0.09974028	0.01550739	M5	0.77247558
ASCRP3002969	hsa_circRNA_001219	chr22/+	exonic	MTMR3	0.17693847	0.05871006	0.00531333	M5	0.75744423
ASCRP3004769	hsa_circRNA_104802	chr9/-	exonic	TLE1	0.26060294	0.10879576	0.02328375	M5	0.74707673
ASCRP3003876	hsa_circRNA_014522	chr1/-	exonic	CLK2	0.19247331	0.07216819	0.01238715	M5	0.74488554
ASCRP3004186	hsa_circRNA_092390	chr11/+	exonic	PPP6R3	0.23025699	0.0932106	0.01962396	M5	0.73505363
ASCRP3007763	hsa_circRNA_104151	chr6/-	exonic	TBX18	0.24025492	0.09974064	0.02258386	M5	0.73249948
ASCRP3001614	hsa_circRNA_104196	chr6/-	exonic	MAP3K5	0.18255205	0.08778773	0.04652256	M5	0.72922586
ASCRP3012567	hsa_circRNA_102678	chr2/+	exonic	CRIM1	0.2008596	0.09448068	0.04214718	M5	0.71271344
ASCRP3001973	hsa_circRNA_403425	chr5/+	exonic	PHAX	0.27359069	0.09523639	0.0075344	M5	0.70554058
ASCRP3002010	hsa_circRNA_402803	chr3/+	exonic	NR1D2	-0.8089296	0.3519938	0.02895689	M6	0.89469405
ASCRP3006813	hsa_circRNA_103457	chr3/-	exonic	TPRA1	-0.6084868	0.25630949	0.02443274	M6	0.88836295
ASCRP3005036	hsa_circRNA_001257	chr22/-	sense overlapping	PLXNB2	-0.4821966	0.23570514	0.04994422	M6	0.85630389
ASCRP3002336	hsa_circRNA_104040	chr6/+	exonic	DUSP22	-0.6353853	0.24521556	0.0148202	M6	0.8558968
ASCRP3000892	hsa_circRNA_003615	chr11/-	exonic	ALG8	-0.4594455	0.21269272	0.03916414	M6	0.85376399
ASCRP3002575	hsa_circRNA_000480	chr13/+	antisense	ZC3H13	-0.5545388	0.23581789	0.02570047	M6	0.82927864
ASCRP3002992	hsa_circRNA_103561	chr3/+	exonic	SENP5	-0.6137306	0.26457498	0.02760072	M6	0.82697052
ASCRP3012503	hsa_circRNA_005279	chr12/+	exonic	ATP2A2	-0.7007767	0.29665507	0.02508935	M6	0.81984686
ASCRP3011050	hsa_circRNA_004121	chr2/-	exonic	RFX8	-0.5300998	0.23895363	0.03451346	M6	0.81747132
ASCRP3007931	hsa_circRNA_024326	chr11/+	exonic	NNMT	-0.2846048	0.10518118	0.01129087	M6	0.80747642

ASCRP3013054	hsa_circRNA_104942	chr9/+	exonic	NUP214	-0.5009155	0.16125614	0.00421025	M6	0.80587128
ASCRP3000768	hsa_circRNA_043366	chr17/+	exonic	PSMB3	-0.339962	0.15537483	0.03687418	M6	0.77922278
ASCRP3007811	hsa_circRNA_000551	chr14/-	exonic	SLC8A3	-0.3293925	0.15261367	0.03931591	M6	0.7698561
ASCRP3005461	hsa_circRNA_037886	chr16/-	exonic	ZC3H7A	-0.4087057	0.17751235	0.0286834	M6	0.75301779
ASCRP3011978	hsa_circRNA_000298	chr11/-	exonic	ARFGAP2	-0.2581876	0.10747347	0.02291737	M6	0.74057624
ASCRP3009290	hsa_circRNA_000178	chr14/+	intronic	SRSF5	-0.4708265	0.18557467	0.01681395	M6	0.73325107
ASCRP3009271	hsa_circRNA_104969	chr9/+	exonic	EHMT1	-0.28011	0.12479745	0.03259686	M6	0.73321926
ASCRP3005489	hsa_circRNA_085362	chr8/-	exonic	TRPS1	-0.2673359	0.10483961	0.01631924	M6	0.72561762
ASCRP3005132	hsa_circRNA_101134	chr12/+	exonic	UNG	-0.2699215	0.09665287	0.00915941	M7	0.86906736
ASCRP3001917	hsa_circRNA_405170	chr13/-	exonic	UGGT2	-0.3121867	0.11024324	0.00832833	M7	0.85433648
ASCRP3010045	hsa_circRNA_001328	chr3/+	exonic	SIDT1	-0.4459471	0.09098788	3.34E-05	M7	0.78502413
ASCRP3004191	hsa_circRNA_104431	chr7/-	exonic	SMURF1	-0.2332906	0.10207365	0.0297791	M7	0.77120202
ASCRP3000591	hsa_circRNA_102823	chr2/+	exonic	RAB3GAP1	-0.189554	0.08682197	0.03725675	M7	0.76565465
ASCRP3005878	hsa_circRNA_104787	chr9/-	exonic	PTAR1	-0.2388903	0.0965745	0.01947344	M7	0.76474987
ASCRP3002334	hsa_circRNA_092505	chr20/-	intronic	CPNE1	-0.2037535	0.09868391	0.0479947	M7	0.75894305
ASCRP3011575	hsa_circRNA_406742	chr6/-	exonic	KIF13A	-0.2331309	0.10826225	0.03973722	M7	0.72461502
ASCRP3011450	hsa_circRNA_075013	chr5/+	exonic	NPM1	-0.2946804	0.083129	0.00135461	M7	0.71937225
ASCRP3008301	hsa_circRNA_080252	chr7/+	exonic	GBAS	-0.1964349	0.07829959	0.01795784	M8	0.83192628
ASCRP3000788	hsa_circRNA_010991	chr1/+	exonic	LIN28A	-0.1897628	0.07755901	0.02071501	M8	0.74076731
ASCRP3008149	hsa_circRNA_405785	chr19/-	intronic	ADCK4	-0.2340716	0.0845337	0.00970067	M8	0.73997002
ASCRP3004702	hsa_circRNA_015279	chr1/+	exonic	KLHL20	-0.1977976	0.0519646	0.00067499	M8	0.72696137
ASCRP3013378	hsa_circRNA_065645	chr3/-	exonic	RHOA	-0.1889056	0.09228419	0.04981486	M8	0.72266809
ASCRP3000523	hsa_circRNA_005585	chr5/+	sense overlapping	NNT	-0.2202702	0.07746897	0.00809707	M9	0.815283
ASCRP3005981	hsa_circRNA_006205	chr4/+	sense overlapping	C4orf22	-0.3040979	0.10715352	0.00820396	M9	0.79427612
ASCRP3005437	hsa_circRNA_100345	chr1/-	exonic	C1orf43	-0.2204489	0.10448191	0.04361161	M9	0.77182837
ASCRP3011470	hsa_circRNA_102251	chr17/+	exonic	TBCD	-0.2633029	0.10505837	0.01806229	M9	0.7624032
ASCRP3002486	hsa_circRNA_404845	chr11/+	exonic	IPO7	-0.2945553	0.12814287	0.02892398	M9	0.74069027
ASCRP3009183	hsa_circRNA_001826	chr21/+	exonic	DYRK1A	-0.2377539	0.09009638	0.01324203	M9	0.71568113
ASCRP3000168	hsa_circRNA_102324	chr18/-	exonic	TMEM241	-0.5177016	0.22791147	0.03071624	M10	0.80024805
ASCRP3000042	hsa_circRNA_000566	chr14/+	exonic	VRK1	-0.2577258	0.08214161	0.00388996	M10	0.77712929
ASCRP3007631	hsa_circRNA_003792	chr12/+	exonic	CACNA1C	-0.2254746	0.1049032	0.04008319	M10	0.76047186
ASCRP3013458	hsa_circRNA_104538	chr7/-	exonic	LMBR1	-0.2980633	0.09882928	0.00528452	M10	0.74089866
ASCRP3006716	hsa_circRNA_102920	chr2/-	exonic	ABCB6	-0.3354041	0.15465548	0.03844602	M10	0.73522876
ASCRP3010153	hsa_circRNA_001072	chr16/+	sense overlapping	TSC2	-0.2479528	0.11265409	0.03584794	M10	0.72544641

Appendix VI: Regression results for circRNA x miRNA interaction effect on mRNA expression *(Study 2)*.

circRNA	miRNA	mRNA	Estimate	Std. Error	t-value	p-value	FDR
ASCRP3011575	hsa-miR-1200	IMP4	1.53054528	0.28882896	5.29914066	1.72E-05	0.00080937
ASCRP3011575	hsa-miR-1200	SSX2IP	2.02378019	0.42024329	4.81573468	6.01E-05	0.00094102
ASCRP3011575	hsa-miR-1200	PRKCB	5.35165333	1.08293375	4.94181048	4.33E-05	0.00094102
ASCRP3011575	hsa-miR-1200	ASTN1	2.06198402	0.52687919	3.91358031	0.00061837	0.00703394
ASCRP3011575	hsa-miR-1200	PCLO	2.560338	0.66692909	3.83899586	0.00074829	0.00703394
ASCRP3011575	hsa-miR-1200	HOMER1	1.78678466	0.48749802	3.66521419	0.00116416	0.00773595
ASCRP3011575	hsa-miR-1200	OSBPL8	1.91611762	0.53436057	3.58581399	0.00142282	0.00773595
ASCRP3011575	hsa-miR-1200	ATP2B2	2.58793864	0.72495034	3.56981504	0.00148135	0.00773595
ASCRP3011575	hsa-miR-1200	HRAS	1.82606095	0.49999695	3.65214416	0.00120332	0.00773595
ASCRP3011575	hsa-miR-1200	IPCEF1	2.09463746	0.60716557	3.44986206	0.00200163	0.00855244
ASCRP3011575	hsa-miR-1200	LDB2	3.51554896	1.01237131	3.47258849	0.00189102	0.00855244
ASCRP3011575	hsa-miR-1200	NDST3	2.73526849	0.81163132	3.37008742	0.00244195	0.00956431
ASCRP3011575	hsa-miR-1200	RAB11FIP2	0.90610204	0.27438872	3.30225692	0.00288906	0.01044506
ASCRP3005132	hsa-miR-665	MLEC	-0.6226648	0.1964143	-3.17016	0.00399749	0.01342016
ASCRP3011575	hsa-miR-1200	RANBP2	0.8802594	0.32381172	2.71842972	0.01174565	0.03680303
ASCRP3010153	hsa-miR-3187-3p	GPD2	-0.7689576	0.29016294	-2.6500891	0.01375386	0.03802538
ASCRP3011575	hsa-miR-1200	RFC2	0.83560553	0.31447229	2.65716745	0.01353182	0.03802538
ASCRP3013378	hsa-miR-571	NR3C1	-1.5578533	0.6327597	-2.4619983	0.02106023	0.05499059
ASCRP3001917	hsa-miR-4310	CELF1	0.6516508	0.29988509	2.17300165	0.03946215	0.0898441
ASCRP3011575	hsa-miR-1200	ACTR2	0.81274224	0.36931016	2.20070369	0.03721356	0.0898441
ASCRP3012325	hsa-miR-361-5p	NEK7	2.25849437	1.0432361	2.16489284	0.04014311	0.0898441
ASCRP3011575	hsa-miR-1200	E2F3	0.90432912	0.42352137	2.1352621	0.04272217	0.0912701
ASCRP3011575	hsa-miR-498	RBFOX1	1.02469005	0.53820813	1.90389181	0.06849601	0.13997012
ASCRP3011575	hsa-miR-1200	PDP1	1.16762774	0.76221328	1.53189109	0.13810705	0.27045965
ASCRP3012301	hsa-miR-361-5p	RALBP1	-0.6320372	0.41954121	-1.5064962	0.1444724	0.27160811
ASCRP3005878	hsa-miR-1207-5p	MLEC	-0.3025057	0.24227865	-1.248586	0.22338302	0.38531688
ASCRP3010524	hsa-miR-3119	MYOF	-2.7366467	2.16538406	-1.2638159	0.21795402	0.38531688
ASCRP3011575	hsa-miR-1200	GPC5	0.72909057	0.59197619	1.23162145	0.22955048	0.38531688
ASCRP3001645	hsa-miR-646	ANP32B	1.64097282	1.40199918	1.17045205	0.25285592	0.40816981
ASCRP3002043	hsa-miR-378c	SEC31A	0.47802494	0.4152337	1.15121902	0.26053392	0.40816981
ASCRP3012325	hsa-miR-361-5p	NDE1	-1.6410513	1.4809833	-1.1080823	0.27837347	0.42205011
ASCRP3013378	hsa-miR-571	NRP2	-0.071787	0.0664586	-1.0801763	0.29037466	0.42648778
ASCRP3011575	hsa-miR-1200	KDM5B	0.61064174	0.60528983	1.0088419	0.32271566	0.45166394
ASCRP3011575	hsa-miR-498	ATP2B1	0.66194684	0.66172879	1.0003295	0.32673562	0.45166394
ASCRP3012325	hsa-miR-361-5p	FGF1	1.07676919	1.11904466	0.96222183	0.3451535	0.46349185
ASCRP3012325	hsa-miR-361-5p	SEC62	0.32745852	0.36698391	0.89229668	0.38074255	0.49708056
ASCRP3011575	hsa-miR-1200	ZNF106	0.25997019	0.32441278	0.80135621	0.43047653	0.53243149
ASCRP3012325	hsa-miR-361-5p	MBOAT2	-0.6832299	0.85140254	-0.8024758	0.42984081	0.53243149
ASCRP3001686	hsa-miR-4760-3p	NEK7	1.6031339	2.98776095	0.53656699	0.59630978	0.71862974
ASCRP3012325	hsa-miR-361-5p	ZEB2	-0.6890341	1.343039	-0.513041	0.61242664	0.7196013
ASCRP3000049	hsa-miR-4762-5p	LSM14A	-0.3283677	0.68567705	-0.4788956	0.63617506	0.72927385
ASCRP3000049	hsa-miR-4762-5p	sec24a	-0.3687521	0.93827517	-0.3930106	0.697643	0.78069574
ASCRP3001645	hsa-miR-646	PAIP2B	0.46946142	2.36500614	0.19850326	0.84425677	0.8956874
ASCRP3012325	hsa-miR-361-5p	SMARCC1	-0.1782521	0.80878717	-0.2203943	0.82735396	0.8956874
ASCRP3013054	hsa-miR-3652	LAMC2	0.07744802	0.42711806	0.18132697	0.85757305	0.8956874
ASCRP3012325	hsa-miR-361-5p	FRYL	-0.1311396	0.88015382	-0.1489962	0.88275205	0.90194231
ASCRP3013054	hsa-miR-193a-3p	LAMC2	0.03529401	0.43576684	0.08099288	0.93609254	0.93609254

Appendix VII: CircRNA linear and SNP x AD interaction eQTL results *(Study 2)*.

	Linear eQTL						Linear cross eQTL (SNP x AD interaction)				
snps	*gene*	*statistic*	*pvalue*	*FDR*	*beta*	*snps*	*circRNA*	*statistic*	*pvalue*	*FDR*	*beta*
rs7991424	ASCRP3002575	-6.4839202	5.97E-07	0.02017828	-2.1202211	rs118155171	ASCRP3008301	5.23348349	1.82E-05	0.09670093	0.19908219
rs61811887	ASCRP3012903	6.15129134	1.42E-06	0.02017828	1.93779544	rs147144673	ASCRP3008301	5.23348349	1.82E-05	0.09670093	0.19908219
rs147100105	ASCRP3012903	6.15129134	1.42E-06	0.02017828	1.93779544	rs148170759	ASCRP3008301	5.23348349	1.82E-05	0.09670093	0.19908219
rs117006970	ASCRP3005461	4.95184011	3.47E-05	0.30222579	2.56672245	rs180683570	ASCRP3008301	5.23348349	1.82E-05	0.09670093	0.19908219
rs4720180	ASCRP3002395	-4.8940485	4.05E-05	0.30222579	-0.4388986	rs151187972	ASCRP3008301	5.23348349	1.82E-05	0.09670093	0.19908219
rs184047156	ASCRP3005461	4.87532064	4.26E-05	0.30222579	2.54766753	rs140694617	ASCRP3008301	5.23348349	1.82E-05	0.09670093	0.19908219
rs149248212	ASCRP3009183	4.50201216	0.00011606	0.69824913	0.75503628	rs138568769	ASCRP3008301	5.23348349	1.82E-05	0.09670093	0.19908219
rs11062213	ASCRP3007631	4.44041383	0.00013689	0.69824913	0.4513061	rs77334228	ASCRP3008301	5.23348349	1.82E-05	0.09670093	0.19908219
rs56322298	ASCRP3002395	4.38946477	0.0001569	0.69824913	0.56086768	rs61827881	ASCRP3004702	5.05996029	2.87E-05	0.13575513	0.05710754
rs1468762	ASCRP3001686	4.34981277	0.00017446	0.69824913	0.27292089	rs2239015	ASCRP3007631	5.01930513	3.19E-05	0.13600717	0.11917738
rs947505	ASCRP3004702	-4.3373903	0.00018035	0.69824913	-0.3228061	chr12:2536700:I	ASCRP3007631	4.86756087	4.77E-05	0.1750147	0.14313142
chr6:139272248:I	ASCRP3005732	-4.2288632	0.00024097	0.75844579	-0.7539022	rs4948043	ASCRP3008301	4.85468939	4.93E-05	0.1750147	0.09318458
rs12492090	ASCRP3002010	-4.1931115	0.00026505	0.75844579	-0.8207713	rs4277019	ASCRP3011126	4.77215527	6.13E-05	0.20089723	1.13301319
rs112113277	ASCRP3003195	-4.1602198	0.00028931	0.75844579	-0.7319037	rs4298454	ASCRP3008301	-4.5847017	0.0001006	0.30603124	-0.1422843
rs181041915	ASCRP3004702	4.14744353	0.00029931	0.75844579	0.73089863	rs7963869	ASCRP3007631	-4.4785861	0.00013311	0.35151965	-2.725036
rs8049561	ASCRP3010153	4.11096678	0.00032978	0.75844579	0.77531915	rs10798295	ASCRP3004702	4.47772271	0.00013341	0.35151965	0.05109809
rs954178	ASCRP3011450	4.0978199	0.0003415	0.75844579	1.06320788	rs6578758	ASCRP3010987	4.45857696	0.00014032	0.35151965	0.17966129
rs147614021	ASCRP3004702	4.05030527	0.00038737	0.75844579	0.71265141	rs10774039	ASCRP3007631	4.40257344	0.00016264	0.35264922	0.14252394
rs7950251	ASCRP3010987	4.0328892	0.00040567	0.75844579	0.73048309	rs143831739	ASCRP3008301	4.39808668	0.00016457	0.35264922	4.50745552
rs61826691	ASCRP3004702	4.03147097	0.0004072	0.75844579	0.71099519	rs35065145	ASCRP3004702	4.39568866	0.00016561	0.35264922	0.08337201
rs192039723	ASCRP3004769	-4.0068284	0.00043465	0.75844579	-1.1806904	rs6681720	ASCRP3004702	-4.2981748	0.00021407	0.4295439	-0.0953619
rs77368889	ASCRP3004769	-4.0068284	0.00043465	0.75844579	-1.1806904	rs2227596	ASCRP3004702	4.27334915	0.00022851	0.4295439	0.08476655
rs11119030	ASCRP3003317	3.99304799	0.00045078	0.75844579	0.31167284	rs1951625	ASCRP3004702	4.21947637	0.00026324	0.4295439	0.08141193
rs114699482	ASCRP3012567	3.96767968	0.00048204	0.75844579	0.43657578	rs6425224	ASCRP3004702	-4.1624815	0.00030569	0.4295439	-0.0808469
rs191164384	ASCRP3011450	3.94298456	0.00051452	0.75844579	1.03832699	chr16:11993187:I	ASCRP3005461	-4.1576308	0.0003096	0.4295439	-2.5465823
rs77560264	ASCRP3011126	-3.9264141	0.00053751	0.75844579	-0.8575376	chr1:173429147:I	ASCRP3004702	4.15048838	0.00031545	0.4295439	0.09916557
rs74086799	ASCRP3000042	3.91324874	0.00055649	0.75844579	0.36590434	rs2208849	ASCRP3004702	4.14770559	0.00031776	0.4295439	0.07350117
rs7001536	ASCRP3010761	3.89703036	0.00058079	0.75844579	0.2986662	rs56037160	ASCRP3007335	-4.1446	0.00032035	0.4295439	-0.9807878
rs7130042	ASCRP3010987	3.887231	0.00059597	0.75844579	0.26369392	rs2283294	ASCRP3007631	-4.1296951	0.00033311	0.4295439	-0.0800983
rs6584077	ASCRP3008631	3.8530278	0.00065206	0.75844579	0.3316877	rs7811548	ASCRP3008301	4.10663718	0.00035383	0.4295439	0.14872392

rs140398314	ASCRP3013224	-3.8507165	0.00065603	0.75844579	-1.6663334
rs111500971	ASCRP3013224	-3.8507165	0.00065603	0.75844579	-1.6663334
rs11755735	ASCRP3001614	3.84337588	0.00066881	0.75844579	0.65991286
rs75023617	ASCRP3008173	-3.8405946	0.00067371	0.75844579	-0.5460872
rs112653441	ASCRP3002992	-3.8196149	0.00071185	0.75844579	-1.390168
rs144961584	ASCRP3008301	3.80412425	0.00074136	0.75844579	1.01078695
rs72909043	ASCRP3010987	3.79809872	0.00075316	0.75844579	0.70590666
rs6915606	ASCRP3002336	-3.7895017	0.00077032	0.75844579	-0.8312831
rs13327482	ASCRP3002992	-3.7871545	0.00077507	0.75844579	-0.9003206
chr3:196876775:I	ASCRP3002992	-3.7871545	0.00077507	0.75844579	-0.9003206
rs3889250	ASCRP3002992	-3.7835403	0.00078244	0.75844579	-1.4146461
rs185016961	ASCRP3002992	-3.7756558	0.00079875	0.75844579	-2.0498858
rs61811927	ASCRP3012903	3.77068586	0.00080921	0.75844579	1.24171491
rs62014212	ASCRP3003348	-3.7547925	0.00084356	0.75844579	-1.4667056
rs118053682	ASCRP3003348	-3.7547925	0.00084356	0.75844579	-1.4667056
rs76154462	ASCRP3009543	-3.7531916	0.00084709	0.75844579	-0.7368734
rs131800	ASCRP3005036	3.74061068	0.0008754	0.75844579	1.82692568
rs139307962	ASCRP3002969	-3.721483	0.00092023	0.75844579	-0.6124716
rs118037742	ASCRP3008301	3.71466694	0.00093674	0.75844579	0.99028196
rs148680552	ASCRP3002969	-3.7052423	0.00096004	0.75844579	-0.6088526
rs72959969	ASCRP3009543	-3.6926099	0.00099217	0.75844579	-0.72277
rs139397465	ASCRP3009543	-3.6926099	0.00099217	0.75844579	-0.72277
rs117316783	ASCRP3009543	-3.6926099	0.00099217	0.75844579	-0.72277
rs183325577	ASCRP3009543	-3.6926099	0.00099217	0.75844579	-0.72277
rs10269598	ASCRP3013458	3.6871386	0.00100641	0.75844579	0.35807415
rs111464093	ASCRP3012903	3.68692945	0.00100696	0.75844579	1.52569259
rs7752106	ASCRP3011575	-3.6838239	0.00101513	0.75844579	-0.3151475
rs57190150	ASCRP3013224	-3.6615299	0.00107575	0.76434385	-1.6026565
rs141353736	ASCRP3013224	-3.6615299	0.00107575	0.76434385	-1.6026565
rs142134601	ASCRP3004492	3.66112995	0.00107687	0.76434385	0.84267438
rs192123345	ASCRP3008301	3.64047046	0.00113625	0.7932691	0.98968076
rs10084688	ASCRP3002010	-3.6281423	0.00117319	0.79508958	-0.774602
rs181374150	ASCRP3013224	-3.6265098	0.00117817	0.79508958	-1.5891561
rs7040470	ASCRP3013054	-3.6116352	0.00122449	0.79508958	-0.3787826
rs11176379	ASCRP3012301	-3.6105738	0.00122787	0.79508958	-0.4033713
rs8061521	ASCRP3002043	-3.6063097	0.00124151	0.79508958	-0.2942108

rs2695582	ASCRP3013458	-4.103989	0.00035629	0.4295439	-0.1448899
rs4948042	ASCRP3008301	4.10016327	0.00035988	0.4295439	0.07381557
rs6661868	ASCRP3004702	4.09888203	0.00036109	0.4295439	0.08007398
chr8:116515360:I	ASCRP3005489	-4.0924627	0.0003672	0.4295439	-1.4690301
rs1951627	ASCRP3004702	4.05645952	0.00040344	0.4295439	0.07868624
chr6:83982034:I	ASCRP3013224	-4.0563507	0.00040356	0.4295439	-0.2389517
rs618513	ASCRP3009543	-4.0349897	0.00042671	0.4295439	-0.7957842
rs16845720	ASCRP3004702	4.01639695	0.00044793	0.4295439	0.09222312
chr1:173832772:I	ASCRP3004702	4.00805274	0.00045779	0.4295439	0.07746833
rs142085364	ASCRP3006716	4.00793637	0.00045793	0.4295439	0.31175239
rs72711419	ASCRP3004702	4.00624618	0.00045995	0.4295439	0.09136714
rs74348266	ASCRP3004702	4.00569976	0.00046061	0.4295439	0.09799906
rs78972925	ASCRP3004702	3.99192899	0.00047745	0.4295439	0.09755645
rs114032493	ASCRP3004702	3.99192899	0.00047745	0.4295439	0.09755645
rs34672369	ASCRP3008301	3.9696333	0.00050601	0.4295439	0.0761465
rs590401	ASCRP3009543	3.96937047	0.00050635	0.4295439	0.85621318
rs670825	ASCRP3009543	3.96937047	0.00050635	0.4295439	0.85621318
rs509870	ASCRP3009543	3.96937047	0.00050635	0.4295439	0.85621318
rs192012531	ASCRP3004702	3.96651327	0.00051014	0.4295439	2.67119152
rs74580411	ASCRP3011126	3.96416704	0.00051326	0.4295439	25.2635431
rs10912724	ASCRP3004702	3.95716565	0.00052271	0.4295439	0.09346551
rs80103586	ASCRP3008301	3.95586008	0.00052449	0.4295439	1.91152011
rs72846848	ASCRP3010987	3.94131944	0.00054471	0.43769376	21.6714802
rs56273514	ASCRP3004702	3.91522607	0.00058296	0.45332814	0.09282595
rs35835531	ASCRP3000614	3.91357849	0.00058546	0.45332814	0.15088015
rs189633691	ASCRP3004702	3.90082208	0.00060519	0.46023723	2.25397145
rs4916354	ASCRP3004702	-3.8928852	0.0006178	0.46143463	-0.0757487
rs9444008	ASCRP3013224	3.88630796	0.00062844	0.46143463	0.19141436
chr1:173853833:D	ASCRP3004702	3.86299024	0.00066763	0.48190492	0.08460472
chr10:132742824:D	ASCRP3011126	3.84789914	0.00069427	0.4847013	26.0565532
rs2397462	ASCRP3011126	-3.8478991	0.00069427	0.4847013	-26.056553
rs2096147	ASCRP3004702	-3.8366335	0.00071483	0.49100784	-0.0563645
chr1:44935102:D	ASCRP3003107	-3.8229843	0.00074055	0.49125135	-0.0785014
rs184604106	ASCRP3008301	3.81112573	0.00076362	0.49125135	3.7145164
rs74677717	ASCRP3008301	3.80919881	0.00076744	0.49125135	1.3084944
chr7:56304197:D	ASCRP3008301	3.80647776	0.00077286	0.49125135	0.1483591

rs111451551	ASCRP3002992	-3.6027758	0.00125292	0.79508958	-1.1773103
rs602609	ASCRP3009543	3.59768677	0.00126954	0.79508958	0.7101108
rs10951458	ASCRP3002395	3.57385008	0.00135029	0.8334059	0.36516123
rs72614028	ASCRP3007019	3.56797629	0.00137095	0.8340655	0.59660383
rs139931431	ASCRP3006716	3.56018874	0.00139881	0.83416777	2.01775705
rs75707618	ASCRP3011978	3.54366307	0.00145976	0.83416777	0.887478
rs144281024	ASCRP3008271	-3.5407766	0.00147067	0.83416777	-0.9868443
rs11921123	ASCRP3002992	-3.5391134	0.00147699	0.83416777	-1.1127463
chr10:98057176:I	ASCRP3008631	3.53591346	0.00148922	0.83416777	0.50294138
rs35339198	ASCRP3006813	3.53142411	0.00150656	0.83416777	1.07133039
rs139566659	ASCRP3001614	3.52693758	0.00152407	0.83416777	0.88265431
rs147813589	ASCRP3001614	3.52598561	0.00152782	0.83416777	0.8810639
rs76345075	ASCRP3002969	-3.5124184	0.00158213	0.85288893	-0.4232376
rs147535393	ASCRP3001614	3.49875065	0.00163874	0.86159515	0.87479701
rs28741382	ASCRP3001614	3.49875065	0.00163874	0.86159515	0.87479701
rs76638263	ASCRP3003107	-3.4826475	0.00170797	0.8648808	-0.5851162
rs58314904	ASCRP3002658	-3.4771112	0.00173242	0.8648808	-0.5332786
rs138447739	ASCRP3008271	-3.4752946	0.00174052	0.8648808	-0.9731142
chr9:88701230:I	ASCRP3008271	-3.4746883	0.00174323	0.8648808	-0.9735232
rs61898465	ASCRP3011978	3.46809149	0.00177298	0.8648808	0.49403331
rs190221363	ASCRP3010153	3.46687897	0.00177851	0.8648808	1.17010006
rs149732000	ASCRP3011050	-3.4605619	0.00180755	0.8648808	-2.6126959
rs149826422	ASCRP3011050	-3.4605619	0.00180755	0.8648808	-2.6126959
rs4845394	ASCRP3003876	3.45447922	0.00183595	0.8648808	0.17537566
chr12:2341396:I	ASCRP3007631	3.45190885	0.00184808	0.8648808	0.92258734
chr17:36957346:I	ASCRP3000768	3.43726998	0.00191866	0.87947543	1.53890503
rs75798658	ASCRP3004513	-3.4368818	0.00192057	0.87947543	-0.6709623
rs8030006	ASCRP3007335	-3.4256808	0.00197638	0.88192193	-0.2083326
rs72953980	ASCRP3009543	-3.4233811	0.00198804	0.88192193	-0.4958911
rs189849094	ASCRP3009543	-3.4233811	0.00198804	0.88192193	-0.4958911
rs75769228	ASCRP3008301	3.80647776	0.00077286	0.49125135	0.1483591
rs111964306	ASCRP3011126	3.79979242	0.00078634	0.49246812	12.6430461
rs2715266	ASCRP3000614	-3.7898676	0.00080677	0.49569924	-0.1412847
rs10193725	ASCRP3006716	3.78604779	0.00081478	0.49569924	0.1693986
rs12057778	ASCRP3004702	3.77177546	0.00084538	0.50032043	0.07368197
rs148117824	ASCRP3005188	3.77082622	0.00084745	0.50032043	0.2049382
rs7295089	ASCRP3007631	-3.7635286	0.00086357	0.50032043	-0.0975674
rs3759177	ASCRP3013402	-3.7542064	0.00088459	0.50032043	-0.1368039
rs72908063	ASCRP3013224	3.75100913	0.00089192	0.50032043	0.19117992
rs2274166	ASCRP3012052	3.75059826	0.00089286	0.50032043	30.8155728
rs150681506	ASCRP3008301	3.73731642	0.00092397	0.50054602	0.16627655
rs10281437	ASCRP3008301	3.73636474	0.00092624	0.50054602	1.90760819
rs118095911	ASCRP3008301	3.72365062	0.00095708	0.50054602	0.16615327
rs2456527	ASCRP3008173	-3.7217153	0.00096186	0.50054602	-0.1708786
chr17:74618265:D	ASCRP3008151	3.71897644	0.00096867	0.50054602	6.35908164
rs72704895	ASCRP3000042	3.71676914	0.00097419	0.50054602	0.1284374
rs79028599	ASCRP3013224	-3.7149955	0.00097865	0.50054602	-6.0667106
rs146708280	ASCRP3007631	3.70896212	0.00099397	0.50054602	3.28500418
rs2561562	ASCRP3008149	-3.7065379	0.00100019	0.50054602	-0.0726742
rs74450739	ASCRP3003607	-3.6891403	0.00104596	0.50054602	-0.1139318
rs12193149	ASCRP3001614	-3.685436	0.00105597	0.50054602	-0.1323333
rs2239116	ASCRP3007631	-3.6844546	0.00105864	0.50054602	-0.119205
rs77369703	ASCRP3013458	3.68319986	0.00106205	0.50054602	3.58517796
rs9695351	ASCRP3008271	3.68247486	0.00106404	0.50054602	0.10143569
rs72724954	ASCRP3004702	3.67751066	0.00107769	0.50054602	0.08419377
rs186642813	ASCRP3008301	3.67620273	0.00108132	0.50054602	0.14455475
rs184778233	ASCRP3013054	3.66961902	0.00109976	0.50142799	19.8874489
rs72724965	ASCRP3004702	3.66714324	0.00110678	0.50142799	2.05867346
rs7304870	ASCRP3007631	3.65904111	0.00113003	0.50657662	0.09917559
rs116342434	ASCRP3004702	3.65034659	0.00115553	0.50860632	0.08249641
rs2836946	ASCRP3013140	3.64310342	0.00117719	0.50860632	0.61690887
rs9975937	ASCRP3013140	3.64310342	0.00117719	0.50860632	0.61690887
rs75234616	ASCRP3009183	3.64140313	0.00118233	0.50860632	3.70807164
rs10774067	ASCRP3007631	-3.6334452	0.0012067	0.51389589	-0.1219746
rs10912588	ASCRP3004702	3.62312832	0.00123901	0.52243298	0.09216293
rs4355583	ASCRP3013224	-3.6114441	0.00127663	0.52243298	-0.1692727

rs57221296	ASCRP3000042	3.610355	0.0012802	0.52243298	0.09751862
rs34906768	ASCRP3004702	-3.6017669	0.00130863	0.52243298	-0.0878348
rs60106275	ASCRP3007631	-3.5999935	0.00131458	0.52243298	-0.1228334
rs7512435	ASCRP3005188	-3.5984536	0.00131977	0.52243298	-0.1321691
rs190877460	ASCRP3013224	-3.5957476	0.00132893	0.52243298	-7.1099615
rs6580826	ASCRP3013402	-3.5944321	0.00133341	0.52243298	-0.6523513
rs2239032	ASCRP3007631	-3.5933357	0.00133715	0.52243298	-0.095827
rs9771073	ASCRP3008301	3.58743879	0.00135745	0.52401851	1.07525445
chr1:173328616:D	ASCRP3004702	-3.5850349	0.00136582	0.52401851	-0.0634902
rs72704130	ASCRP3003876	-3.5811193	0.00137955	0.52411915	-0.134877
rs2283296	ASCRP3007631	-3.5778773	0.00139102	0.52411915	-0.0734301
rs185976327	ASCRP3007631	3.57167157	0.00141323	0.52411915	3.46266226
rs55915731	ASCRP3010153	-3.5709244	0.00141593	0.52411915	-35.980523
rs72819137	ASCRP3004513	3.56770431	0.00142761	0.52411915	1.36398419
rs111687147	ASCRP3004153	3.55552404	0.00147267	0.53603898	0.40412442
rs191215829	ASCRP3008301	3.53264512	0.00156107	0.55892781	3.19672673
rs12122449	ASCRP3005437	-3.5324618	0.0015618	0.55892781	-0.148737
rs2023906	ASCRP3007718	3.52486306	0.0015923	0.56077709	0.09973524
rs4905528	ASCRP3000042	3.52461609	0.0015933	0.56077709	0.09060441
rs7303275	ASCRP3007631	-3.4933724	0.00172501	0.56879004	-0.0949809
rs10410606	ASCRP3008149	-3.4923519	0.00172948	0.56879004	-0.0750106
chr14:97706189:D	ASCRP3000042	3.49192808	0.00173134	0.56879004	0.10488369
rs6670351	ASCRP3003607	-3.4913192	0.00173402	0.56879004	-0.0892654
rs79321848	ASCRP3013402	3.48956907	0.00174174	0.56879004	1.38996702
rs72583243	ASCRP3002957	3.48848163	0.00174656	0.56879004	0.98697944
rs338785	ASCRP3010153	3.48400972	0.00176649	0.56879004	0.14267613
chr12:2634810:I	ASCRP3007631	-3.4824307	0.00177358	0.56879004	-0.1084165
rs11062441	ASCRP3007631	3.480388	0.0017828	0.56879004	0.10227363
rs62457286	ASCRP3008301	3.48026902	0.00178334	0.56879004	0.13986128
rs114698684	ASCRP3006716	-3.4775694	0.00179559	0.56879004	-59.403474
chr11:86154972:D	ASCRP3009543	3.47653685	0.0018003	0.56879004	0.91562649
rs10050565	ASCRP3004492	3.47052487	0.00182796	0.56879004	0.08413053
chr7:156228668:I	ASCRP3013458	3.47017176	0.00182959	0.56879004	0.16000561
rs55741208	ASCRP3008173	-3.4690434	0.00183483	0.56879004	-0.0770597
chr6:83939847:I	ASCRP3013224	-3.4636541	0.00186007	0.56879004	-0.2574582
rs78296603	ASCRP3006716	-3.4608928	0.00187312	0.56879004	-57.862647

rs144308536	ASCRP3013224	-3.4607107	0.00187399	0.56879004	-0.2468993
rs34444541	ASCRP3013458	3.45986398	0.00187801	0.56879004	0.13011341
rs11720857	ASCRP3010045	-3.4587772	0.00188319	0.56879004	-0.0699411
rs61826710	ASCRP3004702	3.45343452	0.00190884	0.57247785	0.08389944
rs3122335	ASCRP3003607	3.44144668	0.00196764	0.58138548	0.09786997
rs272536	ASCRP3003107	-3.4382839	0.00198345	0.58138548	-0.1072511
rs12813847	ASCRP3007631	-3.4368099	0.00199085	0.58138548	-0.1293926
rs7795911	ASCRP3008301	-3.436354	0.00199315	0.58138548	-0.070841

Vita

Education

Ph.D. in Behavioral and Statistical Genetics	Virginia Commonwealth University Richmond, Virginia	2016-present
B.S. in Psychology *(Cum Laude)*	University Of Arizona Tucson, Arizona	2013-2015
A.A. in Liberal Arts	Pima Community College Tucson, Arizona	2010-2013

Funding Awards

F31 Ruth L. Kirschstein Predoctoral Individual National Research Service Award (F31AA028180)

Publications

Vornholt, E., Mamdani, M., Drake, J., McMichael, G., Taylor, Z. N., Bacanu, S. A., ... & Vladimirov, V. I. (2020). Network Preservation Reveals Shared and Unique Biological Processes Associated with Chronic Alcohol Abuse in NAc and PFC. *bioRxiv*. (*UNDER REVIEW*)

Vornholt, E., Mamdani, M., Drake, J., McMichael, G., Taylor, Z.N., Bacanu, S. A., ... & Vladimirov, V. I. (2020). Identifying a novel biological mechanism for alcohol addiction associated with circRNA networks acting as potential miRNA sponges in the nucleus accumbens of chronic alcohol users. (*UNDER REVIEW*)

Vornholt, E., Luo, D., Qiu, W., McMichael, G. O., Liu, Y., Gillespie, N., ... & Vladimirov, V. I. (2019). Postmortem brain tissue as an underutilized resource to study the molecular pathology of neuropsychiatric disorders across different ethnic populations. *Neuroscience & Biobehavioral Reviews*, *102*, 195-207.

Drake, J., McMichael, G. O., **Vornholt, E**., Cresswell, K., Williamson, V., Chatzinakos, C., ... & Riley, B. P. (2020). Assessing the Role of Long-Noncoding RNA in Nucleus Accumbens in Subjects with Alcohol Dependence. *Alcoholism: Clinical and Experimental Research*.

Posters/Presentations

American Society of Human Genetics Meetings

TITLE: Gene network analysis reveals unique and shared modules associated with alcohol dependence within the prefrontal cortex and nucleus accumbens (2019).

TITLE: Assessing circRNA-miRNA-mRNA interactions within the nucleus accumbens of chronic alcohol abusers (2020).

WORLD CONGRESS OF PSYCHIATRIC GENETICS

TITLE: Gene network analysis reveals unique and shared modules associated with alcohol dependence within the prefrontal cortex and nucleus accumbens (2019).

TITLE: Assessing circRNA-miRNA-mRNA interactions within the nucleus accumbens of chronic alcohol abusers (2020).